UNIVERSITAT
ROVIRA i VIRGILI

APPLICATION OF DNA BINDING PROTEIN TAGS AS MEANS FOR DEFINED CO-IMMOBILIZATION IN BIOSENSORS

GÜLSEN BETÜL AKTAS

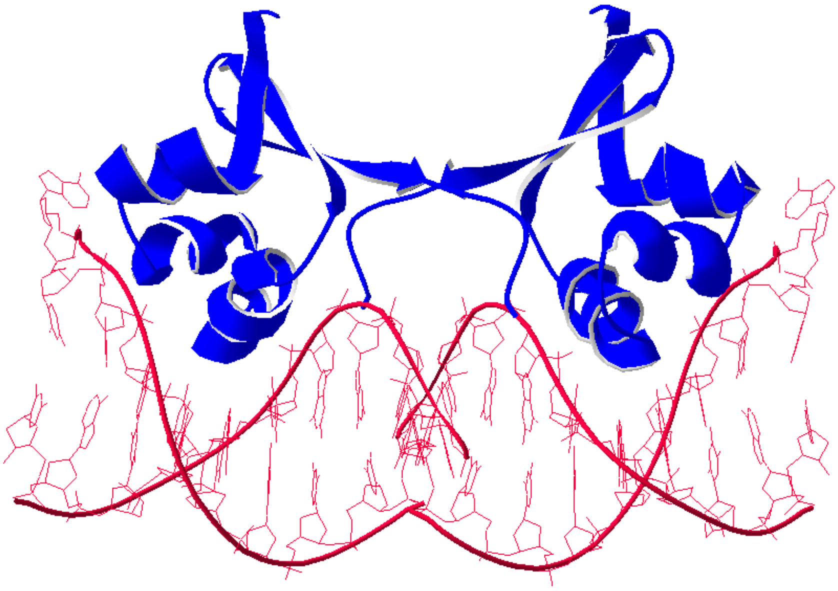

DOCTORAL THESIS

2017

Gülsen Betül Aktas

APPLICATION OF DNA BINDING PROTEIN TAGS AS MEANS FOR DEFINED CO-IMMOBILIZATION IN BIOSENSORS

DOCTORAL THESIS

Departament d'Enginyeria Química

UNIVERSITAT ROVIRA i VIRGILI

Tarragona

2017

UNIVERSITAT
ROVIRA i VIRGILI

Department of Chemical Engineering
University Rovira i Virgili
Av. Països Catalans, 26
43007 - Tarragona, SPAIN
Tel: 977 55 96 58
Fax: 977 55 96 67

I STATE that the present study, entitled "Application of DNA binding protein tags as means for defined co-immobilization in biosensors", presented by Gülsen Betül Aktas for the award of the degree of Doctor, has been carried out under my supervision at the Department of Chemical Engineering of this university, and that is fulfils all the requirements to be eligible for the International Doctoral Award.

Tarragona, 5th June 2017,

Dr. Lluis Masip

ACKNOWLEDGEMENTS

Many people and institutions helped me and my studies during this tough PhD path. It would not be possible to finish my studies without their support. That is why I wish to dedicate this section to recognize their support.

Firstly, my deepest and warmest thanks go to Dr. Vasso Skouridou; my supervisor and mentor since the first day of PhD. I would not be able to complete my studies without her guidance and help. I am thankful for her patience, sharing the invaluable knowledge and encouragement during these years. In addition, of course, being my English dictionary.

I would like to thank and express a sincere gratitude to my director of thesis Dr. Lluis Masip for accepting me in this PhD and teaching me what research is. I am more than grateful and indebted for his full-support and patience. He not only did give me the chance to learn but also made me a member of the scientific world.

To Dr. Aart von Amerongen and Jan Wichers, who gave me opportunity of being part of their group for a three-month research, for their time and kindness. I would like to thank for your guidance not only in the professional way but also in personal life. I wish the best for both of you.

I am also very grateful to all the Interfibio Group for their time to help me during these years, especially Dr. Ciara O'Sullivian, Dr. Ioannis Katakis, Dr. Alex Fragoso, and Dr. Mayreli Ortiz. Of course, to Dr. Miriam Jauset Rubio and Oumaya Meshli, for their friendship and all time support. I am so grateful for the time spent together.

My special thanks to former members of the group, Nouran Yahya and Tania Diaz, for the moments shared in different time and places in the world. I feel so lucky to meet both of you and being my lifelong friends.

To my parents, Fatma and Ali Aktas, the real reason that I have arrived where I am. In addition, my lovely sister Gülseren – my idol and model - and her husband Mehmet, you were amazing with your support every time in long phone calls. I am

so glad to have their unconditional love. Because of you all, I have been inspired to embark on this journey and remained motivated to push through to its completion. Sizi çok seviyorum.

Finally, I would like to thank Nikolas who is so so special to me. I cannot thank you enough for your encouragement, support and of course the time that checking this thesis. Tarragona would be way beyond boring without you. S'agapo poli.

TABLE OF CONTENTS

SUMMARY **1**

LIST OF PUBLICATIONS **5**

LIST OF ABBREVIATIONS **6**

LIST OF FIGURES **9**

LIST OF TABLES **16**

CHAPTER 1: GENERAL INTRODUCTION **8**

1.1 DETECTION METHODS IN BIOSENSORS 8

1.1.1 Fluorescent labeling *10*

1.1.2 Nanoparticle labeling *11*

1.1.3 Enzyme labeling *12*

1.2 PROTEIN IMMOBILIZATION 13

1.2.1 Physical adsorption *13*

1.2.2 Covalent binding *14*

1.2.3 Bioaffinity interactions *15*

1.2.4 Novel affinity-based protein immobilization approach *18*

1.3 DNA BINDING PROTEINS 19

1.3.1 scCro DNA binding protein *20*

1.3.2 LacI headpiece binding protein *21*

1.3.3 Methods to prepare protein-protein conjugates *23*

1.4 THESIS OBJECTIVES 26

1.5 REFERENCES 27

CHAPTER 2: NOVEL SIGNAL AMPLIFICATION APPROACH IN GENOSENSORS BASED ON DNA BINDING PROTEIN TAGS **40**

2.1 ABSTRACT 40

2.2 INTRODUCTION 41

2.3 EXPERIMENTAL 43

2.3.1 Materials 43

2.3.2 Cloning, expression and purification of the DNA binding protein 44

2.3.3 Preparation of the HRP-scCro conjugate 45

2.3.4 SDS-PAGE and Western blot analysis 45

2.3.5 Characterization of the HRP-scCro conjugate by Electrophoretic Mobility Shift Assay (EMSA)46

2.3.6 DNA detection by Enzyme Linked Oligonucleotide Assay (ELONA) 46

2.4 RESULT AND DISCUSSION 47

2.4.1 Choice and production of the DNA binding protein 47

2.4.2 Preparation and characterization of the HRP-DNA binding protein conjugate 48

2.4.3 Design of the DNA detection probes with scCro DNA binding sites 50

2.4.4 ELONA for DNA detection 52

2.5 CONCLUSION 55

2.6 ACKNOWLEDGEMENTS 56

2.7 REFERENCES 57

2.8 SUPPLEMANTARY MATERIAL 61

2.8.1 Preparation of the hybrid ssDNA-dsDNA HPV16 detection probes 62

2.8.2 EMSA for the binding of scCro to the oligonucleotides involved in HPV16 detection 63

2.8.3 Optimization of the HRP-scCro conjugation reaction 64

2.8.4 MALDI-TOF mass spectrometry for the HRP-scCro conjugate 65

CHAPTER 3: NUCLEIC ACID SENSING WITH ENZYME-DNA BINDING PROTEIN CONJUGATES CASCADE AND SIMPLE DNA NANOSTRUCTURES 69

3.1 ABSTRACT 69

3.2 INTRODUCTION 70

3.3 EXPERIMENTAL 72

3.3.1 Materials 72

3.3.2 Preparation of the enzyme-DNA binding protein tag conjugates 73

3.3.3 Preparation and characterization of the hybrid ssDNA-dsDNA detection probes 74

3.3.4 Colorimetric detection of DNA with ELONA *75*

3.3.4.1 Optimization of capture probe concentration 76

3.3.4.2 Optimization of detection probe concentration 76

3.3.4.3 Binding order of the enzyme-DNA binding protein tags conjugates 76

3.3.4.4 Target ssDNA calibration curves 76

3.3.4.5 ELONA assay specificity 77

3.4 RESULT AND DISCUSSION 77

3.4.1 DNA binding protein tags *77*

3.4.2 Enzyme-DNA binding protein tag conjugates *78*

3.4.3 DNA detection probes *81*

3.4.4 Target ssDNA detection with ELONA *83*

3.5 CONCLUSIONS 88

3.6 ACKNOWLEDGEMENTS 89

3.7 REFERENCES 90

3.8 SUPPLEMANTARY MATERIAL 95

3.8.1 Preparation of dimeric single-chain Lac headpiece with N-terminal cysteine (cys-dHP) *95*

3.8.1.1 Cloning 95

3.8.1.2 Expression and purification 96

3.8.2 Preparation of the hybrid ssDNA-dsDNA detection probes *98*

3.8.3 Characterization of the GOx-dHP conjugate by MALDI-TOF mass spectroscopy *100*

3.8.4 DNA detection with ELONA *101*

CHAPTER 4: SANDWICH-TYPE APTASENSOR EMPLOYING MODIFIED APTAMERS AND ENZYME-DNA BINDING PROTEIN CONJUGATES............ 105

4.1 ABSTRACT 105

4.2 INTRODUCTION 106

4.3 EXPERIMENTAL 108

4.3.1 Materials *108*

4.3.2 Preparation and characterization of the modified aptamers *109*

4.3.3 Thrombin colorimetric detection with enzyme-linked aptamer assay (ELAA) *111*

4.3.3.1 Capture aptamer choice 112

4.3.3.2 Optimization of capture aptamer concentration 112

4.3.3.3 Optimization of detection aptamer concentration 112

4.3.3.4 Optimization of DNA binding protein conjugates concentration 113

4.3.4 Detection of thrombin using the enzyme conjugates in a lateral flow assay 113

4.4 RESULTS AND DISCUSSION 114

4.4.1 Design of the colorimetric sandwich-type aptasensor 114

4.4.2 Preparation and characterization of the modified aptamers 115

4.4.3 Colorimetric detection by ELAA 116

4.4.4 Lateral flow assay 119

4.5 CONCLUSIONS 121

4.6 ACKNOWLEDGEMENTS 121

4.7 REFERENCES 122

4.8 SUPPLEMANTARY MATERIAL 126

CHAPTER 5: PAPER-BASED DETECTION OF SHIGA TOXIN-PRODUCING *ESCHERICHIA COLI* USING CARBON NANOPARTICLES-DNA BINDING PROTEIN CONJUGATES 131

5.1 ABSTRACT 131

5.2 INTRODUCTION 132

5.3 EXPERIMENTAL 136

5.3.1 Materials 136

5.3.2 Polymerase Chain Reaction 136

5.3.3 Enzyme-Linked Immunosorbent Assay (ELISA) 137

5.3.4 Preparation of the carbon nanoparticles-protein conjugates 138

5.3.5 Preparation of the nucleic acid lateral flow assay (NALFA) strips 138

5.3.6 Detection of PCR amplicon by NALFA 139

5.4 RESULTS AND DISCUSSION 140

5.4.1 Target gene PCR amplification and ELISA validation 140

5.4.2 NALFA 141

5.4.2.1 Detection with scCro/CNP conjugate 141

5.4.2.2 Detection with HRP-scCro enzyme conjugate 143

5.4.2.3 Detection with HRP-scCro/CNP conjugate 144

5.5 CONCLUSION 147

5.6 ACKNOWLEDGEMENTS 148

5.7 REFERENCES 149

5.8 SUPPLEMANTARY MATERIAL 153

CHAPTER 6: GENERAL CONCLUSION 161

6.1 GENERAL CONCLUSION 161

SUMMARY

There are three main methods used to immobilize proteins for the development of biosensors: physical adsorption, covalent linking and bioaffinity interactions. Each of these methods has advantages and disadvantages but none of them provide a simple and straightforward way to allow the co-immobilization of proteins in a specific pattern. The objective of this doctoral thesis is to develop a novel immobilization system based on bioaffinity interactions with these characteristics in the context of biosensor applications.

Specifically, the aim was to explore the use of DNA binding proteins in biosensors mainly as universal detection molecules. The specificity and high affinity that these proteins exhibit for their respective double stranded DNA (dsDNA) sequence was thus exploited in order to develop a protein immobilization technique that allows the controlled co-immobilization of several proteins. The proposed system is based on the utilization of these DNA binding proteins as fusion tags for the target proteins to be immobilized and the use of dsDNA as the template to direct protein co-immobilization by specific positioning of the target DNA sequences of the DNA binding proteins. The preparation and characterization of two novel enzyme-DNA binding protein conjugates is described and their use for detection and signal amplification in biosensors for the detection of nucleic acid and protein targets is demonstrated.

The thesis is divided in six chapters:

Chapter 1 contains a general introduction and literature review, which includes a brief description of the system for controlled co-immobilization of several proteins. In addition, an overview of DNA binding proteins, their preparation and conjugation are presented in this chapter.

The first application of the proposed system is described in **Chapter 2.** A novel DNA sensing platform is designed based on a scCro DNA binding protein tag-HRP enzyme conjugate and a hybrid single stranded DNA-double stranded DNA (ssDNA-dsDNA) detection probe for the model ssDNA target high-risk human

papillomavirus (HPV16). The number of HRP molecules associated with each target DNA molecule is controlled by the number of DNA binding sites on the hybrid ssDNA-dsDNA detection probe and the ssDNA target is detected using an enzyme linked oligonucleotide assay with improved detection signal. The described platform serves as a proof of concept for the protein co-immobilization system. It is universal since the HRP-scCro protein conjugate can be used for the detection of any ssDNA target by changing only the ssDNA part of the hybrid ssDNA-dsDNA detection probe.

An alternative design of the protein co-immobilization system is demonstrated in **Chapter 3.** Two different DNA binding protein-enzyme conjugates are used together with a simple DNA nanostructure for the detection of ssDNA target, using again the HPV16 as model target. The DNA nanostructure, which is the hybrid ssDNA-dsDNA detection probe, performs two functions: its ssDNA part is complementary to the target sequence and serves for target recognition whereas the dsDNA part provides signal generation through the specific binding sites for the two different DNA binding protein tags of the enzyme conjugates. The two enzyme-DNA binding protein conjugates GOx-dHP and HRP-scCro form an enzymatic cascade which results in signal generation that does not require the external addition of hydrogen peroxide. The effect of enzyme ratio on the obtained signal is also examined by using different designs of the detection probe.

The possibility of using the protein co-immobilization system for non-nucleic acid targets such as proteins is demonstrated in **Chapter 4** by using DNA aptamers. This novel strategy requires a pair of aptamers (dual aptamers) which are modified in a way that each aptamer contains the specific dsDNA binding site for each of the GOx-dHP and HRP-scCro enzyme conjugates. One aptamer serves for target capturing, whereas the second one for detection in a sandwich-type aptasensor, where signal is generated as a result of the simultaneous binding of each enzyme conjugate to each modified aptamer sequence. This system was evaluated for thrombin detection and the limit of detection achieved was comparable to other systems reported in the literature. The possible use of this detection system in low resource settings at the point of care is also demonstrated by a preliminary paper-based, lateral flow assay.

A more detailed study on the use of DNA binding proteins in lateral flow assays is provided in **Chapter 5**. Here, a novel direct detection method of the target DNA sequence after PCR amplification is described utilizing the report system based on DNA binding proteins and specific dsDNA sequences in a lateral flow configuration. Direct detection of the target dsDNA PCR product without the need to generate ssDNA after the PCR step is achieved by incorporating the DNA binding sequence recognized by the DNA binding protein in the reverse PCR primer sequence. The forward primer is also modified with a label (Alexa Fluor 488) to enable target amplicon capture on the lateral flow strip by a specific monoclonal antibody binding the Alexa Fluor 488 label. Detection is accomplished using three different approaches: with a scCro/carbon nanoparticle conjugate (carbon black color), HRP-scCro enzyme conjugate (HRP precipitating red dye color) and HRP-scCro/carbon nanoparticle conjugate (carbon black plus HRP precipitating red dye color). The system is validated for the detection of Shiga-toxin producing *Escherichia coli* and low limits of detection are achieved.

This thesis concludes in **Chapter 6** with a summary and comments on the significance of the completed work and the future perspectives of this research.

LIST OF PUBLICATIONS

1) **Aktas G.B.,** Skouridou V., Masip L. “Novel signal amplification approach for HRP-based colorimetric genosensors using DNA binding protein tags”. Biosensors and Bioelectronics 2015, 74: 1005–1010.

2) **Aktas G.B.,** Skouridou V., Masip L. “Nucleic acid sensing with enzyme-DNA binding protein conjugates cascade and simple DNA nanostructures”. Analytical and Bioanalytical Chemistry 2017, 409:3623–3632.

3) **Aktas G.B.,** Skouridou V., Masip L. “Sandwich-type aptasensor employing modified aptamers and enzyme-DNA binding protein conjugates”. Analytical and Bioanalytical Chemistry 2019, 411: 3581–3589.

4) **Aktas G.B.,** Wichers J.H., Skouridou V., van Amerongen A., Masip L. “Nucleic acid lateral flow assays using a conjugate of a DNA binding protein and carbon nanoparticles”. Microchimica Acta 2019, 2019, 186: 426.

LIST OF ABBREVIATIONS

AuNPs	Gold nanoparticles
BSA	Bovine serum albumin
CNPs	Carbon nanoparticles
Da	Dalton; 1 Da = 1 g/mol
DNA	Deoxyribonucleic acid
DBP	DNA binding protein
dHP	Dimeric headpiece domain of *Escherichia coli* LacI repressor protein
dsDNA	Double stranded DNA
DTT	1,4-dithiothreitol
EDC	1-ethyl-3- (dimethylaminopropyl) carboiimide
ELAA	Enzyme-linked oligonucleotide assay
ELISA	Enzyme-linked immunosorbent assay
ELONA	Enzyme-linked oligonucleotide assay
GOx	Glucose oxidase
HPV	Human papillomavirus
HRP	Horseradish peroxidase
IgA	Human immunoglobulin A
K_D	Dissociation constant
LFA	Lateral flow assay
LFTS	Lateral flow test strips
LOD	Limit of detection
MALDI-TOF	Matrix-Assisted Laser Desorption/Ionisation-Time-Of-Flight

MS	Mass spectrometry
MW	Molecular weight
NALFA	Nucleic acid lateral flow assay
NALFIA	Nucleic acid lateral flow immunoassay
NC	Nitrocellulose
NHS	N-hydroxysuccinimide
PAD	Paper analytical devices
PBS	Phosphate-buffered saline
PBST	PBS plus 0.1% (v/v) Tween-20
PDB	Protein Data Bank
PCR	Polymerase chain reaction
pI	Isoelectric point
POC	Point of care
RT	Room temperature
SA	Streptavidin
SA-HRP	Streptavidin conjugated with horseradish peroxidase
scCro	Dimeric single-chain bacteriophage Cro repressor protein
SE	Standard error
SEM	Standard error of mean
SDS	Sodium dodecyl sulfate
ssDNA	Single strand DNA
TBA	Thrombin-binding aptamer
TCEP	Tris (2-carboxyethyl) phosphine
T_m	Melting temperature
TMB	3,3’,5,5’-tetramethylbenzidine

UV	Ultra violet
v/v	Volume by volume
w/v	Weight by volume

LIST OF FIGURES

CHAPTER 1: GENERAL INTRODUCTION

Figure 1.1: A general biosensor configuration. 8

Figure 1.2: Schematic diagram of biosensor detection methods. 9

Figure 1.3: Schematic diagram of label based biosensor. 10

Figure 1.4: Schematic diagram of fluorescent tagged target detection. 10

Figure 1.5: A) Gold and B) carbon nanoparticles with different ligand modification onto their surfaces, such as DNA and proteins. 12

Figure 1.6: Physical adsorption onto biosensor surface. 14

Figure 1.7: Covalent linking of proteins to a surface. 15

Figure 1.8: Bioaffinity-based protein immobilization. 17

Figure 1.9: Difference between A) random and B) orientated protein immobilization 17

Figure 1.10: Schematic diagram of proposed immobilization system with multiple DNA binding sites on dsDNA 19

Figure 1.11: Origins of DNA-protein binding specificity. 20

Figure 1.12: Scheme of the overall complex of Cro with the operator DNA sequence 21

Figure 1.13: A) LacI DNA binding protein tetramer and B) LacI headpiece binding to its operon (PDB code:1cjg) 22

Figure 1.14: Possible approaches to link target proteins and DNA binding tags.23

Figure 1.15: Conjugation of proteins through genetic fusion 23

Figure 1.16: Protein ligation mechanism of Sortase A 24

CHAPTER 2: NOVEL SIGNAL AMPLIFICATION APPROACH IN GENOSENSORS BASED ON DNA BINDING PROTEIN TAGS

Figure 2.1: (A) Genosensor signal amplification approaches using (i) a detection ssDNA probe conjugated to HRP and (ii) an HRP-DNA binding protein conjugate in combination with hybrid ssDNA-dsDNA detection probes containing one and (iii) three DNA binding sites. (B) Hybrid ssDNA-dsDNA detection probe containing three scCro DNA binding sites (in dark green) with HRP-scCro conjugate bound. The target detection ssDNA part is shown in red and the dsDNA part in light green 43

Figure 2.2: Preparation of the HRP-scCro conjugate. (A) Expression and purification of cys-scCro. Lane 1: *E. coli* soluble lysate; lane 2: IMAC elution fraction; lane 3: cation exchange elution fraction. (B) Synthesis and purification of the HRP-scCro conjugate. Lane 1: maleimide-HRP; lane 2: cys-scCro; lane 3: HRP-scCro conjugation reaction; lane 4: IMAC elution fraction; lane 5: affinity chromatography elution fraction after concentration with 50K MWCO centrifugal filter. (C) Western blot for the HRP-scCro conjugation reaction. Lane 1: maleimide-HRP; lane 2: cys-scCro; lane 3: HRP-scCro conjugation reaction. 50

Figure 2.3: EMSA assay for the binding of the HRP-scCro conjugate to the HPV16 detection probes with one and three DNA binding sites. Bands with asterisks correspond to protein-DNA complexes 52

Figure 2.4: Target DNA calibration curves using a (i) ssDNA-HRP conjugate and (ii) HRP-scCro conjugate with detection probes containing one and (iii) three DNA binding sites. The error bars show the standard error of the mean (SEM). 54

Figure 2.5: Specificity of the genosensor using HPV16 target and control DNA sequences. Detection was achieved with (i) ssDNA-HRP conjugate and (ii) with the HRP-scCro conjugate in combination with detection probes containing one and (iii) three DNA binding sites. The error bars show the standard error of the mean (SEM). 55

Figure S-2.1: Preparation of the hybrid ssDNA-dsDNA HPV16 detection probes. Lane 1: detection probe with one DNA binding site; lane 2: detection probe with one DNA binding site partial complementary strand; lane 3: hybridization reaction of ssDNA oligos in lanes 1 and 2; lane 4: detection probe with three DNA binding sites; lane 5: detection probe with three DNA binding sites partial complementary strand; lane 6: hybridization reaction of ssDNA oligos in lanes 4 and 5. Lanes 1, 2, 4, 5 contain ssDNA whereas lanes 3 and 6 hybrid ssDNA-dsDNA 63

Figure S-2.2: Binding of scCro to the oligonucleotides used for the detection of HPV16 by EMSA. Lane 1: capture probe with target; lane 2: target with detection probe; lane 3: target with detection probe with one DNA binding site (ssDNA oligo); lane 4: target with detection probe with one DNA binding site (ssDNA-dsDNA hybrid); lane 5: capture probe with target and detection probe with one DNA binding site oligo (ssDNA oligo); lane 6: capture probe with target and detection probe with one DNA binding site (ssDNA-dsDNA hybrid). Bands with asterisks show protein-bound DNA 64

Figure S-2.3: Optimization of the HRP-scCro conjugation reaction. Lane 1: maleimide-HRP; lane 2: cys-scCro; lane 3: maleimide-HRP:cys-scCro molar ratio 1:1 (50 μM each); lane 4: maleimide-HRP:cys-scCro molar ratio 3:1 (60 μM:20 μM); lane 5: maleimide-HRP:cys-scCro molar ratio 1:3 (32 μM:96 μM) 65

Figure S-2.4: MALDI-TOF mass spectra of maleimide-HRP and HRP-scCro conjugate. 66

CHAPTER 3: NUCLEIC ACID SENSING WITH ENZYME-DNA BINDING PROTEIN CONJUGATES CASCADE AND SIMPLE DNA NANOSTRUCTURES

Figure 3.1: (A) Detection of target ssDNA based on DNA binding proteins-enzyme conjugates. (B) Hybrid ssDNA-dsDNA detection probes with scCro/dHP DNA binding sites stoichiometry of 1:1, 2:1 and 1:2. The binding sites (highlighting the nucleotide bases that directly participate in the dsDNA-protein interactions) for scCro are shown in green and for dHP in blue 72

Figure 3.2: Preparation of the GOx-dHP conjugate. (A) SDS-PAGE for the conjugation and purification of GOx-dHP. 1: cys-dHP; 2: GOx; 3: maleimide-GOx; 4: GOx-dHP conjugation reaction; 5: IMAC elution fraction; 6: IEC elution fraction. (B) Detection of conjugate by Western blot. 1: cys-dHP; 2: GOx; 3: maleimide-GOx; 4: GOx-dHP conjugation reaction. (C) Native PAGE. 1: GOx; 2: maleimide-GOx; 3: GOx-dHP conjugate. (D) MALDI-TOF mass spectroscopy spectra of GOx and GOx-dHP purified conjugate........ 81

Figure 3.3: EMSA assay for the binding of the DNA binding protein-enzyme conjugates to the HPV16 hybrid detection probe with scCro/dHP DNA binding sites ratio of 1:1. All lanes 1-9 contain the DNA detection probe with different protein species. Lane 1: only DNA; lane 2: HRP; lane 3: GOx; lane 4: cys-scCro; lane 5: HRP-scCro; lane 6: cys-dHP; lane 7: GOx-dHP; lane 8: cys-scCro and cys-dHP; lane 9: HRP-scCro and GOx-dHP........ 83

Figure 3.4: DNA detection with ELONA. (A) Optimization of capture probe concentration. (B) Optimization of detection probe concentration. (C) Optimization of the addition order of the enzyme-DNA binding protein conjugates. The error bars show the standard error of the mean (SEM) from triplicate samples. (D) Target calibration curves using detection probes with scCro/dHP DNA binding sites ratio of 1:1, 2:1 and 1:2. The error bars show the SEM from triplicate samples and three independent experiments........ 86

Figure 3.5: Specificity of the sensing platform. Detection of different target ssDNA molecules was performed using the detection probes with scCro/dHP DNA binding sites ratio of 1:1, 2:1 and 1:2. The error bars show the SEM from triplicate samples 88

Figure S-3.1: SDS-PAGE analysis for the expression and purification of cys-dHP. (A) IMAC purification. 1: *Escherichia coli* soluble fraction; 2: flowthrough fraction; 3-4: wash fractions; 5: elution fraction. (B) IEC purification. 1: IMAC elution fraction after buffer exchange; 2: flowthrough fraction; 3: wash fraction; 4: elution fraction. 97

Figure S-3.2: Agarose gel electrophoresis for the preparation of the HPV16 detection probes with different binding sites stoichiometries. 99

CHAPTER 4: SANDWICH-TYPE APTASENSOR EMPLOYING MODIFIED APTAMERS AND ENZYME-DNA BINDING PROTEIN CONJUGATES

Figure 4.1: The proposed aptamer-based sandwich-type system for target detection via modified dual aptamers and HRP-scCro and GOx-dHP enzyme-DNA binding protein conjugates 108

Figure 4.2: Binding of different protein species to the modified thrombin aptamers by EMSA. Lane 1: Capture aptamer P106 (TBA15-1xCro); lane 2: P106 + scCro; lane 3: P106 + thrombin; lane 4: P106 + scCro + thrombin; lane 5: detection aptamer P96 (1xLacI-TBA29); lane 6: P96 + dHP; lane 7: P96 + thrombin; lane 8: P96 + dHP + thrombin 116

Figure 4.3: Aptamer-based target detection with Enzyme Linked Aptamer Assay. a) Choice of capture aptamer. b) Optimization of capture aptamer concentration. c) Optimization of the detection aptamer concentration. d) Optimization of the enzyme-DNA binding protein conjugates concentration. The error bars show the standard deviation from triplicate samples. 117

Figure 4.4: Target calibration curves using detection aptamers with one or two LacI DNA binding sites. The error bars show the standard deviation from triplicate samples and three independent experiments. ... 119

Figure 4.5: Lateral flow assay for thrombin detection with enzyme-DNA binding protein conjugates. Lane 1-2-3: Negative control (triplicate); lane 4-5-6: Positive control (triplicate). ... 120

Figure S-4.1: Agarose gel electrophoresis for the preparation of the detection aptamer with 2xLacI binding sites. Lane 1: Detection aptamer with two LacI DNA binding sites (P109); lane 2: Complementary to P109 (P110); lane 3: Hybridization reaction of P109 + P110. ... 126

CHAPTER 5: PAPER-BASED DETECTION OF SHIGA TOXIN-PRODUCING *ESCHERICHIA COLI* USING CARBON NANOPARTICLES-DNA BINDING PROTEIN CONJUGATES

Figure 5.1: Scheme of different approaches on the control line NALFA test for the Shiga toxin-producing *E. coli* detection: a) scCro/carbon nanoparticles; b) HRP-scCro enzyme conjugate; and c) HRP-scCro/carbon nanoparticles conjugate.... 134

Figure 5.2: PCR amplified *E. coli* 16S rRNA gene detection by ELISA for one or two scCro DNA binding site ... 141

Figure 5.3: Detection of the PCR amplicon with 1x and 2xCro binding sites on NALFA strips using the scCro/CNPs conjugate. ... 142

Figure 5.4: Detection of the PCR amplicon with 1x and 2xCro binding sites on NALFA strips using the HRP-scCro enzyme conjugate ... 144

Figure 5.5: Detection of the PCR amplicon with 1x and 2xCro binding sites on NALFA strips using the HRP-scCro/CNPs enzyme conjugate ... 146

Figure S-5.1: Agarose gel electrophoresis of the PCR reactions for *E. coli* 16S rRNA target gene amplification with Alexa Fluor 488-labeled forward primer and (A) unlabeled reverse primer, (B) reverse primer with 1xCro binding site, and (C) reverse primer with 2xCro binding sites. Lanes 1, 3, 5 represent the PCR controls and lanes 2, 4, 6 the PCR reactions with genomic DNA template. 153

Figure S-5.2: NALFA strips for PCR amplicon detection using HRP-scCro/CNPs before HRP substrate addition and color development 158

LIST OF TABLES

CHAPTER 1: GENERAL INTRODUCTION

Table 1.1: Reactive functional groups in naturally occurring aminoacids. 25

CHAPTER 2: NOVEL SIGNAL AMPLIFICATION APPROACH IN GENOSENSORS BASED ON DNA BINDING PROTEIN TAGS

Table S-2.1: Sequences of the oligonucleotides used in this work. The specific DNA binding sites for scCro protein are underlined. The length of the oligos is shown in nucleotides (nt). 61

Table S-2.2: Ion species of the proteins analyzed by MALDI-TOF MS. 66

CHAPTER 3: NUCLEIC ACID SENSING WITH ENZYME-DNA BINDING PROTEIN CONJUGATES CASCADE AND SIMPLE DNA NANOSTRUCTURES

Table S-3.1: Primers used for the construction of pVS16.. 96

Table S-3.2: Oligonucleotides used for the preparation of the HPV16 detection probes. The target complementary part is denoted in bold, the HRP-scCro binding sites are shown in italics and the GOX-dHP binding sites are underlined................ 98

Table S-3.3: Ion species and corresponding mass for GOx and GOx-dHP conjugate. mGOx corresponds to GOx enzyme monomer and dGOx corresponds to the homodimer. 100

Table S-3.4: Sequences of oligonucleotides used for DNA detection with ELONA... 101

CHAPTER 4: SANDWICH-TYPE APTASENSOR EMPLOYING MODIFIED APTAMERS AND ENZYME-DNA BINDING PROTEIN CONJUGATES

Table 4.1: Oligonucleotides used for thrombin detection. The thrombin aptamer sequences are in bold, the binding site for HRP-scCro in italics and for GOX-dHP underlined. 110

Table S-4.1: Comparison of various colorimetric detection approaches employed for thrombin detection. 127

CHAPTER 5: PAPER-BASED DETECTION OF SHIGA TOXIN-PRODUCING *ESCHERICHIA COLI* USING CARBON NANOPARTICLES-DNA BINDING PROTEIN CONJUGATES

Table 5.1: Primer sequences used in this work. The scCro DNA binding site(s) are underlined… 137

Table 5.2: Detection limits achieved by ELISA and NALFA. 146

Table S-5.1: ELISA calibration curve results and statistics for the PCR amplicons with (A) 1xCro and (B) 2xCro DNA binding sites. Each replicate corresponds to the average of triplicate sample from three independent experiments, while the sextuplets were used for the blank sample. 154

Table S-5.2: PCR amplicon detection by NALFA using scCro/CNPs. Calibration curve results and statistics for (A) 1x Cro and (B) 2x Cro DNA binding sites. Data shows three independent replicates. 155

Table S-5.3: PCR amplicon detection by NALFA using HRP-scCro. Calibration curve results and statistics for (A) 1x Cro and (B) 2x Cro DNA binding sites. Data shows three independent replicates. 156

Table S-5.4: PCR amplicon detection by NALFA using HRP-scCro/CNPs. Calibration curve results and statistics for (A) 1x Cro and (B) 2x Cro DNA binding sites. Data shows two independent replicates. 157

Chapter 1

General introduction

Chapter 1: General introduction

1.1 DETECTION METHODS IN BIOSENSORS

Biosensors are analytical devices that convert a biological response due to the presence of an analyte to a detection signal. They have a wide range of applications such as medical diagnostics, drug discovery, food safety, process control and environmental monitoring among others [1]. A biosensor is comprised of the bioreceptor, the transducer and the signal producing elements (Fig. 1.1). The bioreceptor element is responsible for the detection of the analyte and can include organelles, tissues, cell receptors, microorganisms, enzymes, antibodies, antigens, nucleic acids and others. An important step in the development of biosensors is the method used to generate a signal from the detection event of the analyte by the bioreceptor.

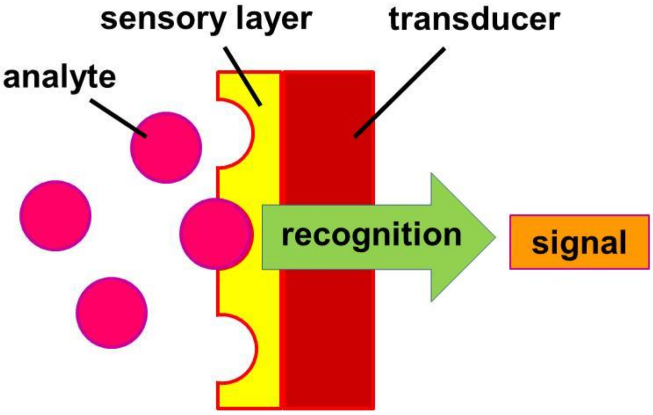

Figure 1.1: A general biosensor configuration.

Several methods have been developed for this signal generation step based on different kinds of processes, such as electrochemical, optical, piezoelectric, radioactive, and others [2]. These methods can be divided in two main groups: label-free and label-based (Fig. 1.2). Label-free technologies have the advantage that the analyte can be observed directly without the use of any labeling but require expensive instruments and trained personnel to perform the experiments and analyze the data [3]. Examples of label-free techniques include mass spectrometry, microcantilevers, surface plasmon resonance (SPR), isothermal titration calorimetry (ITC), surface acoustic wave sensors and differential scanning calorimetry (DSC).

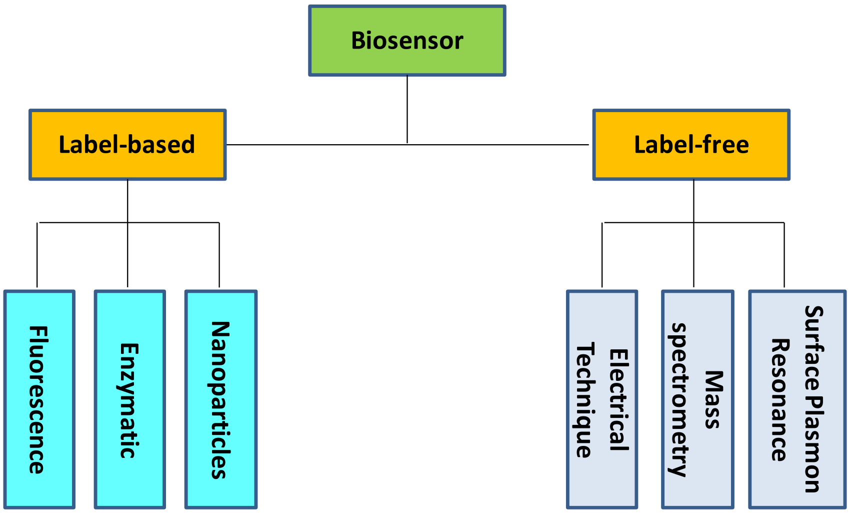
Biosensor
Label-based
Label-free
Fluorescence
Enzymatic
Nanoparticles
Electrical Technique
Mass spectrometry
Surface Plasmon Resonance

Figure 1.2: Schematic diagram of biosensor detection methods.

On the other hand, label-based biosensors in general do not require high cost equipment and in some cases can be integrated as point-of-care (POC) sensors because they can be assessed by naked-eye. Label-based techniques utilize tags that are attached to the analyte (either covalently or non-covalently) for detection. The most common types of labels are fluorescent, enzymatic and nanoparticles (Fig. 1.3).

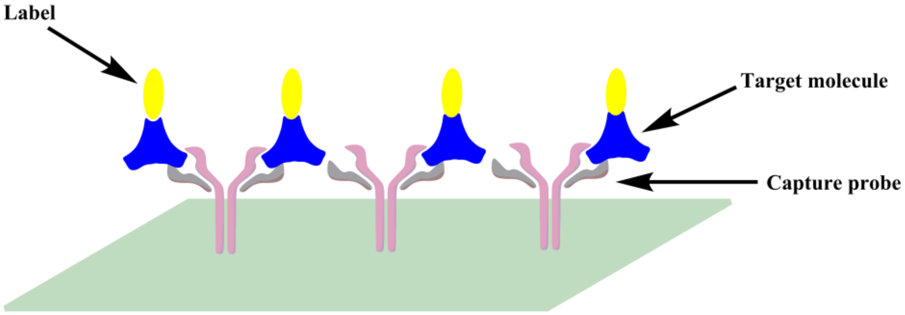

Figure 1.3: Schematic diagram of label based biosensor.

1.1.1 Fluorescent labeling

Fluorescence probes are generally preferred for target labeling since they are stable, easy to manipulate, and provide a sensitive signal. Different types of fluorescent molecules respond to different wavelengths and can be easily detected as different colors [4]. The main advantage of fluorescent dyes lies in the lack of need to add any substrate, unlike in the case of enzymes [5]. However, light exposure is usually needed to excite the fluorophore (Fig. 1.4). Additionally, fluorescent dyes are sensitive to environment conditions such as light, pH, temperature and solvents [6].

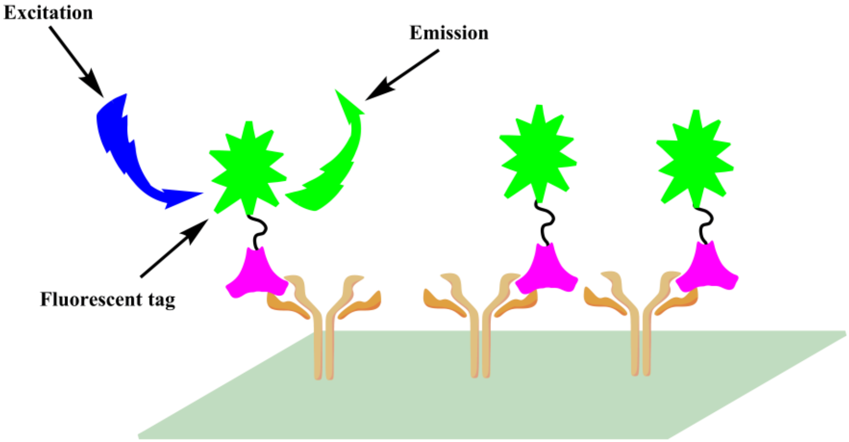

Figure 1.4: Schematic diagram of fluorescent tagged target detection.

1.1.2 Nanoparticle labeling

Nanoparticles have unique optical and electronic properties that make them very suitable for labeling applications [7]. In addition, they allow the immobilization of a large number of detection biomolecules and these results in an increased detection sensitivity and lower target detection limit. Gold nanoparticles (AuNPs) are one the most utilized noble metal nanoparticles for biosensor applications. They are easy to prepare and modify and are compatible with biomolecules. AuNPs can be modified through covalent linking via sulfide bonds (thiol to gold) as well as by physical adsorption. These nanoparticles have been used for coupling to different types of molecules such as proteins [8,9], DNA [10-12], toxic compounds [13] and peptides [14] and a wide variety of colorimetric biosensors have been developed [15].

Carbon based nanoparticles are another common type that provide an easy and well documented functionalization by adsorption of the molecule on the surface. Studies show that carbon nanoparticles labeling provides good sensitivity even for naked-eye detection [16]. Colloidal carbon nanoparticles usually are polydispersed contrary to gold nanoparticles that are monodispersed (Fig. 1.5).

Other types of nanoparticles also exist such as magnetic nanoparticles [17,18], quantum dots [19] and silver nanoparticles that have been developed and utilized in various biosensor sensing platforms [20].

One of the main disadvantages of nanoparticles is their big size compared to the target that can cause steric hindrance effects and prevent efficient binding to the target.

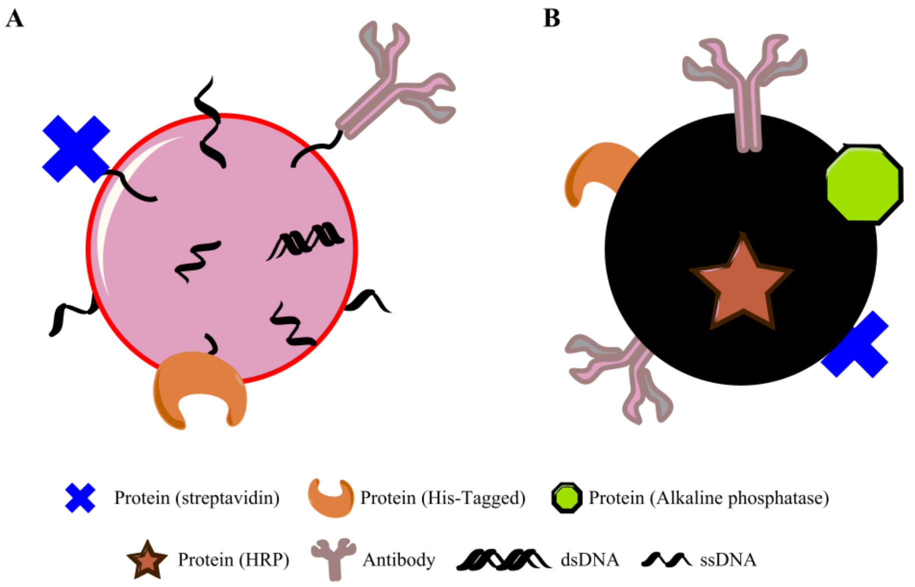

Figure 1.5: A) Gold and B) carbon nanoparticles with different ligand modification onto their surfaces, such as DNA and proteins.

1.1.3 Enzyme labeling

Enzymes are often used for the detection of analytes providing high sensitivity and specific signal generation. Enzyme-based biosensors are among the most widely used ones [21], with the enzymatic glucose biosensors, used for the simple self-monitoring of blood glucose levels, being one of the main examples [22,23]. This type of biosensor uses oxidoreductase enzymes coupled with an electrochemical detection system where an electron transfer process, which is a function of glucose concentration, is quantified [24]. Enzymes have not only been used for electrochemical detection but also for colorimetric. Furthermore, optical and electrochemical biosensors employ enzymes as labels that can be used as tags for signal generation to detect the target of interest. In some cases, enzyme-based biosensors can incorporate nanoparticles for enhanced sensitivity.

Horseradish peroxidase (HRP) is one of the most widely used enzymes for detection because of the straightforward catalytic reaction, small size and high stability. HRP is an oxidoreductase enzyme that uses hydroperoxides as electron acceptor. By means of a redox reaction with redox active molecules that change color, it can easily generate a signal that can be read [25]. A typical example of the utilization of HRP as a label is the detection of ssDNA where a detection probe complementary to the target ssDNA is conjugated to HRP [26,27].

1.2 PROTEIN IMMOBILIZATION

Many of the signal generation methods described above employing labels require the immobilization of a protein. This immobilization may be to a surface, such as the immobilization of an enzyme on the surface of an electrode or an antibody on the surface of a nanoparticle. A different type of immobilization is the union of a reporter to a detection molecule, for example the linking of ssDNA detection molecule to a reporter enzyme such as HRP. The most common types of protein immobilization methods used in the context of biosensors are described next [28].

1.2.1 Physical adsorption

Physical adsorption involves hydrogen bonding, van der Waals forces, electrostatic forces and/or hydrophobic interactions between the protein and the surface. This approach is widely utilized in biosensors because it is easy to perform and at a low cost.

Simple and robust sensing platforms can thus be produced through physical adsorption and used in biosensors [29]. Adsorption results in random orientation of the immobilized protein on the surface (Fig. 1.6). The immobilization process can be reversed by changing the conditions such as pH, ionic strength, temperature, or polarity of the solvent. However, immobilized proteins preserve their function due to the minimum modifications caused by the physical adsorption process.

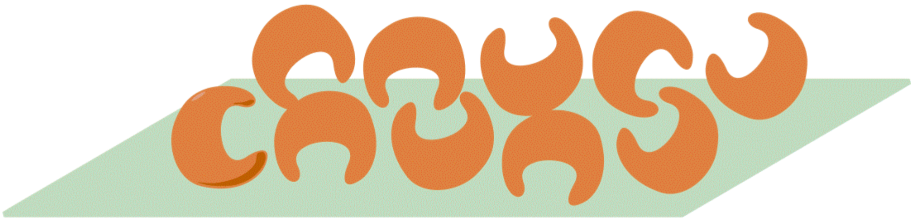

Figure 1.6: Physical adsorption onto biosensor surface.

The physical characteristics of the biosensor matrices determine the performance and conditions of the immobilized protein [30]. Depending on the protein charge and the polarity, various matrices can be chosen: nitrocellulose membranes or polystyrene microtiter plates for hydrophobic adsorption and polylysine-coated slides for electrostatic binding. Due to the non-covalent nature of the immobilization, the protein can leach out from the matrix depending on the interaction strength and result in loss of activity over time. Moreover, since there is no control mechanism for the density of the immobilized proteins on the surface, their activity may be further reduced by steric hindrance effects [31,32].

1.2.2 Covalent binding

Direct covalent linking of proteins to surfaces or other molecules occurs through the chemical reaction with the side groups of the protein's amino acids, like, lysine, cysteine, aspartic acid and arginine. Lysine aminoacids are abundantly present in proteins and can be exposed 6% to 10% over the protein surface [33,34] and they can provide stable chemical linking. On the other hand, cysteine contains a reactive thiol group that can form a disulfide bond. Opposite to the lysine case, cysteine is less commonly present or exposed on the surface of proteins [35]. The side chains of the glutamic and aspartic acid contain a carboxyl group that reacts with amines using the routine coupling chemistry [36].

There are many ways in which the biosensor surface can be modified with reactive groups, such as carboxyl, maleimide, amine, iodoacetamide and isothiocyanate groups to react with the amine, thiol, carboxyl, or carbonyl groups of the proteins to allow for a higher specific activity and stability with controlled protein orientation[29,37,38]. Because covalent binding is usually an irreversible process, proteins immobilized using this approach is stable and do not detach easily from the surface even after multiple utilization cycles of the biosensor.

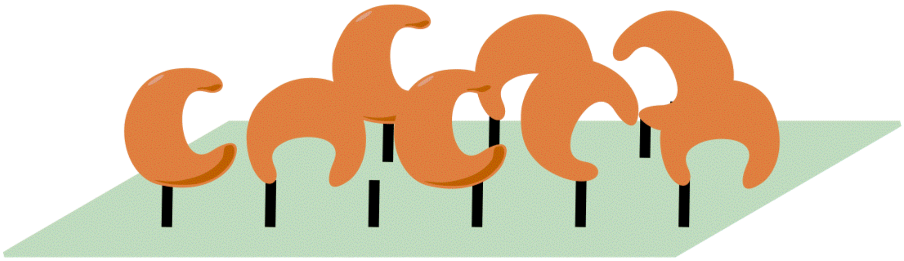

Figure 1.7: Covalent linking of proteins to a surface.

As in the case of physical adsorption, random orientation may also occur if the desired protein has multiple reactive groups on its surface. Thus, covalent binding also suffers from a heterogeneous distribution of protein orientation and this may result in a reduction of activity of the immobilized protein or accessibility to targets in the solution phase [39,40]. Furthermore, the conjugation of a protein aminoacid may also directly affect protein activity and stability [41,42].

In some cases the random orientation can be eliminated with site-specific covalent immobilization through a single engineered surface exposed reactive group. Two unique and mutual reactive groups on protein and surface are needed for this process [43-45].

1.2.3 Bioaffinity interactions

Over the years, a number of protein-protein and protein-small molecule binding interactions have been discovered. The development of bioanalytical assays based on bioaffinity goes back to the early 1960s [46]. Taking advantage of the bioaffinity interactions, a number of proteins have been immobilized onto surfaces by pairing the protein and surface with the respective pair of interaction elements (Fig. 1.8).

Some examples of well known bioaffinity interactions commonly used are (strept)avidin/biotin [47,48], polyhistidine-tag/transition metal ions [49,50], host/guest system [51] and antibody/antigen based interaction [52]. The (strept)avidin/biotin interaction is the strongest bioaffinity interaction that has been discovered, with a dissociation constant of $K_D=10^{-15}$ M. Typically, the surface of a biosensor is modified by introducing biotin groups or (strept)avidin that in turn bind to (strept)avidin or biotin-modified proteins respectively.

Histidine is an aminoacid that exists naturally in proteins and can be engineered at a protein terminal end to interact with immobilized metal ion matrices. The electron donor groups on the histidine imidazole ring readily form coordination bonds with the immobilized transition metal.[53] This method is based on adding a histidine motif (at least six) to the protein of interest that provide a strong interaction to a nickel- or cobalt-coated surface usually by means of an immobilized chelator [38]. One of the limitations is low affinity and specificity due to the existence of other naturally occurring proteins that also display affinity to nickel nitrilotriacetic acid (Ni-NTA) resin. In certain applications this limitation can complicate the specificity of the immobilization procedure [54].

In the antibody-based interaction, protein A is the most widely used protein for the direct immobilization of antibodies due to its strong interaction with the Fc region of immunoglobulins. This interaction with the Fc still allows the antibodies to bind their corresponding antigen targets [38].

The orientation of a protein immobilized through affinity interactions depends on the stoichiometric relationship between affinity elements and ligands that can result in random orientation. In case of the streptavidin/biotin interaction, streptavidin has four biotin binding sites and as a result, the orientation cannot be controlled.

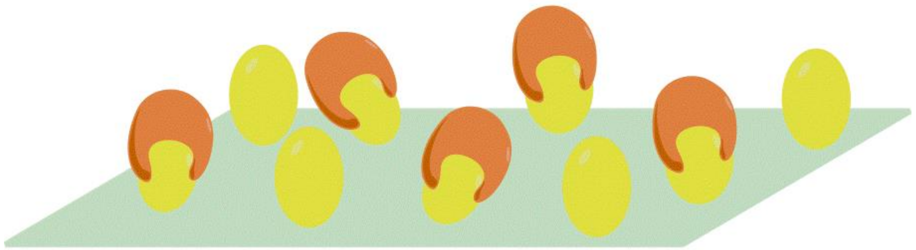

Figure 1.8: Bioaffinity-based protein immobilization.

It is known that controlling the orientation and coupling of different proteins is critical for the optimal biosensor functionality (Fig. 1.9) [55]. Current techniques cannot formulate a general immobilization strategy for controlled co-immobilization in a simple and straightforward way.

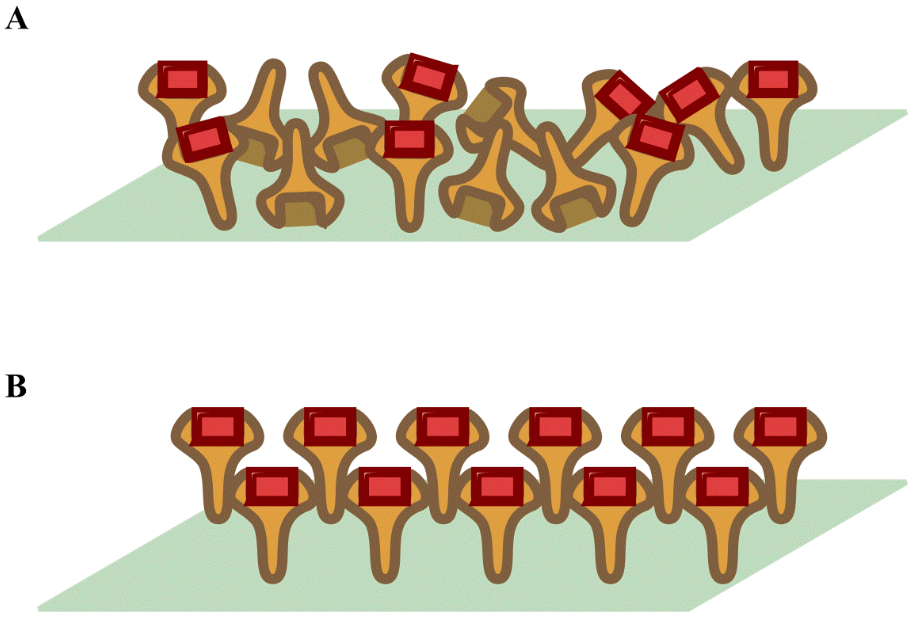

Figure 1.9: Difference between A) random and B) orientated protein immobilization.

1.2.4 Novel affinity-based protein immobilization approach

An additional immobilization approach through bioaffinity is the use of DNA scaffolds to immobilize proteins. One recent example is to use a protein-ssDNA conjugate to immobilize onto a biosensor surface that is covered with the complementary ssDNA sequence [56]. This approach provides a stable and universal biosensor surface based on the high specificity of dsDNA base pairing. The drawback is the requirement of the laborious ssDNA labeling of proteins.

The development of an alternative bioaffinity immobilization approach is the aim of this thesis. The proposed system is based on dsDNA scaffolds to direct organized protein immobilization, by exploiting the highly specific interaction protein/dsDNA that some proteins posses (Fig. 1.10). This method does not need direct conjugation of DNA to a protein. Therefore, sequence specific DNA binding proteins can be used as tags, of the protein of interest to immobilize, that bind to specific sequences of dsDNA with high affinity. This approach allows the easy control of the protein co-immobilization pattern by specifying the distribution of the sequence binding sites of these DNA binding proteins on the dsDNA scaffold. No modification is required of the dsDNA scaffolds, they just need to be designed to contain specific sequences at the desired positions of the DNA binding proteins. This approach is not limited to a single DNA binding protein, the use of multiple DNA binding protein tags with different sequence specificities can also be utilized to obtain co-immobilization of multiple proteins in a specific pattern. This novel methodology not only can be used on the biosensor surface but also as part of the detection element of the biosensor.

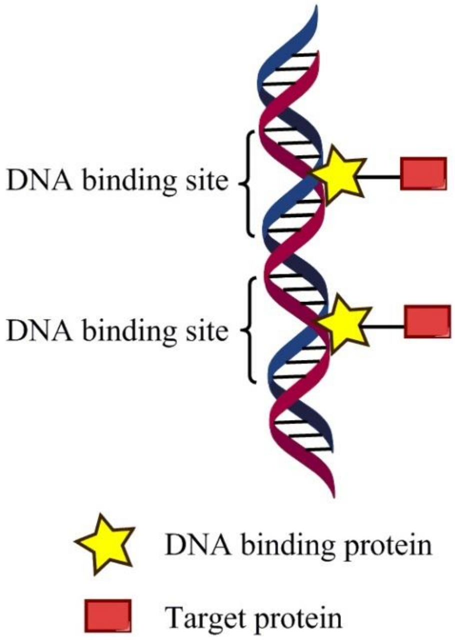

Figure 1.10: Schematic diagram of proposed immobilization system with multiple DNA binding sites on dsDNA.

1.3 DNA BINDING PROTEINS

DNA binding proteins (DBPs) are proteins that have affinity for DNA molecules. These proteins can bind to double or single stranded DNA with sequence specificity or not. DNA binding proteins have different functions *in vivo* to regulate cellular processes such as transcription, translation, gene silencing, microRNA biogenesis and telomere maintenance [57]. DNA-protein binding originated specifically or non-specifically from polymerases and histones. Specific protein-DNA binding is essential for the cells and the organelles, and there has been extensive research in protein-DNA recognition. Proteins utilize specific DNA binding structural motifs to recognize DNA, such as the helix-turn-helix (HTH), homeodomains and other three-dimensional structures of both macromolecules and are bound by a set of hydrogen bonds, electrostatic and non-polar interactions [58]. Furthermore, the specific protein-DNA interactions originate from the base pairs that create a specific DNA structure that is subsequently recognized by the DNA binding protein [59]. Fundamentally, DNA-protein binding mechanisms occur via the recognition of bases and the recognition of DNA shape (Fig. 1.11.). Even though most proteins bind to the major groove of the dsDNA double helix, there are exceptions such as TATA box binding protein and HMG-box proteins [60].

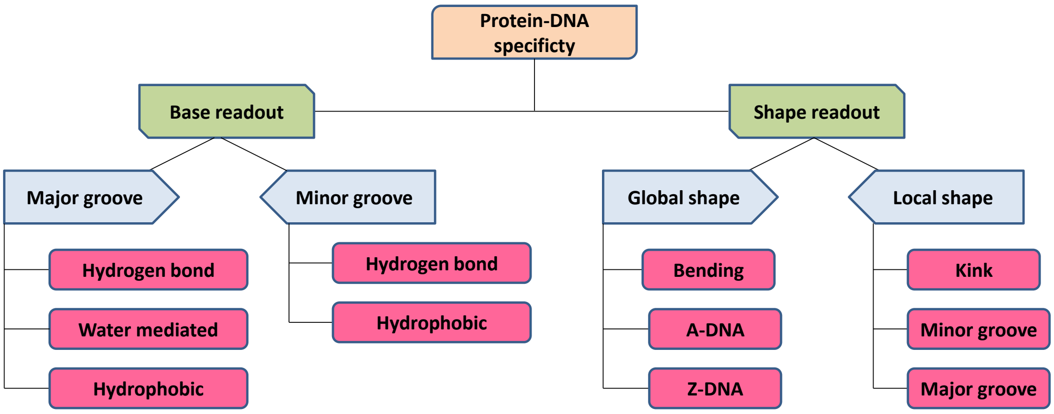
Protein-DNA specificty
Base readout
Shape readout
Major groove
Minor groove
Global shape
Local shape
Hydrogen bond
Water mediated
Hydrophobic
Hydrogen bond
Hydrophobic
Bending
A-DNA
Z-DNA
Kink
Minor groove
Major groove

Figure 1.11: Origins of DNA-protein binding specificity [58].

More than 1500 protein-DNA structures have been deposited in the Protein Data Bank (PDB). The first protein-DNA complexes that have been crystallized and widely investigated are for the Cro repressor [61], λ repressor [62] and Lac repressor headpiece [63] bound to their respective DNA operator sequences.

1.3.1 scCro DNA binding protein

The Cro repressor is a homodimeric DNA binding protein that binds to its operator DNA with very high affinity and specificity [64]. The Cro DNA binding protein has an essential role in bacteriophage λ in gene regulation by turning off early gene transcription during lytic growth [65]. Cro protein is one of first sequence specific DNA binding proteins for which three-dimensional structures were determined [66] (Fig. 1.12).

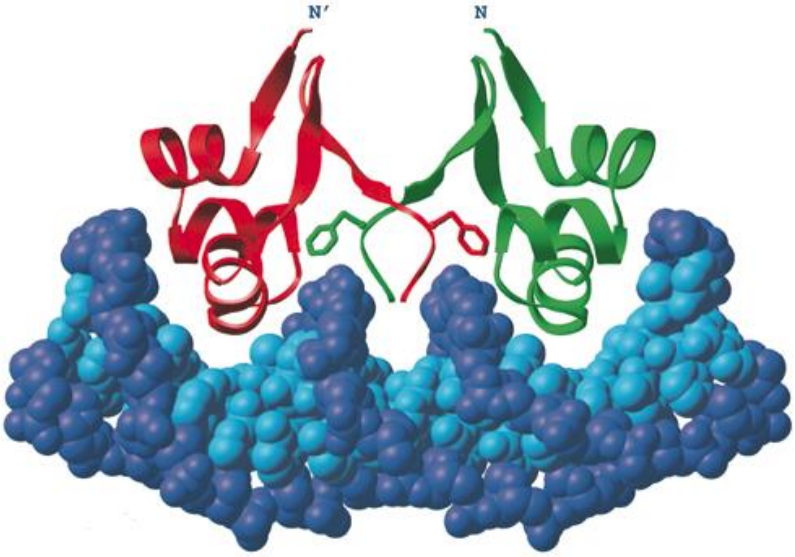

Figure 1.12: Scheme of the overall complex of Cro with the operator DNA sequence [66].

The three-dimensional structure shows that the DNA is bent by 40° through the 19 base-pairs after Cro binding. Hydrogen-bonding and van der Waals contacts within the major groove of the DNA play a role in the recognition and binding of the Cro helix-turn-helix units and its operator [67].

The wild type Cro repressor of bacteriophage λ binds to a 17-bp operator dsDNA as a dimer of two identical 66 residue subunits [68,69]. A single chain version was developed by linking two Cro monomers through a flexible linker (8 or 16 residues) [70]. These versions of the Cro dimer displayed increased affinity to its operator. The dimer Cro with the 16 aminoacid linker (single chain cro, scCro16) resulted in a dissociation constant in the picomolar range, $(4\pm2) \times 10^{-12}$ M, on the 5’-TATCACCGCAAGTGATA-3’ double stranded sequence [70].

1.3.2 LacI headpiece binding protein

LacI is a lactose repressor protein that binds to the promoter of the lac operon to regulate the expression of lactose metabolic genes in *Escherichia coli* [63].

The LacI repressor is a tetramer with 360 aminoacids per subunit which has two differenciated domains: the core and the DNA binding region known as headpiece (Fig. 1.13 (A)). The N-terminal headpiece domains are responsible for DNA binding whereas the inducer binding site is located in the tetrameric core [71].

The wild type lacI headpiece unit binds to a 23 base-pair dsDNA (5'-GAATTGTGAGCGGATAACAATTT- 3') in the major groove of the DNA [72] while the minor groove modulates the hinge helix stability (Fig. 1.13 (B)). Combined structural and biochemical studies demonstrated the headpiece region contains a helix-turn-helix motif responsible for DNA-binding.

It is known that dimerization increases the stability and strengthens protein–protein and protein–DNA interactions [73-75]. Therefore, a Cys52–Cys529 disulfide bond in the hinge region of Lac-HP62 (the first 62 residues of the Lac headpiece) was engineered to increase the binding affinity and stability of the LacI headpiece-DNA complex. Covalent linking of the headpiece monomers through a disulfide bond resulted in enhanced binding affinity towards the operator, four orders of magnitude higher than the wild type monomeric form [76].

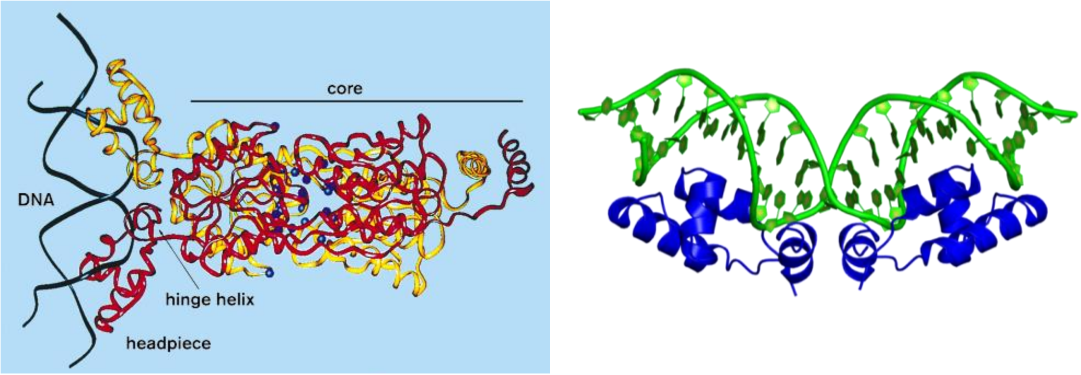

Figure 1.13: A) LacI DNA binding protein tetramer [77] and B) LacI headpiece binding to its operon (PDB code:1cjg) [63].

1.3.3 Methods to prepare protein-protein conjugates

An important step for the proposed system is the linking of the target proteins to the DNA binding protein tags. Several methods exist to conjugate two proteins (Fig. 1.14).

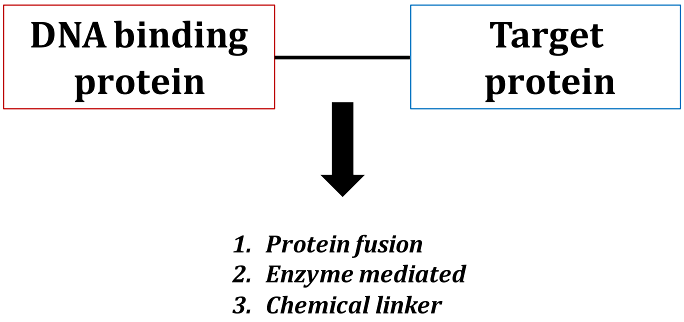
DNA binding protein
Target protein
1. Protein fusion
2. Enzyme mediated
3. Chemical linker

Figure 1.14: Possible approaches to link target proteins and DNA binding tags.

A possible alternative way to conjugate the target protein to DNA binding protein tags is genetic fusion and the subsequent expression (Fig. 1.15). An important advantage of this approach is that it does not require chemical modification since the fusion protein is directly produced [78]. Nonetheless, protein aggregation (insolubility) may arise due to folding issues of the two linked proteins [79,80].

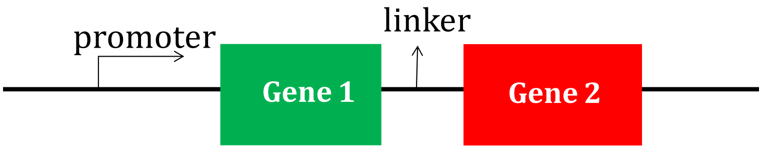
promoter
linker
Gene 1
Gene 2

Figure 1.15: Conjugation of proteins through genetic fusion.

An example of an enzyme based approach for the conjugation of two proteins is the Sortase A enzyme. It is a post-translational *in vitro* protein ligation system that meditates the covalent ligation between LPETG and GGG aminoacid motifs (Fig. 1.16). *Staphylococcus aureus* Sortase A is a bacterial transpeptidase that naturally attaches proteins to the bacterial cell wall by cleaving between threonine and glycine at an LPXTG recognition motif reacting with an N-terminal glycine, regenerating a native amide bond [81]. This approach has been increasingly exploited due to its high specificity [82]. This method requires the cloning of specific amino acid sequences on the proteins to be conjugated.

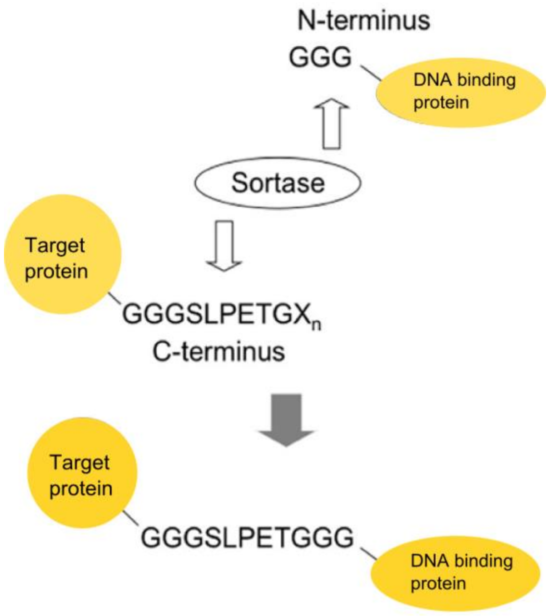
N-terminus
GGG
DNA binding protein
Sortase
Target protein
GGGSLPETGX$_n$
C-terminus
Target protein
GGGSLPETGGG
DNA binding protein

Figure 1.16: Protein ligation mechanism of Sortase A.

Another method of protein-protein conjugation is the covalent attachment between the side chains of two surface exposed reactive groups on the proteins[30]. The functional groups most commonly used to crosslink proteins are lysine, cysteine, aspartic and glutamic acid. (Table 1.1) [83].

Table 1.1: Reactive functional groups in naturally occurring aminoacids [84].

Reactive group		Aminoacid
$-NH_2$	Primary amine	Lysine
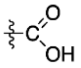	Carboxylic acid	Glutamic acid Ascarpic acid
$-SH$	Thiol	Cysteine
$-OH$	Hydroxyl	Serine Threonine
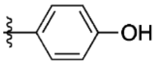	Phenol	Tyrosine
$-CH_2-S-CH_3$	Thioether	Methionine
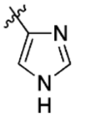	Imidazole	Histidine
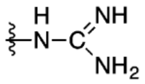	Guanidino	Arginine

The most commonly used chemical groups are amines, thiols and carboxylic acids due to their abundance on protein surfaces [85]. In the case of amines and carboxylic acids, 1-ethyl-3-(3-dimethylaminopropyl) carbodiimide (EDC) and N-hydroxysuccinimide (NHS) are often used as an activating reagent to form the conjugate [86]. This crosslinking reaction is performed under specific conditions (buffer, pH, temperature etc.) in order to avoid protein denaturation.

Cysteine side groups are not as abundant as the amines and carboxylic acids and this low natural abundance can result in site specific coupling. In case cysteines are not present in the protein, they can be easily introduced at a specific position of interest by site-directed mutagenesis [84].

1.4 THESIS OBJECTIVES

The overall objective of the present doctoral thesis is to develop a protein immobilization system that allows the defined and controlled co-immobilization of multiple detection elements. This is achieved by linking them to specific DNA binding protein tags and by controlling the positioning of the DNA binding sequences specific to the DNA binding protein tags on a DNA tether. The proposed immobilization system is utilized to develop novel signal generation methods for biosensors and other applications to showcase the interesting characteristics of this approach.

To accomplish this overall objective, we have focused on the following specific aspects:

- Expression, purification and characterization of the engineered DNA binding proteins (scCro and dHP) to be used as fusion tags.
- Conjugation of these DNA binding protein tags to enzymes and nanoparticles.
- Evaluation of the enzyme-DNA binding protein tag conjugate HRP–scCro and its use as a universal tool for signal enhancement in enzyme-linked assays.
- Development of a DNA sensing platform based on enzyme-DNA binding protein tags HRP-scCro and GOx-dHP conjugates and simple DNA nanostructures.
- Aptamer-based platform for protein detection utilizing the enzyme-DNA binding protein tags HRP-scCro and GOx-dHP conjugates.
- Lateral flow assay for the direct detection of a PCR product via a DNA binding protein tag.
- Use of DNA binding proteins for the immobilization of DNA on the surface of biosensors as an alternative to (strept)avindin/biotin-based approaches.

1.5 REFERENCES

1 Turner, A. P. Biosensors: sense and sensibility. *Chemical Society reviews* **42**, 3184-3196, doi:10.1039/c3cs35528d (2013).

2 Iqbal, S. S. *et al.* A review of molecular recognition technologies for detection of biological threat agents. *Biosensors & bioelectronics* **15**, 549-578 (2000).

3 Shengbo Sang, W. Z. a. Y. Z. Review on the Design Art of Biosensors, State of the Art in Biosensors - General Aspects, Dr. Toonika Rinken (Ed.), InTech,. doi:10.5772/45832 (2013).

4 Stepanenko, O. V. *et al.* Modern fluorescent proteins: from chromophore formation to novel intracellular applications. *BioTechniques* **51**, 313-314, 316, 318 passim, doi:10.2144/000113765 (2011).

5 de Silva, A. P. *et al.* Signaling Recognition Events with Fluorescent Sensors and Switches. *Chemical reviews* **97**, 1515-1566 (1997).

6 Dwight, S. J., Gaylord, B. S., Hong, J. W. & Bazan, G. C. Perturbation of fluorescence by nonspecific interactions between anionic poly(phenylenevinylene)s and proteins: implications for biosensors. *Journal of the American Chemical Society* **126**, 16850-16859, doi:10.1021/ja0469737 (2004).

7 Biju, V. Chemical modifications and bioconjugate reactions of nanomaterials for sensing, imaging, drug delivery and therapy. *Chemical Society reviews* **43**, 744-764, doi:10.1039/c3cs60273g (2014).

8 Burt, J. L., Gutierrez-Wing, C., Miki-Yoshida, M. & Jose-Yacaman, M. Noble-metal nanoparticles directly conjugated to globular proteins. *Langmuir : the ACS journal of surfaces and colloids* **20**, 11778-11783, doi:10.1021/la048287r (2004).

9 You, C. C., De, M., Han, G. & Rotello, V. M. Tunable inhibition and denaturation of alpha-chymotrypsin with amino acid-functionalized gold nanoparticles. *Journal of the American Chemical Society* **127**, 12873-12881, doi:10.1021/ja0512881 (2005).

10 Castaneda, M. T., Merkoci, A., Pumera, M. & Alegret, S. Electrochemical genosensors for biomedical applications based on gold nanoparticles. *Biosensors & bioelectronics* **22**, 1961-1967, doi:10.1016/j.bios.2006.08.031 (2007).

11 Xia, F. *et al.* Colorimetric detection of DNA, small molecules, proteins, and ions using unmodified gold nanoparticles and conjugated polyelectrolytes. *Proceedings of the National Academy of Sciences of the United States of America* **107**, 10837-10841, doi:10.1073/pnas.1005632107 (2010).

12 Taton, T. A., Mirkin, C. A. & Letsinger, R. L. Scanometric DNA array detection with nanoparticle probes. *Science* **289**, 1757-1760 (2000).

13 Hu, S. Q. *et al.* A label-free electrochemical immunosensor based on gold nanoparticles for detection of paraoxon. *Talanta* **61**, 769-777, doi:10.1016/S0039-9140(03)00368-0 (2003).

14 Tkachenko, A. G. *et al.* Multifunctional gold nanoparticle-peptide complexes for nuclear targeting. *Journal of the American Chemical Society* **125**, 4700-4701, doi:10.1021/ja0296935 (2003).

15 Saha, K., Agasti, S. S., Kim, C., Li, X. & Rotello, V. M. Gold nanoparticles in chemical and biological sensing. *Chemical reviews* **112**, 2739-2779, doi:10.1021/cr2001178 (2012).

16 Noguera, P. S. *et al.* Carbon nanoparticles as detection labels in antibody microarrays. Detection of genes encoding virulence factors in Shiga toxin-producing Escherichia coli. *Analytical chemistry* **83**, 8531-8536, doi:10.1021/ac201823v (2011).

17 Akbarzadeh, A., Samiei, M. & Davaran, S. Magnetic nanoparticles: preparation, physical properties, and applications in biomedicine. *Nanoscale research letters* **7**, 144, doi:10.1186/1556-276X-7-144 (2012).

18 Perez, J. M., O'Loughin, T., Simeone, F. J., Weissleder, R. & Josephson, L. DNA-Based Magnetic Nanoparticle Assembly Acts as a Magnetic Relaxation Nanoswitch Allowing Screening of DNA-Cleaving Agents. *Journal of the American Chemical Society* **124**, 2856-2857, doi:10.1021/ja017773n (2002).

19 Medintz, I. L. *et al.* Self-assembled nanoscale biosensors based on quantum dot FRET donors. *Nature materials* **2**, 630-638, doi:10.1038/nmat961 (2003).

20 Prabhu, S. & Poulose, E. K. Silver nanoparticles: mechanism of antimicrobial action, synthesis, medical applications, and toxicity effects. *International Nano Letters* **2**, 32, doi:10.1186/2228-5326-2-32 (2012).

21 Wilson, G. S. & Hu, Y. Enzyme-based biosensors for in vivo measurements. *Chemical reviews* **100**, 2693-2704 (2000).

22 Heller, A. & Feldman, B. Electrochemical glucose sensors and their applications in diabetes management. *Chemical reviews* **108**, 2482-2505, doi:10.1021/cr068069y (2008).

23 Wang, J. Electrochemical glucose biosensors. *Chemical reviews* **108**, 814-825, doi:10.1021/cr068123a (2008).

24 Schuhmann, W. Amperometric enzyme biosensors based on optimised electron-transfer pathways and non-manual immobilisation procedures. *Journal of biotechnology* **82**, 425-441 (2002).

25 Ahirwal, G. K. & Mitra, C. K. Direct electrochemistry of horseradish peroxidase-gold nanoparticles conjugate. *Sensors* **9**, 881-894, doi:10.3390/s90200881 (2009).

26 Civit, L., Fragoso, A., Holters, S., Durst, M. & O'Sullivan, C. K. Electrochemical genosensor array for the simultaneous detection of multiple high-risk human papillomavirus sequences in clinical samples. *Analytica chimica acta* **715**, 93-98, doi:10.1016/j.aca.2011.12.009 (2012).

27 Dequaire, M. & Heller, A. Screen printing of nucleic acid detecting carbon electrodes. *Analytical chemistry* **74**, 4370-4377 (2002).

28 Lebedeva, T. E., Nazarov, N. M. & Siniak Iu, E. [Biocatalysis using immobilized cells or enzymes as a method of water and air purification in habitable enclosed environment]. *Kosmicheskaia biologiia i aviakosmicheskaia meditsina* **25**, 42-45 (1991).

29 Datta, S., Christena, L. R. & Rajaram, Y. R. Enzyme immobilization: an overview on techniques and support materials. *3 Biotech* **3**, 1-9, doi:10.1007/s13205-012-0071-7 (2013).

30 Mohamad, N. R., Marzuki, N. H., Buang, N. A., Huyop, F. & Wahab, R. A. An overview of technologies for immobilization of enzymes and surface analysis techniques for immobilized enzymes. *Biotechnology, biotechnological equipment* **29**, 205-220, doi:10.1080/13102818.2015.1008192 (2015).

31 Yoshimura, S. H. *et al.* Site-specific attachment of a protein to a carbon nanotube end without loss of protein function. *Bioconjugate chemistry* **23**, 1488-1493, doi:10.1021/bc300131w (2012).

32 Kusnezow, W. & Hoheisel, J. D. Solid supports for microarray immunoassays. *Journal of molecular recognition : JMR* **16**, 165-176, doi:10.1002/jmr.625 (2003).

33 Gauthier, M. A. & Klok, H. A. Peptide/protein-polymer conjugates: synthetic strategies and design concepts. *Chemical communications*, 2591-2611, doi:10.1039/b719689j (2008).

34 Jonkheijm, P., Weinrich, D., Schroder, H., Niemeyer, C. M. & Waldmann, H. Chemical strategies for generating protein biochips. *Angewandte Chemie* **47**, 9618-9647, doi:10.1002/anie.200801711 (2008).

35 Menard, A., Huang, Y., Karam, P., Cosa, G. & Auclair, K. Site-specific fluorescent labeling and oriented immobilization of a triple mutant of CYP3A4 via C64. *Bioconjugate chemistry* **23**, 826-836, doi:10.1021/bc200672s (2012).

36 Rusmini, F., Zhong, Z. & Feijen, J. Protein immobilization strategies for protein biochips. *Biomacromolecules* **8**, 1775-1789, doi:10.1021/bm061197b (2007).

37 Fu, J., Reinhold, J. & Woodbury, N. W. Peptide-modified surfaces for enzyme immobilization. *PloS one* **6**, e18692, doi:10.1371/journal.pone.0018692 (2011).

38 Borisov, S. M. & Wolfbeis, O. S. Optical biosensors. *Chemical reviews* **108**, 423-461, doi:10.1021/cr068105t (2008).

39 Butler, J. E. Solid supports in enzyme-linked immunosorbent assay and other solid-phase immunoassays. *Methods* **22**, 4-23, doi:10.1006/meth.2000.1031 (2000).

40 Cha, T., Guo, A. & Zhu, X. Y. Enzymatic activity on a chip: the critical role of protein orientation. *Proteomics* **5**, 416-419, doi:10.1002/pmic.200400948 (2005).

41 Zhou, F. X., Bonin, J. & Predki, P. F. Development of functional protein microarrays for drug discovery: progress and challenges. *Combinatorial chemistry & high throughput screening* **7**, 539-546 (2004).

42 Wong, L. S., Khan, F. & Micklefield, J. Selective covalent protein immobilization: strategies and applications. *Chemical reviews* **109**, 4025-4053, doi:10.1021/cr8004668 (2009).

43 Camarero, J. A. Recent developments in the site-specific immobilization of proteins onto solid supports. *Biopolymers* **90**, 450-458, doi:10.1002/bip.20803 (2008).

44 Duckworth, B. P., Xu, J., Taton, T. A., Guo, A. & Distefano, M. D. Site-Specific, Covalent Attachment of Proteins to a Solid Surface. *Bioconjugate chemistry* **17**, 967-974, doi:10.1021/bc060125e (2006).

45 Zimmermann, J. L., Nicolaus, T., Neuert, G. & Blank, K. Thiol-based, site-specific and covalent immobilization of biomolecules for single-molecule experiments. *Nat. Protocols* **5**, 975-985 (2010).

46 Rogers, K. R. Principles of affinity-based biosensors. *Molecular biotechnology* **14**, 109-129, doi:10.1385/MB:14:2:109 (2000).

47 Dundas, C. M., Demonte, D. & Park, S. Streptavidin-biotin technology: improvements and innovations in chemical and biological applications. *Applied microbiology and biotechnology* **97**, 9343-9353, doi:10.1007/s00253-013-5232-z (2013).

48 Wilchek, M. & Bayer, E. A. The avidin-biotin complex in bioanalytical applications. *Analytical biochemistry* **171**, 1-32 (1988).

49 Bornhorst, J. A. & Falke, J. J. [16] Purification of Proteins Using Polyhistidine Affinity Tags. *Methods in enzymology* **326**, 245-254 (2000).

50 Haddour, N., Cosnier, S. & Gondran, C. Electrogeneration of a poly(pyrrole)-NTA chelator film for a reversible oriented immobilization of histidine-tagged proteins. *Journal of the American Chemical Society* **127**, 5752-5753, doi:10.1021/ja050390v (2005).

51 Holzinger, M., Bouffier, L., Villalonga, R. & Cosnier, S. Adamantane/beta-cyclodextrin affinity biosensors based on single-walled carbon nanotubes. *Biosensors & bioelectronics* **24**, 1128-1134, doi:10.1016/j.bios.2008.06.029 (2009).

52 Byrne, B., Stack, E., Gilmartin, N. & O'Kennedy, R. Antibody-based sensors: principles, problems and potential for detection of pathogens and associated toxins. *Sensors* **9**, 4407-4445, doi:10.3390/s90604407 (2009).

53 Terpe, K. Overview of tag protein fusions: from molecular and biochemical fundamentals to commercial systems. *Applied microbiology and biotechnology* **60**, 523-533, doi:10.1007/s00253-002-1158-6 (2003).

54 Hengen, P. Purification of His-Tag fusion proteins from Escherichia coli. *Trends in biochemical sciences* **20**, 285-286 (1995).

55 Stephanopoulos, N. & Francis, M. B. Choosing an effective protein bioconjugation strategy. *Nature chemical biology* **7**, 876-884, doi:10.1038/nchembio.720 (2011).

56 Boozer, C. *et al.* DNA directed protein immobilization on mixed ssDNA/oligo(ethylene glycol) self-assembled monolayers for sensitive biosensors. *Analytical chemistry* **76**, 6967-6972, doi:10.1021/ac048908l (2004).

57 Hudson, W. H. & Ortlund, E. A. The structure, function and evolution of proteins that bind DNA and RNA. *Nature reviews. Molecular cell biology* **15**, 749-760, doi:10.1038/nrm3884 (2014).

58 Rohs, R. *et al.* Origins of specificity in protein-DNA recognition. *Annual review of biochemistry* **79**, 233-269, doi:10.1146/annurev-biochem-060408-091030 (2010).

59 Koudelka, G. B., Mauro, S. A. & Ciubotaru, M. Indirect readout of DNA sequence by proteins: the roles of DNA sequence-dependent intrinsic and extrinsic forces. *Progress in nucleic acid research and molecular biology* **81**, 143-177, doi:10.1016/S0079-6603(06)81004-4 (2006).

60 Bewley, C. A., Gronenborn, A. M. & Clore, G. M. Minor groove-binding architectural proteins: structure, function, and DNA recognition. *Annual*

review of biophysics and biomolecular structure **27**, 105-131, doi:10.1146/annurev.biophys.27.1.105 (1998).

61 Anderson, W. F., Ohlendorf, D. H., Takeda, Y. & Matthews, B. W. Structure of the cro repressor from bacteriophage lambda and its interaction with DNA. *Nature* **290**, 754-758 (1981).

62 Pabo, C. O. & Lewis, M. The operator-binding domain of lambda repressor: structure and DNA recognition. *Nature* **298**, 443-447 (1982).

63 Spronk, C. A. *et al.* The solution structure of Lac repressor headpiece 62 complexed to a symmetrical lac operator. *Structure* **7**, 1483-1492 (1999).

64 Pabo, C. O. & Sauer, R. T. Protein-DNA recognition. *Annual review of biochemistry* **53**, 293-321, doi:10.1146/annurev.bi.53.070184.001453 (1984).

65 Ohlendorf, D. H., Tronrud, D. E. & Matthews, B. W. Refined structure of Cro repressor protein from bacteriophage lambda suggests both flexibility and plasticity. *Journal of molecular biology* **280**, 129-136, doi:10.1006/jmbi.1998.1849 (1998).

66 Albright, R. A. & Matthews, B. W. Crystal structure of lambda-Cro bound to a consensus operator at 3.0 A resolution. *Journal of molecular biology* **280**, 137-151, doi:10.1006/jmbi.1998.1848 (1998).

67 Jana, R., Hazbun, T. R., Mollah, A. K. & Mossing, M. C. A folded monomeric intermediate in the formation of lambda Cro dimer-DNA complexes. *Journal of molecular biology* **273**, 402-416, doi:10.1006/jmbi.1997.1256 (1997).

68 Takeda, Y., Sarai, A. & Rivera, V. M. Analysis of the sequence-specific interactions between Cro repressor and operator DNA by systematic base substitution experiments. *Proceedings of the National Academy of Sciences of the United States of America* **86**, 439-443 (1989).

69 Brennan, R. G., Roderick, S. L., Takeda, Y. & Matthews, B. W. Protein-DNA conformational changes in the crystal structure of a lambda Cro-operator complex. *Proceedings of the National Academy of Sciences of the United States of America* **87**, 8165-8169 (1990).

70 Jana, R., Hazbun, T. R., Fields, J. D. & Mossing, M. C. Single-chain lambda Cro repressors confirm high intrinsic dimer-DNA affinity. *Biochemistry* **37**, 6446-6455, doi:10.1021/bi980152v (1998).

71 Lamerichs, R. M. *et al.* H NMR study of a complex between the lac repressor headpiece and a 22 base pair symmetric lac operator. *Biochemistry* **28**, 2985-2991 (1989).

72 Lewis, M. *et al.* Crystal structure of the lactose operon repressor and its complexes with DNA and inducer. *Science* **271**, 1247-1254 (1996).

73 Matsumura, M., Becktel, W. J., Levitt, M. & Matthews, B. W. Stabilization of phage T4 lysozyme by engineered disulfide bonds. *Proceedings of the National Academy of Sciences of the United States of America* **86**, 6562-6566 (1989).

74 Matthews, B. W., Nicholson, H. & Becktel, W. J. Enhanced protein thermostability from site-directed mutations that decrease the entropy of unfolding. *Proceedings of the National Academy of Sciences of the United States of America* **84**, 6663-6667 (1987).

75 Robinson, C. R. & Sauer, R. T. Striking stabilization of Arc repressor by an engineered disulfide bond. *Biochemistry* **39**, 12494-12502 (2000).

76 Kalodimos, C. G., Folkers, G. E., Boelens, R. & Kaptein, R. Strong DNA binding by covalently linked dimeric Lac headpiece: evidence for the crucial role of the hinge helices. *Proceedings of the National Academy of Sciences of the United States of America* **98**, 6039-6044, doi:10.1073/pnas.101129898 (2001).

77 Sauer, R. T. Lac repressor at last. *Structure* **4**, 219-222 (1996).

78 Berger, S., Lowe, P. & Tesar, M. Fusion protein technologies for biopharmaceuticals: Applications and challenges. *mAbs* **7**, 456-460, doi:10.1080/19420862.2015.1019788 (2015).

79 Demain, A. L. & Vaishnav, P. Production of recombinant proteins by microbes and higher organisms. *Biotechnology advances* **27**, 297-306, doi:10.1016/j.biotechadv.2009.01.008 (2009).

80 Costa, S., Almeida, A., Castro, A. & Domingues, L. Fusion tags for protein solubility, purification and immunogenicity in Escherichia coli: the novel Fh8 system. *Frontiers in microbiology* **5**, doi:10.3389/fmicb.2014.00063 (2014).

81 Levary, D. A., Parthasarathy, R., Boder, E. T. & Ackerman, M. E. Protein-protein fusion catalyzed by sortase A. *PloS one* **6**, e18342, doi:10.1371/journal.pone.0018342 (2011).

82 Matsumoto, T., Tanaka, T. & Kondo, A. Sortase A-catalyzed site-specific coimmobilization on microparticles via streptavidin. *Langmuir : the ACS journal of surfaces and colloids* **28**, 3553-3557, doi:10.1021/la2047933 (2012).

83 Guisan, J. M. in *Immobilization of Enzymes and Cells* (ed Jose M. Guisan) 1-13 (Humana Press, 2006).

84 Steen Redeker, E. *et al.* Protein engineering for directed immobilization. *Bioconjugate chemistry* **24**, 1761-1777, doi:10.1021/bc4002823 (2013).

85 Foley, T. L. & Burkart, M. D. Site-specific protein modification: advances and applications. *Current opinion in chemical biology* **11**, 12-19, doi:10.1016/j.cbpa.2006.11.036 (2007).

86 Pei, Z. *et al.* Optimizing immobilization on two-dimensional carboxyl surface: pH dependence of antibody orientation and antigen binding capacity. *Analytical biochemistry* **398**, 161-168, doi:10.1016/j.ab.2009.11.038 (2010).

Chapter 2

Novel signal amplification approach in genosensors based on DNA binding protein tags

Biosensors and Bioelectronics 2015, 74: 1005–1010

Chapter 2: Novel signal amplification approach in genosensors based on DNA binding protein tags

2.1 ABSTRACT

The need for sensitive detection of DNA is growing as more specific DNA sequences are being correlated to gene markers for disease diagnosis, food safety and other security related applications. Assays based on DNA hybridization have been routinely used for this purpose especially in combination with reporter enzyme labels like HRP that provide signal amplification. Detection is usually achieved with target-specific ssDNA probes conjugated directly to HRP or with nanoparticles functionalized with DNA and multiple HRP molecules. In order to overcome some of the drawbacks presented by these approaches, we developed a unique DNA sensing platform based on an HRP-DNA binding protein tag conjugate and a hybrid ssDNA-dsDNA detection probe. This approach facilitates the association of more HRP molecules per target molecule compared to the ssDNA-HRP conjugates but with a universal conjugate of smaller size and with known stoichiometry of reporter enzyme to target molecules compared to nanoparticles. By using HRP conjugated to scCro DNA binding protein together with a hybrid detection probe containing three scCro-specific dsDNA binding sites, we demonstrate an improvement by over 3-fold in both sensitivity and limit of detection of high-risk human papillomavirus (HPV16), compared to the standard ssDNA-HRP conjugate. These results show that the HRP-DNA binding protein tag conjugate can be used as an alternative and universal tool for signal enhancement in enzyme-linked assays suitable for integration in point-of-care systems.

2.2 INTRODUCTION

With a world market value of US$ 13 billion for 2013 and around 4500 papers published every year the field of biosensors is booming both commercially and scientifically [1]. Genosensors in specific have gained a lot of interest since the detection of specific DNA sequences has become essential in medical diagnostics, gene expression analysis, detection of infectious diseases and biological warfare agents among others. Different approaches have been developed for the detection of DNA using colorimetric, fluorescence, electrochemical and optical sensors [2-4]. Enzyme-linked assays have been routinely used because they are fast, cost-effective, relatively easy to perform and they provide amplification of the detection signal as a consequence of the rapid conversion of substrates to products that can be readily visualized and measured. The principle of signal enhancement in enzyme-linked assays is based upon the use of a detection platform that enables the association of each target molecule with a reporter enzyme. Horseradish peroxidase (HRP) is one of the most common enzymes used in these assays, in various bioconjugate formats with DNA probes, nanoparticles or other molecules [5,6]. Direct conjugation of the ssDNA detection probe with HRP (ssDNA-HRP conjugate) has been used in both colorimetric and electrochemical assays as an alternative to biotinylated detection probe in combination with streptavidin-HRP [7-10]. The signal generated though is limited since in general a maximum of one HRP molecule can be linked to each target molecule. Furthermore, a new chemical conjugation step is required for each additional specific DNA target to be detected (such as different targets or multiplex configurations), a process that is both expensive and laborious. Functionalized nanoparticles on the other hand have also been used extensively for the detection of biomolecules like DNA and proteins [11-15]. Their use in biosensing applications presents various advantages like large surface areas for functionalization with enzyme probes and other detection elements, biocompatibility with biological systems and the possibility for “naked-eye” detection [16]. Usually the signals obtained are very high but the size of the particles can lead to steric hindrance effects and prevent the association of each target molecule with one nanoparticle. Moreover, functionalization of the particles in order to provide the link between the target DNA and the detection element can be laborious and costly like in the case of ssDNA-HRP conjugates. Differences in size distribution and labeling efficiencies with DNA detection probes and reporter enzymes have also limited their use [17,18].

In this work we propose a DNA sensing platform that facilitates the association of more HRP molecules per target molecule compared to the ssDNA-HRP conjugates (Fig. 2.1A, i) but with a well-defined and reproducible conjugate that provides known stoichiometry of the reporter enzyme to target molecules compared to nanoparticles. It relies on the use of a DNA binding protein tag conjugated to HRP in conjunction with hybrid ssDNA-dsDNA detection probes as illustrated in Fig.2.1A (ii and iii). The ssDNA part of the detection probe is complementary to the target while specific DNA binding sites for the DNA binding protein tag are arranged on the dsDNA part in order to facilitate the simultaneous co-immobilization of multiple HRP molecules through the binding of the HRP-DNA binding protein tag conjugate (Fig 2.1B). Increase of the number of DNA binding sites on the detection probe is expected to increase the number of HRP molecules associated with each target molecule, ultimately leading to higher signal amplification. In this work, we demonstrate such increase in signal amplification for an enzyme-linked genosensor assay. Specifically, the proposed method has been evaluated for the detection of high-risk human papillomavirus (HPV16) DNA. HPV testing using a DNA-based assay is a fundamental element in cervical cancer screening, especially for type 16 that is one of the two most carcinogenic genotypes [19].

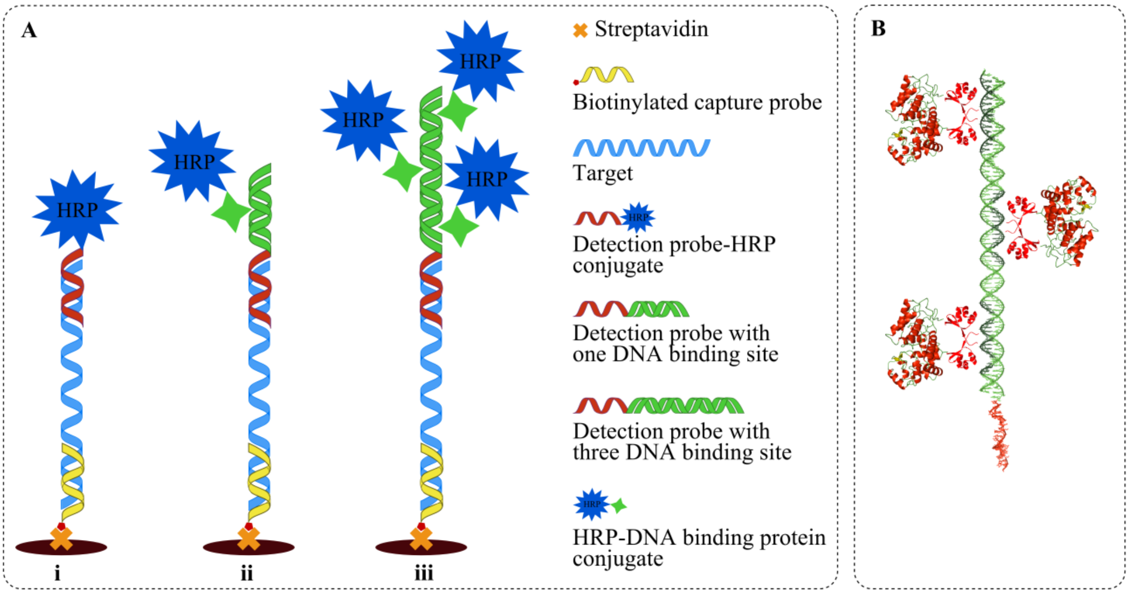
A
HRP
i
ii
iii
Streptavidin
Biotinylated capture probe
Target
Detection probe-HRP conjugate
Detection probe with one DNA binding site
Detection probe with three DNA binding site
HRP-DNA binding protein conjugate
B

Figure 2.1: (A) Genosensor signal amplification approaches using (i) a detection ssDNA probe conjugated to HRP and (ii) an HRP-DNA binding protein conjugate in combination with hybrid ssDNA-dsDNA detection probes containing one and (iii) three DNA binding sites. (B) Hybrid ssDNA-dsDNA detection probe containing three scCro DNA binding sites (in dark green) with HRP-scCro conjugate bound. The target detection ssDNA part is shown in red and the dsDNA part in light green.

2.3 EXPERIMENTAL

2.3.1 Materials

PCR reagents, restriction enzymes, maleimide-activated HRP, HisPure Ni-NTA-agarose, SP Sepharose FF and streptavidin-coated microplate strip plates were purchased from Fisher Scientific (Barcelona, Spain). Con-A sepharose 4B and antibodies were obtained from Sigma-Aldrich (Madrid, Spain) and the Immun-Blot PVDF membrane from Bio-rad (Barcelona, Spain). The pscCro16 construct was kindly provided by Prof. M. C. Mossing (University of Mississippi, USA). The DNA oligonucleotides were purchased from Sigma-Aldrich (Madrid, Spain) and Biomers.net (Ulm, Germany) and their sequences are shown in Table S-2.1 in the supplementary material. All other reagents were purchased from Scharlau (Barcelona, Spain), Fisher Scientific (Barcelona, Spain) and Sigma-Aldrich (Madrid, Spain).

2.3.2 Cloning, expression and purification of the DNA binding protein

Covalently linked homodimeric *cro* repressor gene (*sccro16*) was PCR-amplified from pscCro16 construct [20] using forward and reverse primers designed appropriately in order to add an N-terminal cysteine residue and a C-terminal polyhistidine tag to the expressed protein. The gene was digested with *Nde*I and *Hin*dIII restriction enzymes and ligated into *Nde*I- and *Hin*dIII-digested pET22b plasmid. After confirmation of the correct sequence by DNA sequencing, the resulting construct was transformed in chemically competent *E. coli* BL21(DE3) cells, the culture was grown at 37°C until OD600nm ≈ 1 and the expression of cys-scCro was induced by the addition of 0.05 mM IPTG. The culture was grown post-induction for 3 h at 30°C, the cells were harvested, resuspended in lysis buffer (50 mM Tris-HCl pH 7, 5 mM DTT, 5 % glycerol, 5 µg/ml DNase I, 0.5 % Triton X-100) at 5 ml per gram of wet cell weight and then lysed by sonication on ice for 10 min. The cell lysate was centrifuged at 14,000 rpm at 4°C and the soluble fraction (supernatant) was loaded on an immobilized metal ion affinity chromatography (IMAC) gravity column packed with HisPure Ni-NTA-agarose resin pre-washed with equilibration buffer (10 mM phosphate buffer, 300 mM NaCl, 10 mM imidazole). The column was washed with equilibration buffer containing 15 mM imidazole and the protein was eluted with the same buffer containing 500 mM imidazole. The buffer of the IMAC elution fraction was exchanged to 50 mM potassium phosphate pH 7, 1 mM EDTA, 5 mM DTT and the sample was loaded on a cation exchange gravity column packed with SP Sepharose FF resin equilibrated with the same buffer. The column was washed with buffer containing 0.2 M NaCl and cys-scCro was eluted with the same buffer containing 1 M NaCl. The buffer of the elution fraction was exchanged to PBS pH 7 containing 50 % glycerol before storage at -20°C. The process was monitored by SDS-PAGE and Western blot.

2.3.3 Preparation of the HRP-scCro conjugate

Maleimide-activated HRP was dissolved in water and the solution was buffer-exchanged to PBS pH 7. The protein was then mixed with cys-scCro at equimolar concentrations (50 µM each protein in PBS pH 7) and the mixture was allowed to react overnight at 4°C. The HRP-scCro conjugate was purified by IMAC and affinity chromatography. For IMAC, a gravity column packed with HisPur Ni-NTA-agarose was equilibrated with 10 mM phosphate buffer pH 7.4, 0.3 M NaCl, loaded with the conjugation mixture, washed with equilibration buffer containing 25 mM imidazole and eluted with the same buffer containing 250 mM imidazole. The buffer of the IMAC elution fraction was exchanged to binding buffer (20 mM Tris-HCl pH 7, 0.5 M NaCl, 1 mM $CaCl_2$, 1 mM $MgCl_2$) and the sample was loaded on a Con-A sepharose 4B-packed column equilibrated with the same buffer. The column was washed with wash buffer (20 mM Tris-HCl pH 7, 0.5 M NaCl) and the conjugate was eluted with wash buffer containing 0.38 M methyl α-D-mannopyranoside. The elution fraction was concentrated with a 50K MWCO centrifugal filter and the buffer was exchanged to PBS with 50 % glycerol. The process was monitored by SDS-PAGE and Western blot. The exact molecular weight of the conjugate was calculated with MALDI-TOF mass spectrometry (see supplementary material Fig. S-2.4 and Table S-2.2).

2.3.4 SDS-PAGE and Western blot analysis

Protein expression, purification and the conjugation reaction were monitored by SDS-PAGE and Western blot using standard protocols. For Western blot, the PVDF membrane after transfer was probed with monoclonal mouse anti-polyhistidine antibody and then with polyclonal rabbit anti-mouse-HRP antibody. Colorimetric detection of the bands was achieved using 1-STEP TMB-Blot solution.

2.3.5 Characterization of the HRP-scCro conjugate by Electrophoretic Mobility Shift Assay (EMSA)

The binding of the HRP-scCro conjugate and of its individual protein components to the different oligonucleotides involved in the detection of HPV16 was evaluated by EMSA. Pre-hybridized ssDNA-dsDNA detection probes (see supplementary material for details) with one or three scCro binding sites (600 nM and 200 nM respectively) were mixed with maleimide-activated HRP, cys-scCro or HRP-scCro (600 nM) in binding buffer (20 mM Tris-HCl pH 7.5, 150 mM NaCl, 1 mM EDTA, 0.05 % Tween-20, 5 % glycerol). The concentrations of DNA and proteins were chosen in order to maintain a DNA:protein molar ratio of 1:1. The mixtures were incubated for 30 min at room temperature and then loaded on a 10% polyacrylamide/TAE gel. The gels were run for 1.5 h at 100 V in TAE buffer and then stained with GelRed DNA gel stain in TAE.

2.3.6 DNA detection by Enzyme Linked Oligonucleotide Assay (ELONA)

HPV16 target DNA was detected with an ELONA assay. Biotinylated HPV16 capture probe (50µl of 20 nM) was immobilized for 15 min at room temperature on streptavidin-coated microplate strip wells followed by three washes with 300 µl ELONA buffer (20 mM potassium phosphate pH 7.5, 50 mM NaCl, 1 mM EDTA, 0.5 % BSA, 0.05 % Tween-20). Target DNA (50 µl of concentrations up to 100 pM) was then added and hybridization was allowed to proceed for 1 h at 37°C. The wells were washed and 50 µl of 0.2 nM of detection probe (ssDNA-HRP conjugate or pre-hybridized ssDNA-dsDNA detection probes containing one or three DNA binding sites) was added followed by incubation at 37°C for 1 h. For target detection using the hybrid ssDNA-dsDNA probes, HRP-scCro conjugate was added (50ul of 1 nM) after three washes and incubated for 30 min at room temperature. Five washing steps were performed before the addition of TMB substrate. Color was allowed to develop for 20 min, an equal volume of 1 M H_2SO_4 was added and the absorbance was recorded at 450 nm. All incubation and washing steps were conducted in

ELONA buffer whereas the step of HRP-scCro binding was performed in binding buffer (20 mM Tris-HCl pH 7.5, 150 mM NaCl, 1 mM EDTA, 0.5 % BSA, 0.05 % Tween-20). Each sample was measured in triplicate with three independent experiments whereas the blank measurements were conducted in sextuplets. Average values of sensitivity and limit of detection (LOD) for each detection approach were calculated without blank subtraction and are shown with the standard error of the mean (SEM). For the specificity experiments, the same conditions were used as described above but with a fixed 1 nM concentration of DNA, HPV16 target and non-complementary control sequences of cancer (CDH1) and celiac disease (HLA-DQ1*0201) gene markers.

2.4 RESULT AND DISCUSSION

2.4.1 Choice and production of the DNA binding protein

The DNA binding protein used for conjugation to HRP was chosen based on several criteria: it had to bind only dsDNA with high affinity and specificity, be relatively small in size, monomeric and without co-factor requirements that would enable its facile expression and purification in soluble form in *Escherichia coli*, and with available three-dimensional structure if possible. Several DNA binding proteins were identified that fulfil these criteria and the bacteriophage lambda Cro repressor was finally chosen. Cro is a sequence-specific dsDNA binding protein that binds as a homodimer to its operator DNA with very high affinity and specificity [21]. The single chain dimeric form that was used in this work (scCro), where the two monomers are covalently linked by a 16 amino acid linker, has an approximate size of 16 kDa and a reported dissociation constant of $(4 \pm 2) \times 10^{-12}$ M [20]. Also, the three-dimensional structure of Cro bound to a consensus DNA operator [22] revealed that the N-terminal of the protein is at a distant position compared to the DNA binding sites, indicating that the conjugation of the protein at its N-terminal is not expected to change its DNA binding properties. Additionally, Cro does not contain any cysteine residues and the addition of one at its N-terminal would provide a single thiol group for conjugation to maleimide-activated HRP, thus enabling us to have better control over the conjugation reaction and achieve an equimolar 1:1 ratio of the two proteins in the final conjugate. HRP isoenzyme C, the main source of HRP available commercially, contains only three surface exposed lysine groups [23]. The limited number of surface-exposed amine groups are located very close to each other (distance between the two lysines further apart is 20 Å) which would further facilitate the covalent linking of one HRP molecule with only one DNA binding protein tag. Finally, the expression of the DNA binding protein tag with a C-terminal polyhistidine tag would facilitate its detection and purification and therefore of the conjugate as well. Taking all these into account, we cloned and expressed cys-scCro in soluble form in *E. coli* (Fig.2.2A, lane 1). The majority of protein contaminants were removed by IMAC (Fig. 2.2A, lane 2) and by further polishing of the IMAC elution fraction with cation exchange chromatography, we were able to obtain cys-scCro at more than 90 % purity (Fig. 2.2A, lane 3) at a total yield of approximately 2 mg per liter of bacterial culture.

2.4.2 Preparation and characterization of the HRP-DNA binding protein conjugate

Commercially available maleimide-activated HRP was covalently linked to cys-scCro via amine-to-sulfhydryl chemistry. The protein contains an average of two maleimide groups per molecule (as indicated by the manufacturer) whereas cys-scCro DNA binding protein tag contains only one thiol group. The conjugation was performed using an equimolar mixture of the two proteins in order to achieve the desired 1:1 molar ratio in the final conjugate. The reaction yielded a single conjugation product as assessed by SDS-PAGE after overnight incubation at 4°C with around 30 % efficiency when 50 μM of each protein were used (Fig.2.2B, lane 3). The efficiency was estimated from the intensity of the SDS-PAGE bands corresponding to maleimide-HRP before and after conjugation (Fig. 2.2B, lanes 1 and 3) using the ImageJ program. The use of molar excess of either protein did not improve the conjugation efficiency (see Fig. S-2.3 in supplementary material). Purification of the conjugate and removal of unreacted proteins was achieved by a two-step process. The first step involved the use of IMAC for the removal of unreacted maleimide-HRP that does not contain a polyhistidine tag. The second step was designed in order to remove unreacted cys-scCro using an affinity resin (Con-A sepharose 4B) containing immobilized concanavalin A protein suitable for capturing glycosylated biomolecules like HRP. The purification process was monitored by SDS-PAGE, and as it can be seen in Fig. 2.2B, the majority of unreacted HRP was removed after IMAC (Fig. 2.2B, lane 4) whereas unreacted cys-scCro was removed after affinity chromatography and concentration with a 50 K MWCO centrifugal filter (Fig. 2.2B, lane 5). The amount of unreacted HRP in the final conjugate preparation was estimated at approximately 5 %. The conjugation reaction was also analyzed by Western blot that indicated as well a single conjugation product with an apparent size of 75 kDa (Fig. 2.2C, lane 3). In order to verify that the conjugate contained only one molecule of each protein, MALDI-TOF mass spectrometry was used. Both maleimide-HRP and the HRP-scCro conjugate were analyzed (see Fig. S-2.4 and Table S-2.2 in the supplementary material). From the spectra of both proteins and the expected molecular weight of cys-scCro (calculated *in silico* as 17.4 kDa), it is concluded that the HRP-scCro conjugate has an approximate size of 61 kDa and contains one molecule of HRP (43 kDa) and one molecule of scCro (17.4 kDa).

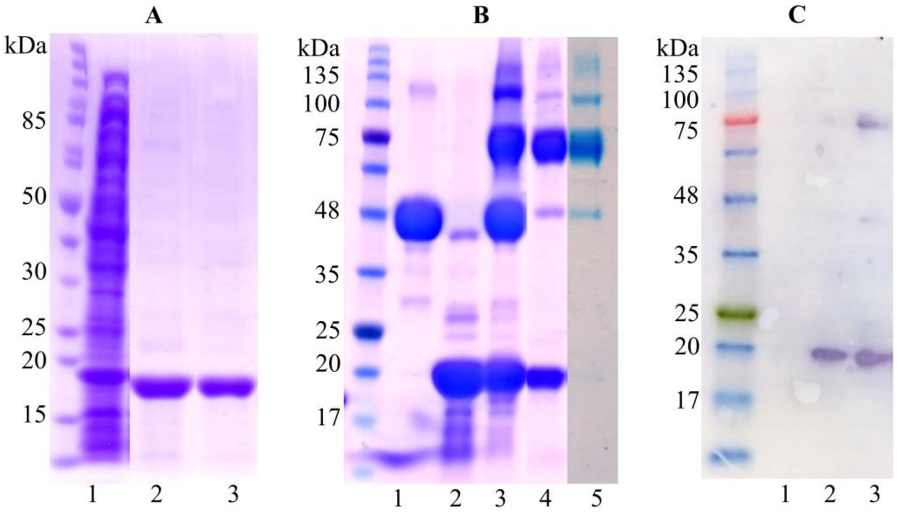

Figure 2.2: Preparation of the HRP-scCro conjugate. (A) Expression and purification of cys-scCro. Lane 1: *E. coli* soluble lysate; lane 2: IMAC elution fraction; lane 3: cation exchange elution fraction. (B) Synthesis and purification of the HRP-scCro conjugate. Lane 1: maleimide-HRP; lane 2: cys-scCro; lane 3: HRP-scCro conjugation reaction; lane 4: IMAC elution fraction; lane 5: affinity chromatography elution fraction after concentration with 50K MWCO centrifugal filter. (C) Western blot for the HRP-scCro conjugation reaction. Lane 1: maleimide-HRP; lane 2: cys-scCro; lane 3: HRP-scCro conjugation reaction.

2.4.3 Design of the DNA detection probes with scCro DNA binding sites

The hybrid ssDNA-dsDNA detection probes were designed taking into account that (i) the target detection ssDNA part would have to be separated enough from the first scCro binding site in order to avoid steric hindrance effects after target hybridization with the detection probe; and (ii) the DNA binding sites would have to be separated enough between them so as to enable their positioning on opposite faces of the dsDNA part of the detection probe. A structure of the detection probe containing three scCro DNA binding sites with HRP-scCro bound was generated using molecular modeling (model.it® server, [24]) and visualization tools (PyMOL

Molecular Graphics System, Schrödinger, LLC) and it is illustrated in Fig. 2.1 B. In this final design of the probe, a 5-bp spacer between the ssDNA and the dsDNA part of the probe was used and 8-bp spacers between the DNA binding sites. Simultaneous co-binding of three cys-scCro molecules on this hybrid ssDNA-dsDNA molecule was demonstrated by EMSA as shown in Fig. 2.3. With this assay, free and protein-bound DNA were separated due to the reduced mobility of bound DNA through a polyacrylamide matrix. When an equimolar mixture of DNA (in terms of binding sites) and cys-scCro was used, cys-scCro was able to bind to each DNA binding site simultaneously, and form DNA-protein complexes of increasing size, depending on the number of binding sites, resulting in bands in the polyacrylamide gel with decreased mobility (bands with asterisks). The binding properties of HRP-scCro were then assessed by EMSA. The conjugate and its individual protein components were used in binding mixtures with the designed HPV16 detection probes containing one or three scCro DNA binding sites and analyzed by polyacrylamide gel electrophoresis (described in the experimental section). As it is demonstrated in Fig. 2.3, the binding of HRP-scCro to the DNA detection probes (bands with asterisks) is a consequence of the presence of the DNA binding protein component (scCro) since no protein-DNA complex can be observed with the HRP molecule alone. Moreover, cys-scCro binds only to the hybridized DNA oligonucleotides with HPV16 target and capture/detection probes containing the specific dsDNA sequences whereas no binding can be detected in the presence of ssDNA (see Fig. S-2.2 in the supplementary material).

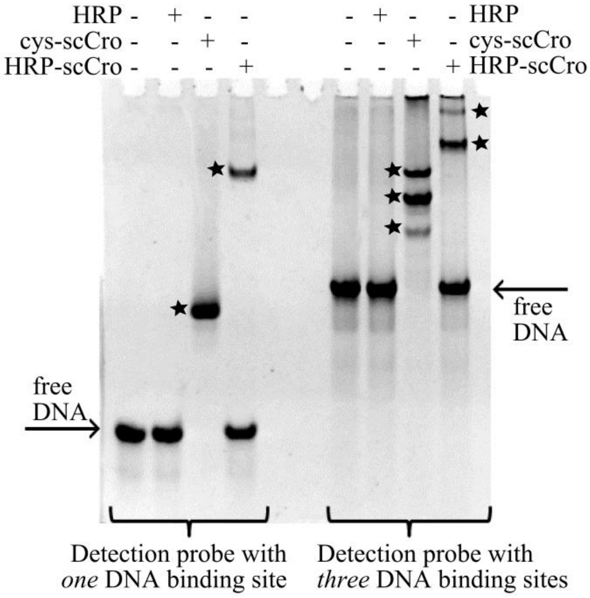
HRP - + - -
cys-scCro - - + -
HRP-scCro - - - +
- + - - HRP
- - + - cys-scCro
- - - + HRP-scCro
★
free DNA
free DNA
Detection probe with *one* DNA binding site
Detection probe with *three* DNA binding sites

Figure 2.3: EMSA assay for the binding of the HRP-scCro conjugate to the HPV16 detection probes with one and three DNA binding sites. Bands with asterisks correspond to protein-DNA complexes.

2.4.4 ELONA for DNA detection

After demonstrating the specificity of binding of the HRP-scCro conjugate to the DNA detection probes containing the specific dsDNA binding sequences, the probes and the conjugate were used to detect the target HPV16 DNA. Synthetic target ssDNA was detected using the three approaches illustrated in Fig. 2.1A: (i) direct detection with the detection ssDNA-HRP conjugate, (ii) detection using hybrid ssDNA-dsDNA detection probes containing one and (iii) three scCro DNA binding sites in conjunction with the HRP-scCro conjugate. Target calibration curves were acquired with independent triplicate experiments and as it can be seen in Fig. 2.4, the optical response increased linearly with the increase of target concentration up to 100 pM. For higher target concentrations, the signal starts to get progressively saturated for all three detection approaches described (data not shown). The sensitivity of each detection approach was calculated as the slope of the linear range of the target calibration curves (AU/pM) and it was found to be (15.5 ± 1.1) x 10^{-4} AU/pM for the ssDNA-HRP conjugate, (19.3 ± 0.8) x 10^{-4} AU/pM for the hybrid detection probe containing one DNA binding site and (56.0 ± 9.0) x 10^{-4} AU/pM for the detection probe containing three scCro DNA binding sites. These results demonstrate that the incorporation of multiple DNA binding sites on the detection probe enables the association of each target molecule with multiple HRP molecules, leading to improved assay sensitivity. In the case of detection probe with three DNA binding sites, the sensitivity improved by a factor of 3.5 compared with the ssDNA-HRP conjugate. It should be pointed out that the sensitivity obtained for the DNA detection using the ssDNA–HRP conjugate, that served as an internal control for the assay, is very similar to the sensitivity reported (18 x 10^{-4} AU/pM) for the detection of a different target (beta-actin) using a similar colorimetric ELONA assay with a ssDNA–HRP conjugate [25]. This eliminates the possibility that the increased sensitivity of the proposed detection system is due to a poor performance of the ssDNA–HRP bench mark control. The limit of detection (LOD) of the assay was also calculated as three times the standard deviation of the blank measurements (no target in the presence of each detection probe) divided by the slope [26]. For all three detection approaches the LOD was calculated in the low picomolar range: 7.4 ± 2.6 pM for the ssDNA-HRP conjugate, 4.0 ± 1.3 pM for the hybrid detection probe containing one DNA binding site and 2.1 ± 1.3 pM for the hybrid detection probe containing three DNA binding sites. Even though these limits of detection are very similar, there is still a 3.5-fold improvement between detection with the ssDNA-HRP and the detection probe containing three DNA binding sites. This may reflect better accessibility of the reporter protein HRP to the target molecules through the spacing that is provided by the use of the hybrid detection probe. Optimization of the detection probes in terms of number of DNA binding sites and the spacing between the different elements (target hybridization part and DNA binding sites) as well as assay conditions (buffers and concentrations of the individual components) may allow us to further improve the performance of the sensor. Nonetheless, the LODs calculated for HPV16 based on HRP–scCro and hybrid detection probes are among the lowest ones reported for HPV using different detection approaches like fluorescence, electrochemical, magnetic and nanoparticle-based optical methods [27].

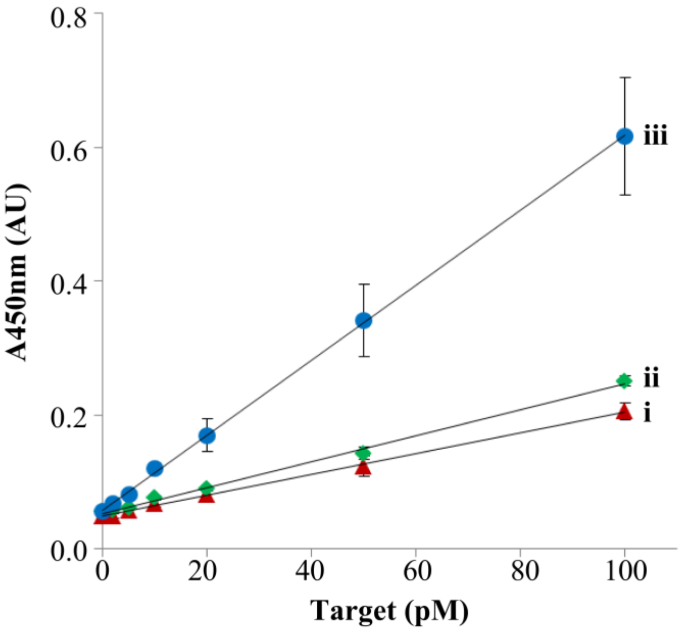

	i	ii	iii
Slope·10^4 (AU/pM)	15.5	19.3	56.0
Intercept (AU)	0.0494	0.0536	0.0579
R^2	0.9985	0.9967	0.9997

Figure 2.4: Target DNA calibration curves using a (i) ssDNA-HRP conjugate and (ii) HRP-scCro conjugate with detection probes containing one and (iii) three DNA binding sites. The error bars show the standard error of the mean (SEM).

Another important aspect of the performance of a sensor is its selectivity towards the detection of the target without interfering signals from non-specific interactions. For this purpose, we evaluated the specificity of the genosensor using target and non-complementary control DNA sequences from different gene markers and the three detection approaches. As shown in Fig. 2.5 independent of the detection approach used, a high specific signal was obtained at saturating target DNA concentration (1 nM) whereas no signal could be detected for two different control DNA sequences.

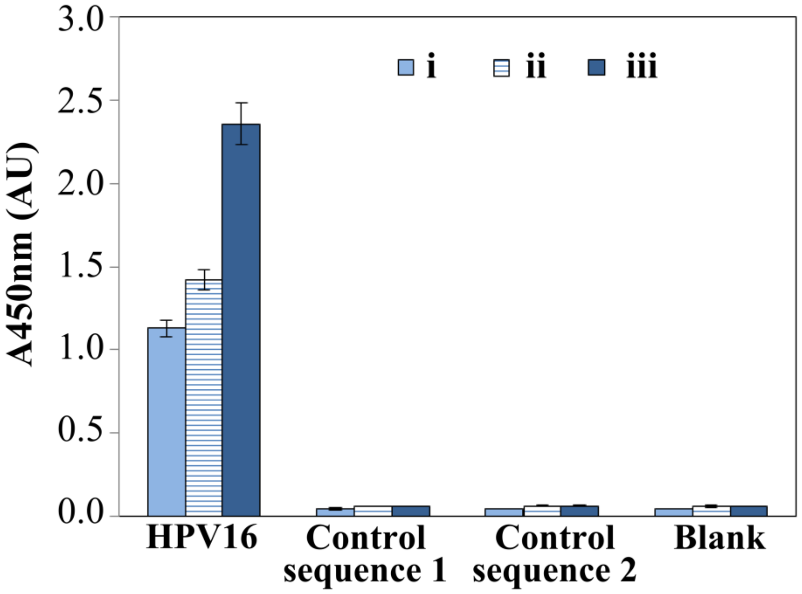

Figure 2.5: Specificity of the genosensor using HPV16 target and control DNA sequences. Detection was achieved with (i) ssDNA-HRP conjugate and (ii) with the HRP-scCro conjugate in combination with detection probes containing one and (iii) three DNA binding sites. The error bars show the standard error of the mean (SEM).

2.5 CONCLUSION

In this work we describe the preparation of a novel HRP-DNA binding protein tag conjugate and its use for signal amplification in a genosensor. Characterization of the conjugate with MALDI-TOF mass spectroscopy confirmed the direct covalent linking of one HRP molecule with one molecule of scCro, the DNA binding protein tag used in this work. The specificity of the binding of the conjugate only to dsDNA sequences containing the scCro specific DNA binding sites was demonstrated by EMSA. Finally, the conjugate was used for the detection of HPV16 target DNA in a sandwich format in conjunction with hybrid ssDNA-dsDNA detection probes containing scCro DNA binding sites. By incorporating three scCro DNA binding sites on the detection probe we were able to improve the assay performance by 3.5-fold, compared to ssDNA-HRP conjugate, in terms of both sensitivity and limit of detection. The results corroborate that the high affinity and specificity of the DNA binding protein tag for its binding sequence enabled its simultaneous co-immobilization on the multiple positions on the detection probe, ultimately leading to the positioning of multiple HRP molecules on the probe and providing a signal enhancement effect. In this work three DNA binding sites were included in the detection probe in order to demonstrate the feasibility of the proposed method but this number can be increased to further increase the signal. Optimization of the assay conditions in terms of incubation times, buffer composition and the design of the detection probes regarding number and spacing between the DNA binding sites could enable further improvement of the assay performance. The proposed signal amplification approach is not dependent on the target DNA sequence of the genosensor circumventing the expensive and laborious preparation of ssDNA-HRP conjugates for each target; only the hybrid ssDNA-dsDNA detection probes have to be prepared specifically for each target. Furthermore, the detection step can be tailored for each application by controlling the number of DNA binding sites on the detection probe, thus increasing or decreasing the signal as needed. Overall, this novel HRP-DNA binding protein conjugate can be used as a universal signal amplification tool in enzyme-linked assays, providing higher signal than ssDNA-HRP direct conjugates while still exhibiting a better defined stoichiometry and smaller size than functionalized nanoparticles. The low cost and simplicity of this approach also make it suitable for integration with point-of-care systems.

2.6 ACKNOWLEDGEMENTS

This work was supported financially by the FP7-PEOPLE-2011-CIG DeCoDeB project grant awarded to LM. GBA acknowledges the Universitat Rovira i Virgili for the doctoral fellowship. The authors thank Prof. M. C. Mossing (University of Mississippi, USA) for the gift of the pscCro16 construct and Dr. C.K. O'Sullivan and Dr. A. Fragoso (Universitat Rovira i Virgili, Spain) for oligonucleotides.

2.7 REFERENCES

1 Turner, A. Biosensors: then and now. *Trends in Biotechnology* **31**, 119-120, doi:10.1016/j.tibtech.2012.10.002.

2 Batchelor-McAuley, C., Wildgoose, G. G. & Compton, R. G. The physicochemical aspects of DNA sensing using electrochemical methods. *Biosensors and Bioelectronics* **24**, 3183-3190, doi:https://doi.org/10.1016/j.bios.2009.01.045 (2009).

3 Niemz, A., Ferguson, T. M. & Boyle, D. S. Point-of-care nucleic acid testing for infectious diseases. *Trends in Biotechnology* **29**, 240-250, doi:10.1016/j.tibtech.2011.01.007.

4 Sassolas, A., Leca-Bouvier, B. D. & Blum, L. J. DNA biosensors and microarrays. *Chemical reviews* **108**, 109-139, doi:10.1021/cr0684467 (2008).

5 Merkoçi, A. Nanoparticles-based strategies for DNA, protein and cell sensors. *Biosensors and Bioelectronics* **26**, 1164-1177, doi:https://doi.org/10.1016/j.bios.2010.07.028 (2010).

6 Wang, J. Nanoparticle-based electrochemical DNA detection. *Analytica Chimica Acta* **500**, 247-257, doi:**HTTP://DX.DOI.ORG/10.1016/S0003-2670(03)00725-6** (2003).

7 Civit, L., Fragoso, A., Hölters, S., Dürst, M. & O'Sullivan, C. K. Electrochemical genosensor array for the simultaneous detection of multiple high-risk human papillomavirus sequences in clinical samples. *Analytica Chimica Acta* **715**, 93-98, doi:https://doi.org/10.1016/j.aca.2011.12.009 (2012).

8 Dequaire, M. & Heller, A. Screen printing of nucleic acid detecting carbon electrodes. *Analytical chemistry* **74**, 4370-4377 (2002).

9 Ortiz, M., Torrens, M., Fragoso, A. & O'Sullivan, C. K. Highly sensitive colorimetric enzyme-linked oligonucleotide assay based on cyclodextrin-

modified polymeric surfaces. *Analytical and bioanalytical chemistry* **403**, 195-202, doi:10.1007/s00216-012-5791-3 (2012).

10 Zhijie Wang, Y. Y., Kailiang Leng, Jishan Li, Fan Zheng, Guoli Shen & Ruqin Yu. A Sequence-Selective Electrochemical DNA Biosensor Based on HRP-Labeled Probe for Colorectal Cancer DNA Detection. *Analytical Letters* **41**, 24-35, doi:10.1080/00032710701746873 (2008).

11 Alfonta, L., Singh, A. K. & Willner, I. Liposomes Labeled with Biotin and Horseradish Peroxidase: A Probe for the Enhanced Amplification of Antigen−Antibody or Oligonucleotide−DNA Sensing Processes by the Precipitation of an Insoluble Product on Electrodes. *Analytical chemistry* **73**, 91-102, doi:10.1021/ac000819v (2001).

12 Genç, R., Murphy, D., Fragoso, A., Ortiz, M. & O'Sullivan, C. K. Signal-Enhancing Thermosensitive Liposomes for Highly Sensitive Immunosensor Development. *Analytical chemistry* **83**, 563-570, doi:10.1021/ac1023765 (2011).

13 Niemeyer, C. M. Nanoparticles, Proteins, and Nucleic Acids: Biotechnology Meets Materials Science. *Angewandte Chemie International Edition* **40**, 4128-4158, doi:10.1002/1521-3773(20011119)40:22<4128::AID-ANIE4128>3.0.CO;2-S (2001).

14 Rosi, N. L. & Mirkin, C. A. Nanostructures in Biodiagnostics. *Chemical reviews* **105**, 1547-1562, doi:10.1021/cr030067f (2005).

15 Wajs, E., Caldera, F., Trotta, F. & Fragoso, A. Peroxidase-encapsulated cyclodextrin nanosponge immunoconjugates as a signal enhancement tool in optical and electrochemical assays. *Analyst* **139**, 375-380, doi:10.1039/C3AN01643A (2014).

16 Mirkin, C. A., Letsinger, R. L., Mucic, R. C. & Storhoff, J. J. A DNA-based method for rationally assembling nanoparticles into macroscopic materials. *Nature* **382**, 607-609 (1996).

17 Xu, K., Huang, J., Ye, Z., Ying, Y. & Li, Y. Recent development of nano-materials used in DNA biosensors. *Sensors* **9**, 5534-5557, doi:10.3390/s90705534 (2009).

18 Zanoli, L. M., D'Agata, R. & Spoto, G. Functionalized gold nanoparticles for ultrasensitive DNA detection. *Analytical and bioanalytical chemistry* **402**, 1759-1771, doi:10.1007/s00216-011-5318-3 (2012).

19 Gibson, J. S. Nucleic acid-based assays for the detection of high-risk human papillomavirus: A technical review. *Cancer Cytopathology* **122**, 639-645, doi:10.1002/cncy.21451 (2014).

20 Jana, R., Hazbun, T. R., Fields, J. D. & Mossing, M. C. Single-Chain Lambda Cro Repressors Confirm High Intrinsic Dimer–DNA Affinity. *Biochemistry* **37**, 6446-6455, doi:10.1021/bi980152v (1998).

21 Pabo, C. O. & Sauer, R. T. Protein-DNA recognition. *Annual review of biochemistry* **53**, 293-321, doi:10.1146/annurev.bi.53.070184.001453 (1984).

22 Albright, R. A. & Matthews, B. W. Crystal structure of λ-Cro bound to a consensus operator at 3.0 Å resolution1. *Journal of molecular biology* **280**, 137-151, doi:https://doi.org/10.1006/jmbi.1998.1848 (1998).

23 Gajhede, M., Schuller, D. J., Henriksen, A., Smith, A. T. & Poulos, T. L. Crystal structure of horseradish peroxidase C at 2.15 A resolution. *Nature structural biology* **4**, 1032-1038 (1997).

24 Munteanu, M. G., Vlahovicek, K., Parthasarathy, S., Simon, I. & Pongor, S. Rod models of DNA: sequence-dependent anisotropic elastic modelling of local bending phenomena. *Trends in biochemical sciences* **23**, 341-347 (1998).

25 Acero Sanchez, J. L. *et al.* Colorimetric quantification of mRNA expression in rare tumour cells amplified by multiple ligation-dependent probe

amplification. *Analytical and bioanalytical chemistry* **397**, 2325-2334, doi:10.1007/s00216-010-3830-5 (2010).

26 Gumustas, M. O., S. A. . The Role of and the Place of Method Validation in Drug Analysis Using Electroanalytical Techniques. *The Open Analytical Chemistry Journal* **5**, 1-21 (2011).

27 Tasoglu, S. *et al.* Advances in Nanotechnology and Microfluidics for Human Papillomavirus Diagnostics. *Proceedings of the IEEE* **103**, 161-178, doi:10.1109/JPROC.2014.2384836 (2015).

2.8 SUPPLEMANTARY MATERIAL

Table S-2.1: Sequences of the oligonucleotides used in this work. The specific DNA binding sites for scCro protein are underlined. The length of the oligos is shown in nucleotides (nt).

ssDNA oligo (length) (5' to 3' sequence)
***sccro16* forward primer (39 nt)** CTCTCCATATGTGTGAACAACGCATAACTTTAAAAGATT
***sccro16* reverse primer (33 nt)** GAGTAACAAAAAAACAACAGCAAAGCTTGAGAG
HPV16 capture probe (24 nt) biotin-C6-GAGGAGGAGGATGAAATAGATGGT
HPV16 target (159 nt) GCCCATTAACAGGTCTTCCAAAGTACGAATGTCTACGTGTGTGCTTTGTACGCACAACCGAAGCGTAGAGTCACACTTGCAACAAAAGGTTACAATATTGTAATGGGCTCTGTCCGGTTCTGCTTGTCCAGCTGGACCATCTATTTCATCCTCCTCCTC
Detection probe-HRP conjugate (21 nt) TTGGAAGACCTGTTAATGGGC-HRP
Detection probe with one scCro DNA binding site (46 nt) TTGGAAGACCTGTTAATGGGCGCAACTATCACCGCAAGTGATACGA
Complementary strand for detection probe with one scCro DNA binding site (25 nt) TCGTATCACTTGCGGTGATAGTTGC
Detection probe with three scCro DNA binding sites (93 nt) TTGGAAGACCTGTTAATGGGCGCAACTATCACCGCAAGTGATAAAAAAAAATATCACCGCAAGTGATAAAAAAAAATATCACCGCAAGTGATA

Table S-2.1: (continued)

ssDNA oligo (length) (5' to 3' sequence)
Complementary strand for detection probe with three scCro DNA binding sites (72 nt)
TATCACTTGCGGTGATATTTTTTTTTATCACTTGCGGTGATATTTTTTTTTATCACTTGCGGTGATAGTTGC
Control sequence 1 (CDH1) (133 nt)
GGGTTCCCTAAGGGTTGGACCTTGGAGGAATTCTTGCTTTGCTAATTCTGATTCTGCTGCTCTTGCTGTTTCTTCGGAGGAGAGCGATAGGCTGGTTCGTAATCGGTCTAGATTGGATCTTGCTGGCGCGTCC
Control sequence 2 (HLA-DQA1*0201) (97 nt)
GAGAGGAAGGAGACTGCCTGGCGGTGGCCTGAGTTCAGCAAATTTGGAGGTTTTGACCCGCAGGGTGCACTGAGAAACATGGCTGTGGCAAAACACA

2.8.1 Preparation of the hybrid ssDNA-dsDNA HPV16 detection probes

Partially complementary ssDNA oligos (see the sequences in Table S2-1) were hybridized by mixing 10 μM of each oligo in 10 mM potassium phosphate pH 7.5, 50 mM NaCl, 5 mM EDTA, 5 % glycerol. The mixtures were heated in a thermal cycler for 5 min at 95°C and then cooled down to 25°C by reducing the temperature 1°C per minute. The efficiency of the hybridization reactions was monitored by DNA gel electrophoresis using a 10 % polyacrylamide in TAE buffer that was run for 90 min at 100 V in TAE buffer and stained with SYBR Safe DNA gel stain in the same buffer for 5 min (see Fig. S-2.1).

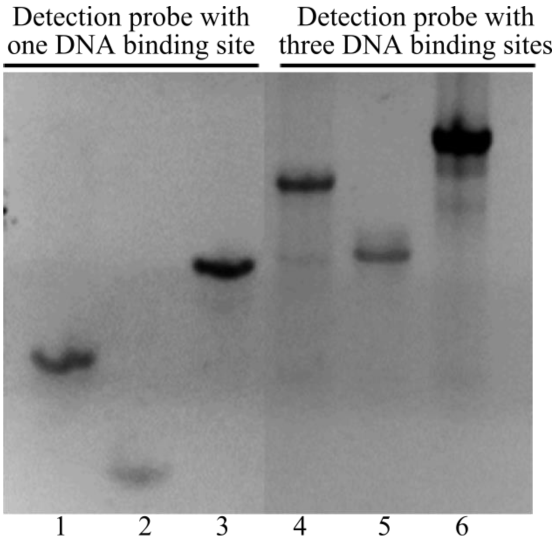
Detection probe with one DNA binding site
Detection probe with three DNA binding sites
1
2
3
4
5
6

Figure S-2.1: Preparation of the hybrid ssDNA-dsDNA HPV16 detection probes. Lane 1: detection probe with one DNA binding site; lane 2: detection probe with one DNA binding site partial complementary strand; lane 3: hybridization reaction of ssDNA oligos in lanes 1 and 2; lane 4: detection probe with three DNA binding sites; lane 5: detection probe with three DNA binding sites partial complementary strand; lane 6: hybridization reaction of ssDNA oligos in lanes 4 and 5. Lanes 1, 2, 4, 5 contain ssDNA whereas lanes 3 and 6 hybrid ssDNA-dsDNA.

2.8.2 EMSA for the binding of scCro to the oligonucleotides involved in HPV16 detection

The binding of scCro to different combinations of the oligonucleotides involved in the detection of HPV16 was evaluated by EMSA. Combinations of the capture probe, the detection probe with one DNA binding site and the target HPV16 (100 nM each) were pre-hybridized as described above and then each mixture was incubated with scCro (500 nM) and run on 6 % polyacrylamide gel in TAE buffer. As it can be seen in Fig. S-2.2, scCro binds only to the combination of oligos that contain the specific dsDNA binding sites (bands with asterisks).

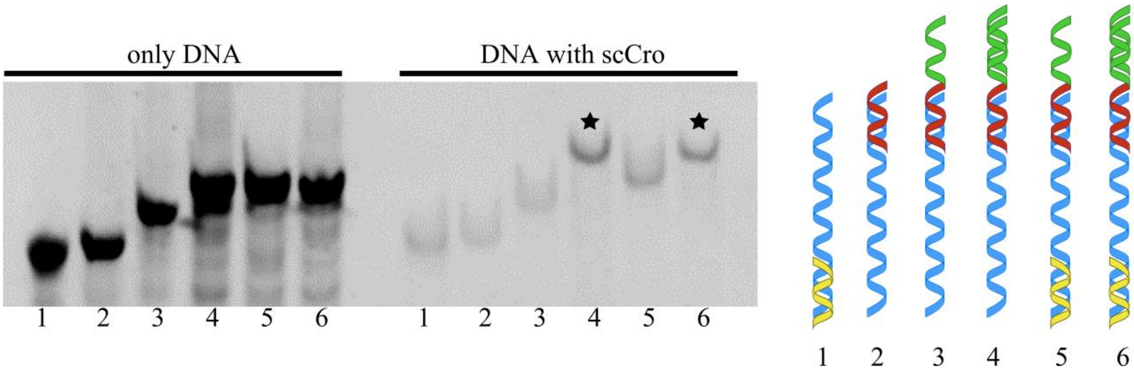

Figure S-2.2: Binding of scCro to the oligonucleotides used for the detection of HPV16 by EMSA. Lane 1: capture probe with target; lane 2: target with detection probe; lane 3: target with detection probe with one DNA binding site (ssDNA oligo); lane 4: target with detection probe with one DNA binding site (ssDNA-dsDNA hybrid); lane 5: capture probe with target and detection probe with one DNA binding site oligo (ssDNA oligo); lane 6: capture probe with target and detection probe with one DNA binding site (ssDNA-dsDNA hybrid). Bands with asterisks show protein-bound DNA.

2.8.3 Optimization of the HRP-scCro conjugation reaction

Maleimide-activated HRP and cys-scCro were mixed at different molar ratios: equimolar mixtures and mixtures with excess of one of the two proteins. Reactions were conducted in PBS pH 7 with overnight incubation at 4°C. Samples were analyzed by SDS-PAGE (Fig. S-2.3) and the optimum conditions (equimolar mixture) were chosen for scale-up reaction.

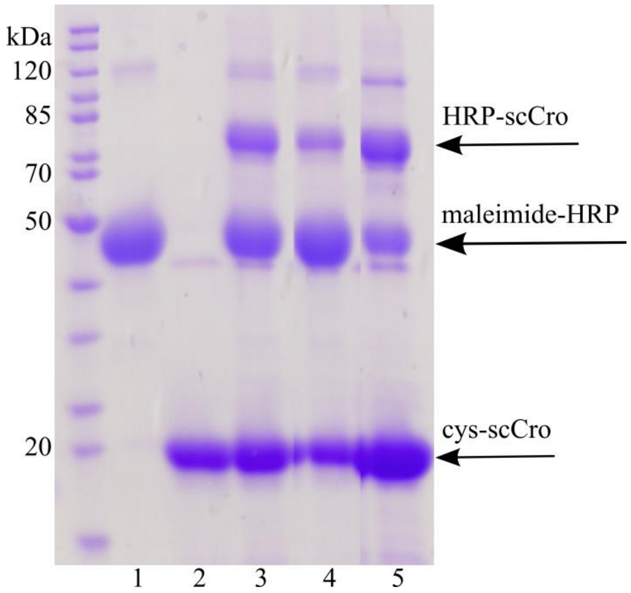

Figure S-2.3: Optimization of the HRP-scCro conjugation reaction. Lane 1: maleimide-HRP; lane 2: cys-scCro; lane 3: maleimide-HRP:cys-scCro molar ratio 1:1 (50 µM each); lane 4: maleimide-HRP:cys-scCro molar ratio 3:1 (60 µM:20 µM); lane 5: maleimide-HRP:cys-scCro molar ratio 1:3 (32 µM:96 µM).

2.8.4 MALDI-TOF mass spectrometry for the HRP-scCro conjugate

Protein samples (30 µM in 0.1 % TFA) were mixed with DHAP matrix solution prior to spotting on a ground steel target plate. For external quadratic calibration, the Bruker "Protein Calibration Standard 2" was used. All spectra were acquired on the new ultrafleXtreme MALDI-TOF/TOF mass spectrometer equipped with a 2 kHz Bruker smartbeam-II solid state laser and a FlashDetector. Prior to calibration, the spectra were processed with Flex analysis using smoothing and baseline subtraction. The analysis was performed using the equipment of Servei de Recursos Científics i Tècnics (Universitat Rovira i Virgili, Reus, Spain). The spectra and the ion species of the proteins analyzed are shown in Fig. S-2.4 and Table S-2.2.

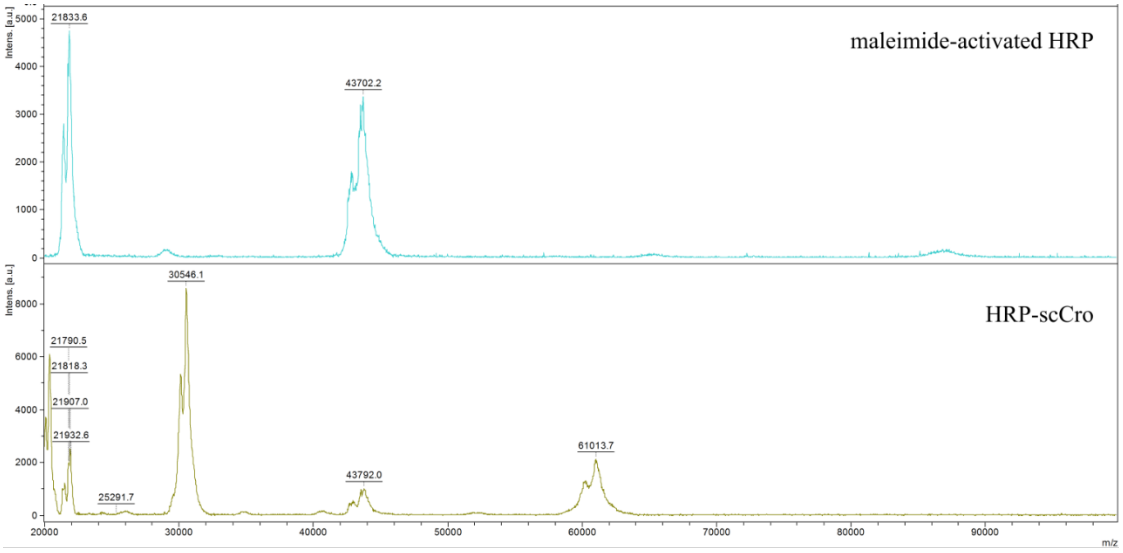

Figure S-2.4: MALDI-TOF mass spectra of maleimide-HRP and HRP-scCro conjugate.

Table S-2.2: Ion species of the proteins analyzed by MALDI-TOF MS.

Protein	**Ion**	**Mass**
maleimide-HRP	[M+2H]2+	21859.6
maleimide-HRP	[M+H]+	43717.1
HRP-scCro	[M+2H]2+	30546.0
HRP-scCro	[M+H]+	61170.6

Chapter 3

Nucleic acid sensing with enzyme-DNA binding protein conjugates cascade and simple DNA nanostructures

Analytical and Bioanalytical Chemistry 2017, 409:3623–3632

Chapter 3: Nucleic acid sensing with enzyme-DNA binding protein conjugates cascade and simple DNA nanostructures

3.1 ABSTRACT

A versatile and universal DNA sensing platform is presented based on enzyme-DNA binding protein tags conjugates and simple DNA nanostructures. Two enzyme conjugates were thus prepared, HRP-scCro and GOx-dHP, and were used in conjunction with a hybrid ssDNA-dsDNA detection probe. This probe served as a simple DNA nanostructure allowing first for target recognition through its target-complementary ssDNA part and then for signal generation after conjugate binding on the dsDNA containing the specific binding sites for the dHP and scCro DNA binding proteins. The DNA binding proteins chosen in this work have different sequence specificity, high affinity and lack of cross-reactivity. The proposed sensing system was validated for the detection of model target ssDNA from high-risk human papillomavirus (HPV16) and a limit of detection at the low picomolar range was achieved. The performance of the platform in terms of limit of detection was comparable to direct HRP systems using target-specific oligonucleotide-HRP conjugates. The ratio of the two enzymes can be easily manipulated by changing the number of binding sites on the detection probe, offering further optimization possibilities of the signal generation step. Moreover, since the signal is obtained in the absence of externally added hydrogen peroxide, the described platform is compatible with paper-based assays for molecular diagnostics applications. Finally, just by changing the ssDNA part of the detection probe, this versatile nucleic acid platform can be used for the detection of different ssDNA target sequences or in a multiplex detection configuration without the need to change any of the conjugates.

3.2 INTRODUCTION

The field of molecular diagnostics is one of the fastest growing sectors in clinical analysis [1], with the DNA diagnostics market expected to generate $19 billion globally by 2020 [2]. Clinical applications of molecular diagnostics are usually found in the areas of genetic diseases, cancer, infectious diseases, pharmacogenomics as well as special applications like HLA typing and forensic science [3]. The association of specific DNA sequences with disease as well as the recent outbreaks of infectious diseases like Ebola, MERS and Zika viruses has increased the demand for rapid, sensitive and point-of-care testing.

Usually, the platforms used for DNA detection rely on hybridization of the target ssDNA sequence with complementary sequences in order to facilitate the recognition and detection with specific capture and detection probes, respectively. For the detection step, a signal amplification strategy is often used in order to generate a reliable signal after target identification that will subsequently allow its quantification [4]. Target-specific labeled oligonucleotides are commonly used for this purpose, resulting in elevated assay costs due to the additional labeling. In our previous work we reported the development of a universal, target-independent signal amplification approach in DNA biosensors. A novel horseradish peroxidase-DNA binding protein conjugate (HRP-scCro) was described and used for the detection of a model target ssDNA through the binding of the scCro DNA binding protein with its specific sequence contained in the hybrid ssDNA-dsDNA detection probe [5]. A signal enhancement effect was observed according to the number of conjugate binding sites on the detection probe leading to increased biosensor sensitivity.

In the present report, we combine the synergistic action of HRP with glucose oxidase (GOx) to provide a measurable signal with the properties of DNA binding proteins of high affinity and specificity regarding their dsDNA binding sequences in order to detect the target ssDNA (Fig. 3.1). The system relies on target recognition by a specific capture probe while target detection is accomplished by using a hybrid ssDNA-dsDNA detection probe and the two enzymes as DNA binding protein conjugates. The detection probe contains the specific sequence required for target hybridization (ssDNA) and the two distinct sequences for the binding of the enzyme-DNA binding protein tag conjugates (dsDNA) (Fig. 3.1 (B)). The bienzymatic HRP/GOx cascade system has been used extensively over the decades due to the numerous advantages it presents, such as rapid signal generation, high enzyme stability, possibility for immobilization without significant loss of activity, low cost and high turnover numbers [6-11]. At the same time, the *in situ* generation of hydrogen peroxide from the GOx-catalyzed oxidation of glucose has promoted the wide use of this bienzymatic system as a convenient method to avoid the direct utilization and storage of hydrogen peroxide in point-of-care biosensors. The catalytic efficiency of this cascade enzyme reaction strongly depends on the diffusion of hydrogen peroxide since HRP has a much higher turnover rate than GOx [11] and this diffusion is regulated by the distance between the active sites of the two enzymes. In the system described herein, the target detection probe served as a simple DNA nanostructure for the spatial organization of the two enzyme conjugates in such a way as to allow their simultaneous binding avoiding steric hindrance effects, minimize hydrogen peroxide diffusion and provide improved performance of the sensor for target detection. Furthermore, the signal generation step could be further optimized by altering the ratio of the two enzymes and this was easily accomplished by changing the number of the DNA binding sites on the detection probe. The preparation and characterization of the enzyme-DNA binding protein tag conjugates, along with optimization of conditions for DNA detection are discussed in detail. The proposed platform was used to detect ssDNA from the model target high-risk human papillomavirus HPV type 16.

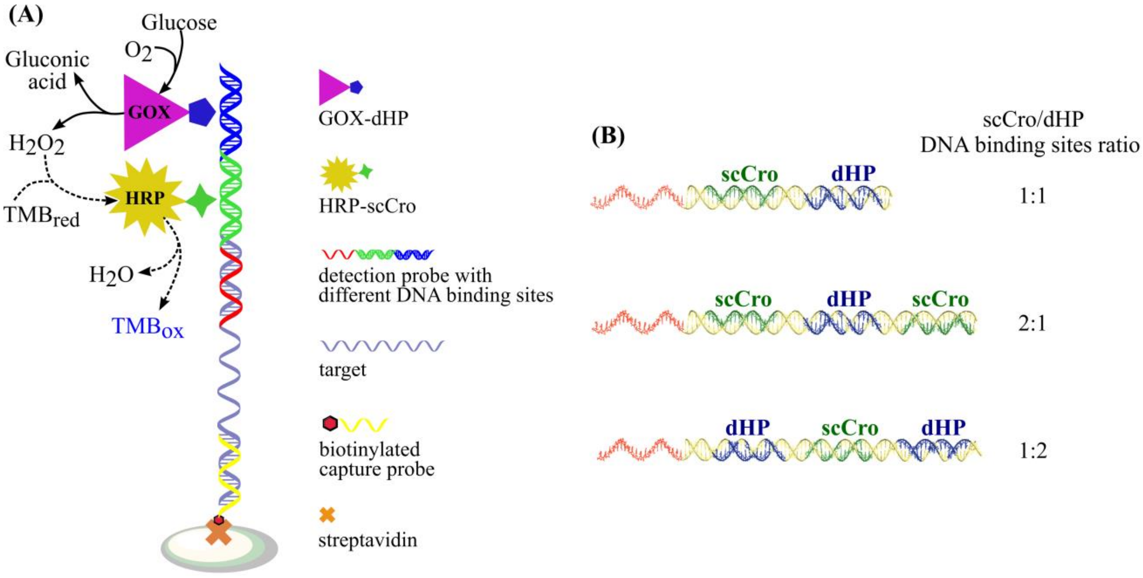
(A)
Glucose
O_2
Gluconic acid
GOX
H_2O_2
TMB_{red}
HRP
H_2O
TMB_{ox}
GOX-dHP
HRP-scCro
detection probe with different DNA binding sites
target
biotinylated capture probe
streptavidin
(B)
scCro/dHP DNA binding sites ratio
scCro
dHP
1:1
scCro
dHP
scCro
2:1
dHP
scCro
dHP
1:2

Figure 3.1: (A) Detection of target ssDNA based on DNA binding proteins-enzyme conjugates. (B) Hybrid ssDNA-dsDNA detection probes with scCro/dHP DNA binding sites stoichiometry of 1:1, 2:1 and 1:2. The binding sites (highlighting the nucleotide bases that directly participate in the dsDNA-protein interactions) for scCro are shown in green and for dHP in blue.

3.3 EXPERIMENTAL

3.3.1 Materials

PCR reagents, restriction enzymes (*Nco*I and *Hind*III), plasmid pBADmychisA, sulfo-SMCC, HisPure Ni-NTA-agarose, SP Sepharose FF, maleimide-activated HRP and neutravidin-coated microplate strip plates were purchased from Fisher Scientific (Barcelona, Spain). Glucose oxidase from *Aspergillus niger* and antibodies were obtained from Sigma (Madrid, Spain) and the Immun-Blot PVDF membrane from Bio-rad (Barcelona, Spain). The DNA oligonucleotides were purchased from Biomers.net (Ulm, Germany) and Eurofins (Ebersberg, Germany) and their sequences are shown in Table S-3.2 (Supplementary material). The sequences of the oligonucleotides used for HPV16 detection (ssDNA capture and detection probes, ssDNA synthetic HPV16 target) were based on previously reported sequences, which were verified for the detection of DNA extracted from cervical scrapes through PCR [12]. All other reagents were purchased from Fisher Scientific (Barcelona, Spain), Sigma-Aldrich (Madrid, Spain) and Scharlau (Barcelona, Spain).

3.3.2 Preparation of the enzyme-DNA binding protein tag conjugates

The HRP-scCro conjugate was prepared as described previously [5]. For the preparation of the GOx-dHP conjugate, glucose oxidase was initially reacted with a ten-fold excess of sulfo-SMCC for 1 h at 25°C in conjugation buffer (PBS, pH 7) in order to label the protein's free amines with maleimide groups. Excess crosslinker was removed using a desalting column equilibrated with conjugation buffer. Then, maleimide-activated GOx and cys-dHP (prepared as detailed in part S1 of the Supplementary material) were mixed at equimolar concentrations in conjugation buffer and the mixture was incubated overnight at 4°C. The GOx-dHP conjugate was purified by immobilized metal affinity chromatography (IMAC) and ion exchange chromatography (IEC). For IMAC, a HisPur Ni-NTA-agarose column was washed with equilibration buffer (10 mM potassium phosphate, 300 mM NaCl, pH 7.4) and then loaded with the conjugation mixture. The column was washed with equilibration buffer containing 10 mM imidazole and the conjugation product was eluted with the same buffer containing 500 mM imidazole. The buffer of the IMAC elution fraction was exchanged to IEC buffer (20 mM Tris-HCl, pH 7) and the sample was loaded on a DEAE Sepharose FF weak cation exchange resin-packed column equilibrated with the same buffer. The conjugate was eluted with IEC buffer containing 1 M NaCl and the buffer was exchanged to storage buffer (100 mM potassium phosphate pH 5.1, 50 % glycerol). The concentration of the conjugate was calculated using the absorbance at 452 nm of the FAD cofactor of GOx (ε_{452nm}=12.83 cm^{-1} mM^{-1}) [13]. The process was monitored by SDS-PAGE, native PAGE and Western blot. For Western blot, the PVDF membrane after transfer was probed with monoclonal mouse anti-His antibody and then with polyclonal rabbit anti-mouse-HRP antibody and finally the bands were detected with 1-STEP TMB-Blot solution. For native PAGE, proteins were separated on a 7.5% polyacrylamide gel in Tris-glycine buffer (pH ~ 8.3). MALDI-TOF mass spectrometry was used to calculate the exact molecular weight of the conjugate.

3.3.3 Preparation and characterization of the hybrid ssDNA-dsDNA detection probes

The detection probes, containing binding sites for the enzyme-DNA binding protein tag conjugates at different stoichiometries, were prepared by the hybridization of partially complementary ssDNA oligonucleotides (pairs P88/P89, P92/P93, P94/P95) with sequences as described in Table S-3.2 (Supplementary material). Each oligonucleotide pair were mixed in hybridization buffer (10 mM Tris-HCl pH 7.5, 50 mM NaCl, 1 mM EDTA) at a final concentration of 10 µM each oligo in a total of 20 µl, heated for 5 min at 95°C and then cooled to 25°C by 1°C/min. Hybridization was validated by gel electrophoresis of the hybridization reactions as shown in Fig. S-3.2 (Supplementary material). Electrophoretic mobility shift assay (EMSA) was also used to evaluate the binding of the enzyme conjugates HRP-scCro and GOx-dHP to the prepared detection probe containing one binding site for each enzyme conjugate. The binding mixtures were prepared in a total volume of 20 µl in binding buffer (20 mM potassium phosphate pH 7.5, 50 mM NaCl, 1 mM EDTA, 0.05 % Tween-20, 5 % glycerol). The detection probe (final concentration 200 nM) was incubated for 1 hour at room temperature with each protein species separately (final concentration 600 nM of each maleimide-activated HRP, maleimide-activated GOx, cys-scCro, cys-dHP, HRP-scCro and GOx-dHP) and also in mixtures of the two DNA binding proteins and their conjugates. The binding mixtures were then separated on a 5 % polyacrylamide/TAE gel for 60 min at 80V in TAE buffer and finally visualized by GelRed DNA gel staining.

3.3.4 Colorimetric detection of DNA with ELONA

Detection of the model target HPV16 ssDNA was achieved with a colorimetric enzyme linked oligonucleotide assay (ELONA) using neutravidin-coated microplate wells. The buffer used for DNA immobilization and the hybridization steps was ELONA buffer (20 mM potassium phosphate pH 7.5, 50 mM NaCl, 1 mM EDTA, 0.5 % BSA, 0.05 % Tween-20), whereas for washing the same buffer was used without BSA. The immobilization of the biotinylated capture probe (50 µl) was performed for 15 min at room temperature and the wells were washed three times with 300 µl of wash buffer before the addition of target ssDNA (50 µl). Capture probe-target hybridization was allowed to proceed for 1 h at 37°C followed by three washes with 300 µl of wash buffer and the addition of 50 µl of pre-hybridized ssDNA-dsDNA detection probes (with one or two binding sites for each DNA binding protein, prepared as described in Section 2.3). Hybridization was carried out for 1 h at 37°C and after three washes with 300 µl of wash buffer, the equimolar mixture of the two conjugates HRP-scCro and GOx-dHP was added and incubation proceeded for 1 h at room temperature. After a final washing step (three times of 300 µl wash buffer), 50 µl of a mixture of 250 mM glucose and 1 mM TMB (freshly prepared in 100 mM potassium phosphate pH 5) were added to the wells and the absorbance at 650 nm was monitored for 45 min at room temperature using a Cary 100 Bio UV visible Spectrophotometer. Color development was stopped by the addition of 50 µl of 1 M H_2SO_4 and finally the absorbance at 450 nm was measured. Optimization of the ELONA assay was performed in terms of capture and detection probes concentration as well as the addition order of the enzyme-DNA binding proteins conjugates using the general ELONA assay setup described above. Optimized conditions were finally used to obtain target calibration curves.

3.3.4.1 Optimization of capture probe concentration

The capture probe concentration used to immobilize on the neutravidin-coated microplate was titrated from 10 nM to 50 nM. The target ssDNA was used at 1 nM, the detection probes with scCro/dHP DNA binding sites ratio of 2:1 and 1:2 at 3 nM and the enzyme conjugates (HRP-scCro and GOx-dHP) at 5 nM each with simultaneous addition.

3.3.4.2 Optimization of detection probe concentration

Using a capture probe concentration of 20 nM and the target ssDNA at 1 nM, the concentration of the detection probes was titrated from 0.2 nM to 3 nM. The three detection probes with scCro/dHP DNA binding sites ratio of 1:1, 2:1 and 1:2 were used, while the enzyme conjugates were added simultaneously (5 nM each).

3.3.4.3 Binding order of the enzyme-DNA binding protein tags conjugates

The capture probe, target ssDNA and each of the three detection probes were used at constant concentrations of 50 nM, 1 nM and 3 nM, respectively. The two conjugates HRP-scCro and GOx-dHP (5 nM each) were added either simultaneously (GOx-dHP + HRP-scCro) or in two steps: the first conjugate was allowed to bind initially, then the wells were washed three washes with 300 µl wash buffer and finally the second conjugate was added (first HRP-scCro and second GOx-dHP or first GOx-dHP and second HRP-scCro).

3.3.4.4 Target ssDNA calibration curves

The biotinylated HPV16 capture probe was used at 20 nM, target ssDNA at concentrations up to 1 nM, the detection probes (with one or two binding sites for each DNA binding protein, prepared as described in Section 2.3) at 3 nM and finally the two conjugates HRP-scCro and GOx-dHP (5 nM each) were finally added simultaneously. Each sample was measured in triplicate with three independent experiments, whereas the blank measurements were conducted in sextuplets. Limit of detection (LOD) for each detection probe was calculated as the average of blank measurements plus three times the standard deviation of the blank measurements.

3.3.4.5 ELONA assay specificity

The specificity of the detection platform was studied by performing the ELONA assay using optimized conditions (as described above for the target calibration curves) with 5 nM of ssDNA from the target HPV16 and control non-complementary sequences from breast cancer markers (CDH1 and HUWE1) and a celiac disease marker (HLA-DQ1*0201). All the sequences used are shown in Table S-3.4 (Supplementary material).

3.4 RESULT AND DISCUSSION

3.4.1 DNA binding protein tags

The DNA sensing platform described in this work is based on the synergistic action of two enzymes, HRP and GOx, in order to link the step of target ssDNA recognition and signal generation for detection (Fig. 3.1A). Therefore, two DNA binding proteins with different dsDNA binding sequence specificities were needed to be conjugated to the two enzymes respectively. In a previous work we developed a single-chain dimeric DNA binding protein of the bacteriophage lambda repressor protein (Cro) with an N-terminal cysteine for conjugation purposes [5]. It was then conjugated to HRP and the enzyme-DNA binding protein tag conjugate was used for signal amplification in the detection of model target ssDNA. Here, a second DNA binding protein was chosen, the headpiece domain of LacI protein, for conjugation to GOx based on the same criteria of size, affinity and specificity used for the first DNA binding protein tag chosen, Cro. The two proteins have different sequence specificities, a property that will ensure their specific binding to their respective sequences, avoiding cross-reactivity issues. LacI is a homotetrameric repressor protein from *Escherichia coli* which regulates the transcriptional activity of the lactose operon [14]. It has a promoter-operator interaction region [headpiece domain, LacI(1-58)] which binds to a specific dsDNA sequence with very high affinity and specificity (K_D=30 pM, [15]). Using this DNA binding domain, a new DNA binding protein was engineered by linking together two LacI headpiece domains since the native protein binds DNA as a homodimer. The crystal structure of the homodimeric headpiece domain bound to an operator DNA sequence [15,16] suggested that a GGSGGS flexible peptide linker could be used to link the two monomers because of the close proximity of the polypeptide ends to be linked. In addition, it also indicated that a C-terminal poly-histidine tag could be added for purification purposes without impacting binding. In order to facilitate conjugation of the DNA binding protein, a single cysteine residue was added to its N-terminus taking advantage of the absence of cysteine residues in the native headpiece sequence. This single-chain homodimeric LacI headpiece domain protein with an engineered N-terminal cysteine (cys-dHP) was cloned and expressed in soluble form in *E. coli* (see Supplementary material, part S3-1). The majority of protein contaminants were removed by IMAC via the C-terminal poly-histidine tag and the IMAC elution fraction was further polished with cation exchange chromatography. The purified protein cys-dHP was finally obtained at more than 90% purity with a total yield of approximately 2 mg/L of bacterial culture.

3.4.2 Enzyme-DNA binding protein tag conjugates

The proposed DNA detection system relies on the use of two DNA binding protein-enzyme conjugates, HRP-scCro and GOx-dHP, for signal generation. The preparation and characterization of the HRP-scCro conjugate has already been described in our previous work [5]. To prepare the GOx-dHP conjugate the heterobifunctional crosslinker sulfo-SMCC was used in order to covalently link solvent accessible amine groups of GOx with the single thiol group of dHP. GOx is a homodimeric glycosylated protein with a molecular weight of 130-320 kDa depending on the extent of the glycosylation pattern [17]. The enzyme most commonly used in biochemical assays is isolated from *Aspergillus niger* with two subunits with a molecular weight of 80 kDa each and approximately 18% sugars. According to its amino acid sequence and crystal structure (using the structure 3QVP.pdb), there are 14 amine groups on the surface of the protein that can potentially react with sulfo-SMCC. On the other hand, the DNA binding protein cys-dHP contains only one thiol group that has been specifically engineered (in the form of a single cysteine residue) at its N-terminal to enable its conjugation with maleimide-containing molecules. The amine groups of GOx were activated with an excess of sulfo-SMCC and the conjugation with cys-dHP was performed using an equimolar mixture of the two proteins in order to achieve a low conjugation ratio. After overnight incubation at 4°C, the efficiency of the conjugation reaction was estimated at approximately 25% by comparing the intensity of the SDS-PAGE bands corresponding to cys-dHP before and after conjugation (Fig. 3.2 (A), lanes 1 and 4) using the ImageJ program. Different conditions for the activation of GOx with sulfo-SMCC as well as the use of molar excess of either protein in the conjugation reaction did not improve the conjugation efficiency (results not shown). The GOx-dHP conjugate was purified with a two-step procedure enabling the removal of unreacted proteins. With IMAC purification it was possible to remove unreacted maleimide-GOx that did not contain any His-tag (Fig. 3.2 (A), lane 5), whereas IEC was used for the removal of unreacted cys-dHP (Fig. 3.2(A), lane 6) based on the charge difference between the two proteins (GOx pI ~ 4.2 according to the supplier, cys-dHP pI ~7.9 calculated from its amino acid sequence). Based on SDS-PAGE analysis, three protein bands are associated with the conjugate: one at approximately 75 kDa corresponding to the GOx monomer, and two bands at 100 kDa and 100-130 kDa corresponding to potential conjugates of GOx monomers with one and two dHP per monomer, respectively (calculated size of cys-dHP ~16.5 kDa). Western blot analysis revealed two distinct protein species with incorporated His-tag (Fig. 3.2 (B), lane 4) corresponding to the two bands between 100 and 130 kDa identified with SDS-PAGE. These results suggested the synthesis of two conjugation products: one product with one dHP per GOx dimer and one product with two dHP per GOx dimer. To further characterize the conjugate, we performed native PAGE as shown in Fig. 3.2 (C). GOx in its native form migrates on the gel as a single band corresponding to the homodimer (Fig. 3.2 (C), lanes 1 and 2) whereas the conjugate migrates slower as a single band with higher molecular weight (Fig. 3.2 (C) lane 3), corresponding to a single conjugation product. To accurately determine the size of the conjugation product(s) and the GOx:dHP stoichiometry within the conjugate, MALDI-TOF mass spectroscopy was performed. As shown in Fig. 3.2(D), there is one single conjugation product with a molecular weight of approximately 168 kDa corresponding to one GOx homodimer conjugated with one dHP (see Supplementary material for more information). The three distinct bands of the GOx-dHP conjugate identified by SDS-PAGE with molecular weights in the range of 75-120 kDa can be assigned to GOx monomer, and to GOx monomer with one dHP conjugated at different locations on the enzyme molecule surface, resulting in two molecules with different morphologies and electrophoretic mobility within the polyacrylamide gel matrix.

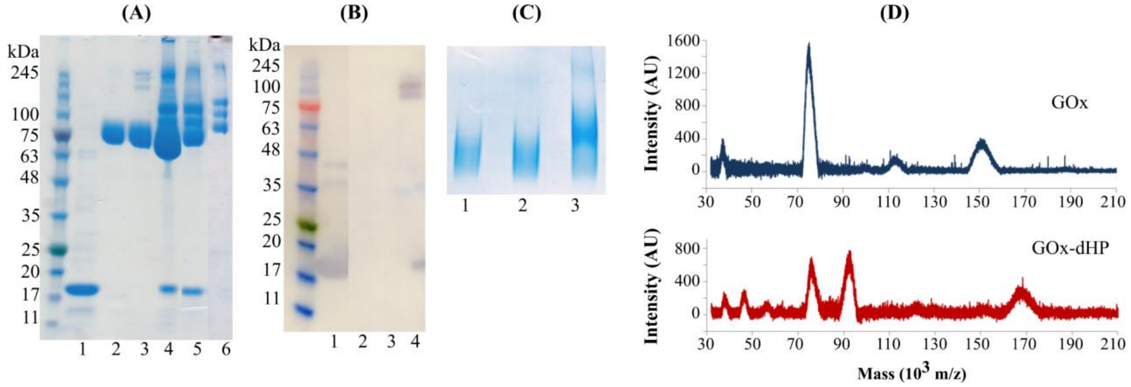

Figure 3.2: Preparation of the GOx-dHP conjugate. (A) SDS-PAGE for the conjugation and purification of GOx-dHP. 1: cys-dHP; 2: GOx; 3: maleimide-GOx; 4: GOx-dHP conjugation reaction; 5: IMAC elution fraction; 6: IEC elution fraction. (B) Detection of conjugate by Western blot. 1: cys-dHP; 2: GOx; 3: maleimide-GOx; 4: GOx-dHP conjugation reaction. (C) Native PAGE. 1: GOx; 2: maleimide-GOx; 3: GOx-dHP conjugate. (D) MALDI-TOF mass spectroscopy spectra of GOx and GOx-dHP purified conjugate.

3.4.3 DNA detection probes

For optimal target detection, the design of the detection probes was performed taking into account the two distinct roles it had to perform, target recognition and signal generation. As detailed in our previous work [5], the detection probes were hybrid consisting of a ssDNA and a dsDNA part: target recognition is accomplished by hybridization with the ssDNA part, whereas the dsDNA contains the specific DNA binding sites for the binding of the DNA binding protein-enzyme conjugates that will ultimately provide the signal for detection. To generate these hybrid detection probes, partially complementary oligonucleotides were hybridized as detailed in the Supplementary material (part S2). A 5-bp spacer was used to separate the two parts and the distinct functions of the probe, hybridization with the target and binding of the enzyme conjugates. In turn, the DNA binding sites were specifically arranged on the dsDNA part of the detection probes and separated by 3-bp spacers to try to minimize steric hindrances and allow the co-binding of both HRP-scCro and GOx-dHP conjugates. Different configurations of the detection probe were designed and prepared in order to vary the stoichiometry of the two enzymes HRP and GOx and study their effect on target detection. For this reason, HRP-scCro/GOx-dHP stoichiometries of 1:1, 2:1 and 1:2 were chosen. Models of the three different detection probes were generated using the online molecular modeling tool model.it® [18], visualized with the PyMOL Molecular Graphics System (Schrödinger, LLC) and they are illustrated in Fig. 3.1(B). As it can be seen, the constant 3-bp spacing between the binding sequences results in different relative orientations of the binding sites on the dsDNA double helix structure. This should facilitate the simultaneous binding of multiple conjugates and minimize any steric hindrance effects that might be encountered due to the size of the conjugates (61 kDa for HRP-scCro and 168 kDa for GOx-dHP).

Successful simultaneous binding of the two DNA binding protein-enzyme conjugates to the detection probe with one binding site for each conjugate was verified with an electrophoretic mobility shift assay (EMSA). The detection probe was incubated separately with different protein species and the samples were separated in a polyacrylamide gel. Free DNA and protein-bound DNA could be separated efficiently because of differences in their mobility. As it is shown in Fig. 3.3, the DNA binding protein tags cys-scCro and cys-dHP as well as their respective enzyme conjugates HRP-scCro and GOx-dHP were able to bind the detection probe and cause a decrease in their mobility depending on the size of the protein bound. The highest decrease was observed for the DNA detection probe bound with the two enzyme conjugates HRP-scCro and GOx-dHP simultaneously (Fig. 3.3 lane 9) because of the total size of proteins bound (approximately 229 kDa). Therefore, EMSA results validated the design of the detection probes and co-binding of the enzyme conjugates.

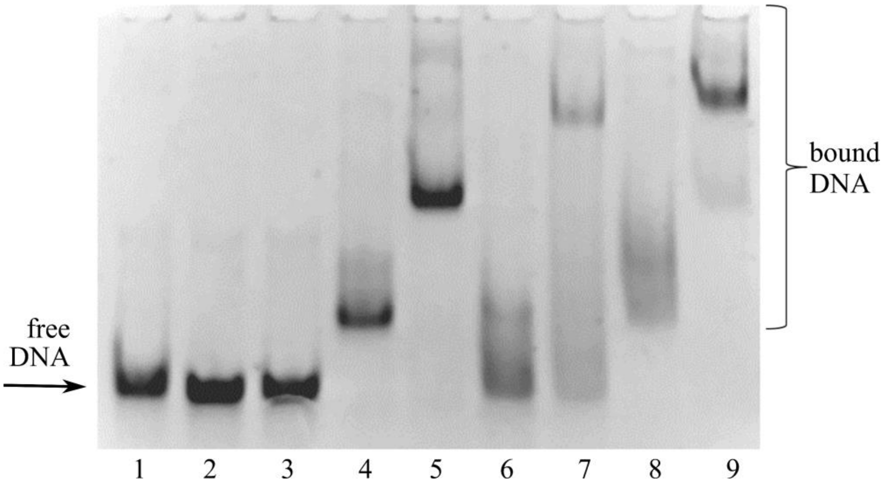

Figure 3.3: EMSA assay for the binding of the DNA binding protein-enzyme conjugates to the HPV16 hybrid detection probe with scCro/dHP DNA binding sites ratio of 1:1. All lanes 1-9 contain the DNA detection probe with different protein species. Lane 1: only DNA; lane 2: HRP; lane 3: GOx; lane 4: cys-scCro; lane 5: HRP-scCro; lane 6: cys-dHP; lane 7: GOx-dHP; lane 8: cys-scCro and cys-dHP; lane 9: HRP-scCro and GOx-dHP.

3.4.4 Target ssDNA detection with ELONA

In the proposed system, DNA detection is based on the use of hybrid ssDNA-dsDNA detection probes and HRP-scCro and GOx-dHP enzyme conjugates for signal generation. The combination of HRP and GOx in a cascade configuration has been reported extensively in the literature in a variety of assays and applied to commercial devices for the detection of various analytes. The system developed in this work is outlined in Fig. 3.1 and it is based on (a) the recognition of target ssDNA by a specific capture probe immobilized on a microtiter plate and (b) detection by the hybrid ssDNA-dsDNA probe containing binding sites for the DNA binding protein-enzyme conjugates HRP-scCro and GOx-dHP. Addition of glucose and TMB initiates the GOx-mediated oxidation of glucose and production of gluconic acid and hydrogen peroxide. Hydrogen peroxide is then scavenged by HRP that reduces it to water using TMB as the electron donor that eventually turns to blue after oxidation and provides the signal. For optimal assay performance, the ELONA was initially optimized in terms of capture and detection probes concentration, as well as the addition order of the DNA binding protein-enzyme conjugates. Firstly, the capture probe concentration was varied from 10 nM to 50 nM while maintaining constant the concentrations of target, detection probes (with one or two binding sites for each enzyme conjugate) and enzyme conjugates. As it can be seen in Fig. 3.4 (A), the use of more than 20 nM of capture probe concentration did not significantly increase the signal irrespectively of the detection probe used, therefore a concentration of 20 nM capture probe was chosen. Next, the concentration of the detection probes was titrated from 0.2 nM to 3 nM. All three detection probes with a HRP-scCro/GOx-dHP stoichiometry of 1:1, 2:1 and 1:2 were used and the enzyme conjugates were added simultaneously at 5 nM each. The data in Fig. 3.4 (B) show a signal increase with the increase of the detection probes concentration thus a concentration of 3 nM was chosen for further work. In addition, the effect of the order in which the enzyme conjugates are added was also explored. The GOx-dHP conjugate is bigger in size (approximately 168 kDa) compared to the HRP-scCro conjugate (61 kDa) and binding of either conjugate might be obstructed by binding of the other depending on the arrangement of the specific DNA binding sites on the detection probe. As it can be seen in Fig. 3.4 (C), the highest signal was obtained when the two enzyme conjugates were added simultaneously, whereas hindrance was observed mainly in the case where the bulkier GOx-dHP conjugate was added first and bound to the detection probe prior to the addition of the second smaller conjugate HRP-scCro.

Using the optimized conditions detailed above, target ssDNA calibration curves were obtained for each of the three detection probes as shown in Fig. 5.4 (D). All three curves were successfully fitted to a quadratic model, to relate the amount of signal (absorbance) to the target ssDNA concentration. This type of polynomial calibration curves have been reported before when these two enzymes were used for analyte detection [19-21]. The limit of detection (LOD) of the assay was also calculated as three times the standard deviation of the blank plus the average of blank measurements. The LODs achieved were all in the low picomolar range: 45

pM, 26 pM and 21 pM for detection using the probes with scCro/dHP DNA binding sites ratio of 1:1, 2:1 and 1:2, respectively. Overall, higher sensitivity and lower LODs were obtained using the detection probe containing one binding site for HRP-scCro and two for GOx-dHP. Also, the performance of the described system in terms of LOD is comparable to the majority of electrochemical biosensors (LODs between 100 pM and 50 nM) that are the most common type used for DNA-based HPV detection (for an extensive review, see [22]). Regarding DNA biosensors in general, the LODs achieved vary from femtomolar to nanomolar and some examples are shown in Table S-3.5 (see Supplementary Material). The electrochemical assays offer the advantage of sensitivity and shorter analysis times but usually require complex surface functionalization and specialized equipment that are not suitable for point-of-care applications [12,23,24]. On the other hand, fluorescence-based detection [25-27] is also very sensitive especially when functionalized silica nanoparticles are employed. As in the case of colorimetric systems [28,29], they rely on biotin/streptavidin interactions or employ target-specific conjugates. For the colorimetric detection of HPV16 ssDNA using a direct HRP-labeled reporter probe for example, an LOD of 7.4 pM was achieved as reported in our previous work [5] which is comparable to the LOD of 21 pM achieved with the combination of the two universal enzyme-DNA binding protein conjugates reported here. Ultrasensitive colorimetric systems employing hybridization chain reaction have also been reported with LOD reaching low femtomolar range [30,31]. but these systems rely on complex DNA nanostructures that are target-dependent, slow to assemble, highly dependent on the specific conditions used, and also require purification before analysis. The results presented in this work highlight the efficiency, simplicity, and sensitivity of the proposed platform compared to other systems as discussed above. It offers the possibility for multiplex detection of analytes, for example in microarrays and lateral flow assays, just by changing the capture probe and the ssDNA part of the ssDNA-dsDNA hybrid detection probe for each specific target. Furthermore, since many optical DNA detection systems rely on biotin/streptavidin interactions, the system could serve as an alternative thus leading to reduced assay costs, as in the case of direct HRP systems, by eliminating the need for specific modification of each target detection oligonucleotide. The replacement of hydrogen peroxide with glucose as enzyme substrate is an additional advantage the proposed platform offers, because it avoids the direct utilization and storage of hydrogenperoxide that is susceptible to decomposition and as a consequence incompatible with paper-based assays. Point-of-care devices using paper-based lateral flow or dipstick assays have dominated the field of rapid diagnostics especially in low-resource settings because of their excellent features and versatility and the proposed bi-enzymatic DNA-based nanostructure platform is compatible with these type of assays.

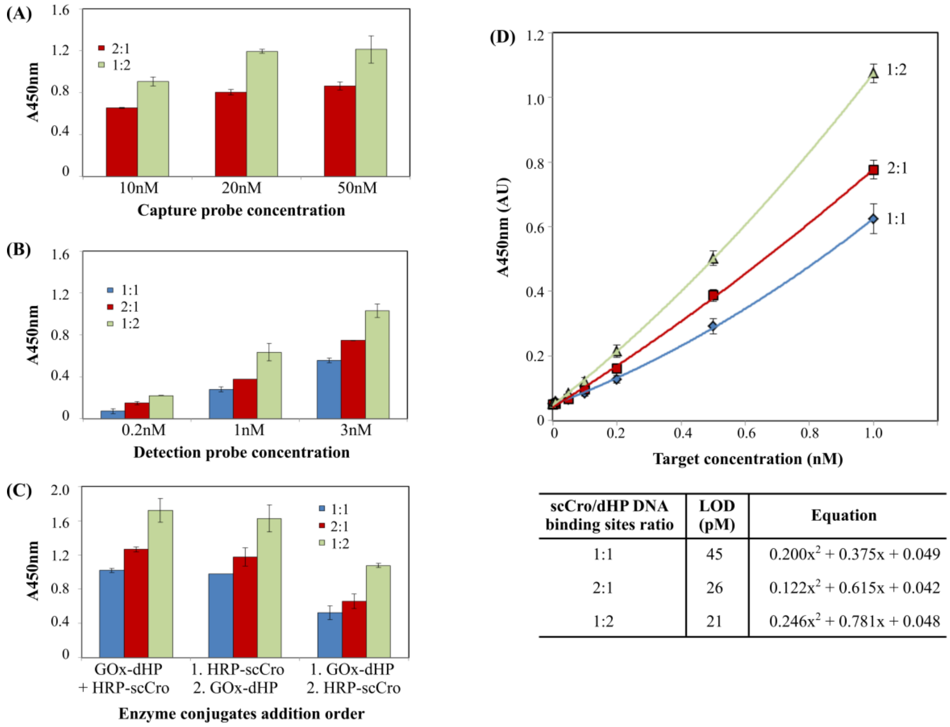

scCro/dHP DNA binding sites ratio	LOD (pM)	Equation
1:1	45	$0.200x^2 + 0.375x + 0.049$
2:1	26	$0.122x^2 + 0.615x + 0.042$
1:2	21	$0.246x^2 + 0.781x + 0.048$

Figure 3.4: DNA detection with ELONA. (A) Optimization of capture probe concentration. (B) Optimization of detection probe concentration. (C) Optimization of the addition order of the enzyme-DNA binding protein conjugates. The error bars show the standard error of the mean (SEM) from triplicate samples. (D) Target calibration curves using detection probes with scCro/dHP DNA binding sites ratio of 1:1, 2:1 and 1:2. The error bars show the SEM from triplicate samples and three independent experiments.

The data obtained in this work also accentuates the importance of the ratio of the HRP and GOx enzymes for optimal performance, with an excess of GOx being favorable for increased assay sensitivity. Since the rate limiting step in the cascade reaction is the production of hydrogen peroxide, excess of GOx increases the amount produced which is in turn scavenged by HRP and used for signal generation. Similar observations have been reported before [32] during the co-immobilization of the two enzymes in copper phosphate-based nanoflowers were the excess of GOx resulted in higher assay sensitivity. In the sensing platform described here, the ratio of the two enzymes was easily manipulated just by changing the sequence of the hybrid ssDNA-dsDNA detection probe, thus demonstrating the flexibility of the proposed immobilization system based on the DNA binding protein tags which allowed further optimization of the signal generation step. Further improvement may be achieved by testing different spacing and orientations of the DNA binding sites, since several reports in the literature demonstrated the importance of the distance between HRP and GOx in a cascade configuration for optimal performance in order to reduce the diffusion of hydrogen peroxide in the bulk solvent, and prevent its decomposition [11,19,33,34].

Finally, the specificity of the detection system, another important feature of biosensors, was evaluated by testing its response to three irrelevant sequences from different disease markers: CDH1 and HUWE1 for breast cancer and HLA-DQA1*0201 for celiac disease. All four sequences including the target were used at high concentration (5 nM) under optimized assay conditions. As it is shown in Fig. 3.5, the system is very specific for the target sequence from HPV16 since extremely low, background-level signal was obtained for the control sequences used.

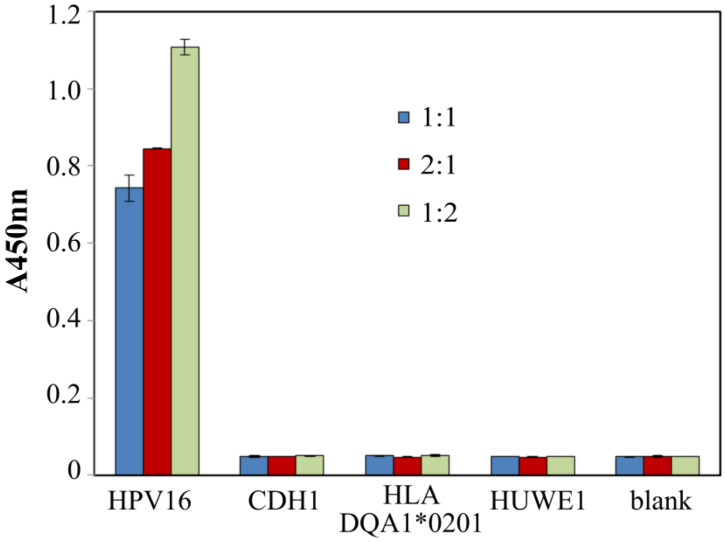

Figure 3.5: Specificity of the sensing platform. Detection of different target ssDNA molecules was performed using the detection probes with scCro/dHP DNA binding sites ratio of 1:1, 2:1 and 1:2. The error bars show the SEM from triplicate samples.

3.5 CONCLUSIONS

A DNA sensing platform was described in this work based on an HRP/GOx bi-enzymatic DNA nanostructure exploiting DNA binding protein tags. Two enzyme-DNA binding protein tag conjugates and hybrid ssDNA-dsDNA detection probes containing specific sites for the binding of the enzyme conjugates were thus designed and used for the detection of model target HPV16 ssDNA. The preparation and characterization of the GOx-dHP conjugate was detailed in this work and the conjugate was subsequently used together with the previously reported HRP-scCro conjugate for the sensitive detection of target ssDNA. Under optimized assay conditions, increased DNA detection sensitivity and lower LOD were achieved when a detection probe containing one binding site for the HRP-scCro conjugate and two for the GOx-dHP conjugate was used compared to a detection probe providing an enzyme stoichiometry of 1:1. The performance of the biosensor in terms of LOD was comparable to direct HRP systems using target-specific oligonucleotide-HRP conjugate further highlighting the advantageous use of the proposed DNA detection platform to provide fast signal generation with lower cost. The approach described herein allows the easy control of the pattern of co-immobilization of the two enzymes by simply selecting the distribution of the specific sequences for binding of the enzyme-DNA binding protein tags conjugates, providing facile manipulation of the ratio of the two enzymes for tailored signal generation. The enzyme conjugates could also be used as universal reporters for multiplex analyte detection in conjunction with multiple target-specific capture and ssDNA-dsDNA detection probes. Finally, the versatility of the proposed system is further demonstrated by its compatibility with paper-based diagnostics for point-of-care testing since the unstable hydrogen peroxide is substituted with glucose as enzyme substrate.

3.6 ACKNOWLEDGEMENTS

This work was supported financially by the FP7-PEOPLE-2011-CIG DeCoDeB project grant awarded to LM. GBA acknowledges the Universitat Rovira i Virgili for the doctoral fellowship. The authors thank Dr. Gert Folkers (Utrecht University, Netherlands) for the generous gift of the construct containing the LacI headpiece domain gene.

3.7 REFERENCES

1 Jain, K. K. Nanodiagnostics: application of nanotechnology in molecular diagnostics. *Expert review of molecular diagnostics* **3**, 153-161, doi:10.1586/14737159.3.2.153 (2003).

2 Shields D, D. S. https://**WWW.ALLIEDMARKETRESEARCH.COM/DNA-DIAGNOSTICS-MARKET**. (2014).

3 FL., K. in *Molecular diagnostics: techniques and applications for the clinical laboratory* Vol. 4 (ed Nakaruma RM Grody WW, Strom CM, Kiechle FL) 9–106 (Academic Press;, 2010).

4 M., P. in *Molecular diagnostics: techniques and applications for the clinical laboratory* (ed Nakaruma RM Grody WW, Strom CM, Kiechle FL) 15–19. (Academic Press, 2010).

5 Aktas, G. B., Skouridou, V. & Masip, L. Novel signal amplification approach for HRP-based colorimetric genosensors using DNA binding protein tags. *Biosensors & bioelectronics* **74**, 1005-1010, doi:10.1016/j.bios.2015.07.077 (2015).

6 Ariga, K. *et al.* Enzyme nanoarchitectonics: organization and device application. *Chemical Society reviews* **42**, 6322-6345, doi:10.1039/c2cs35475f (2013).

7 Riccardi, C. M. *et al.* Covalent interlocking of glucose oxidase and peroxidase in the voids of paper: enzyme-polymer "spider webs". *Chemical communications* **52**, 2593-2596, doi:10.1039/c6cc00037a (2016).

8 Kuchler, A., Yoshimoto, M., Luginbuhl, S., Mavelli, F. & Walde, P. Enzymatic reactions in confined environments. *Nature nanotechnology* **11**, 409-420, doi:10.1038/nnano.2016.54 (2016).

9 Wu, D. *et al.* Electrochemical aptasensor for the detection of adenosine by using PdCu@MWCNTs-supported bienzymes as labels. *Biosensors & bioelectronics* **74**, 391-397, doi:10.1016/j.bios.2015.07.003 (2015).

10 Lai, Y.-H., Lee, C.-C., King, C.-C., Chuang, M.-C. & Ho, J.-a. A. Exploitation of stem-loop DNA as a dual-input gene sensing platform: extension to subtyping of influenza A viruses. *Chemical Science* **5**, 4082-4090, doi:10.1039/C4SC01289E (2014).

11 Xin, L., Zhou, C., Yang, Z. & Liu, D. Regulation of an enzyme cascade reaction by a DNA machine. *Small* **9**, 3088-3091, doi:10.1002/smll.201300019 (2013).

12 Civit, L., Fragoso, A., Holters, S., Durst, M. & O'Sullivan, C. K. Electrochemical genosensor array for the simultaneous detection of multiple high-risk human papillomavirus sequences in clinical samples. *Analytica chimica acta* **715**, 93-98, doi:10.1016/j.aca.2011.12.009 (2012).

13 Gao, F., Courjean, O. & Mano, N. An improved glucose/O2 membrane-less biofuel cell through glucose oxidase purification. *Biosensors and Bioelectronics* **25**, 356-361, doi:https://doi.org/10.1016/j.bios.2009.07.015 (2009).

14 Hudson, J. M. & Fried, M. G. Co-operative interactions between the catabolite gene activator protein and the lac repressor at the lactose promoter. *Journal of Molecular Biology* **214**, 381-396, doi:**HTTP://DX.DOI.ORG/10.1016/0022-2836(90)90188-R** (1990).

15 Kalodimos, C. G., Folkers, G. E., Boelens, R. & Kaptein, R. Strong DNA binding by covalently linked dimeric Lac headpiece: Evidence for the crucial role of the hinge helices. *Proceedings of the National Academy of Sciences of the United States of America* **98**, 6039-6044, doi:10.1073/pnas.101129898 (2001).

16 Spronk, C. A. *et al.* Hinge-helix formation and DNA bending in various lac repressor-operator complexes. *The EMBO Journal* **18**, 6472-6480, doi:10.1093/emboj/18.22.6472 (1999).

17 Kohen, A., Jonsson, T. & Klinman, J. P. Effects of Protein Glycosylation on Catalysis: Changes in Hydrogen Tunneling and Enthalpy of Activation in the Glucose Oxidase Reaction. *Biochemistry* **36**, 2603-2611, doi:10.1021/bi962492r (1997).

18 Munteanu, M. G., Vlahovicek, K., Parthasarathy, S., Simon, I. & Pongor, S. Rod models of DNA: sequence-dependent anisotropic elastic modelling of local bending phenomena. *Trends in biochemical sciences* **23**, 341-347 (1998).

19 Manera, M. *et al.* A multisyringe flow injection system with immobilized glucose oxidase based on homogeneous chemiluminescence detection. *Analytica chimica acta* **508**, 23-30, doi:https://doi.org/10.1016/j.aca.2003.11.050 (2004).

20 Wilner, O. I. *et al.* Enzyme cascades activated on topologically programmed DNA scaffolds. *Nature nanotechnology* **4**, 249-254, doi:10.1038/nnano.2009.50 (2009).

21 Freeman, R., Sharon, E., Teller, C. & Willner, I. Control of Biocatalytic Transformations by Programmed DNA Assemblies. *Chemistry – A European Journal* **16**, 3690-3698, doi:10.1002/chem.200902559 (2010).

22 Isaac A. M. Frías, K. Y. P. S. A., Rafael R. Silva, César A. S. Andrade and Maria D. L. Oliveira. Trends in Biosensors for HPV: Identification and Diagnosis. *Journal of Sensors* **2015**, 16, doi:10.1155/2015/913640 (2015).

23 Ortiz, M. *et al.* Amperometric supramolecular genosensor self-assembled on cyclodextrin-modified surfaces. *Electrochemistry Communications* **13**, 578-581, doi:**HTTP://DX.DOI.ORG/10.1016/J.ELECOM.2011.03.014** (2011).

24 Bartolome, J. P., Echegoyen, L. & Fragoso, A. Reactive Carbon Nano-Onion Modified Glassy Carbon Surfaces as DNA Sensors for Human Papillomavirus Oncogene Detection with Enhanced Sensitivity. *Analytical Chemistry* **87**, 6744-6751, doi:10.1021/acs.analchem.5b00924 (2015).

25 Zhao, X., Tapec-Dytioco, R. & Tan, W. Ultrasensitive DNA Detection Using Highly Fluorescent Bioconjugated Nanoparticles. *Journal of the American Chemical Society* **125**, 11474-11475, doi:10.1021/ja0358854 (2003).

26 Riccò, R., Meneghello, A. & Enrichi, F. Signal enhancement in DNA microarray using dye doped silica nanoparticles: Application to Human Papilloma Virus (HPV) detection. *Biosensors and Bioelectronics* **26**, 2761-2765, doi:**HTTP://DX.DOI.ORG/10.1016/J.BIOS.2010.10.024** (2011).

27 Lee, C.-C., Liao, Y.-C., Lai, Y.-H. & Chuang, M.-C. Recognition of Dual Targets by a Molecular Beacon-Based Sensor: Subtyping of Influenza A Virus. *Analytical Chemistry* **87**, 5410-5416, doi:10.1021/acs.analchem.5b00810 (2015).

28 Li, H. & Rothberg, L. Colorimetric detection of DNA sequences based on electrostatic interactions with unmodified gold nanoparticles. *Proceedings of the National Academy of Sciences of the United States of America* **101**, 14036-14039, doi:10.1073/pnas.0406115101 (2004).

29 Li, J. *et al.* Enzyme-Based Multi-Component Optical Nanoprobes for Sequence- Specific Detection of DNA Hybridization. *Advanced Materials* **20**, 497-500, doi:10.1002/adma.200701918 (2008).

30 Ma, C., Wang, W., Mulchandani, A. & Shi, C. A simple colorimetric DNA detection by target-induced hybridization chain reaction for isothermal signal amplification. *Analytical Biochemistry* **457**, 19-23, doi:**HTTP://DX.DOI.ORG/10.1016/J.AB.2014.04.022** (2014).

31 Lu, S., Hu, T., Wang, S., Sun, J. & Yang, X. Ultra-Sensitive Colorimetric Assay System Based on the Hybridization Chain Reaction-Triggered Enzyme

Cascade Amplification. *ACS Applied Materials & Interfaces* **9**, 167-175, doi:10.1021/acsami.6b13201 (2017).

32 Sun, J. *et al.* Multi-enzyme co-embedded organic-inorganic hybrid nanoflowers: synthesis and application as a colorimetric sensor. *Nanoscale* **6**, 255-262, doi:10.1039/C3NR04425D (2014).

33 Fu, J., Liu, M., Liu, Y., Woodbury, N. W. & Yan, H. Interenzyme Substrate Diffusion for an Enzyme Cascade Organized on Spatially Addressable DNA Nanostructures. *Journal of the American Chemical Society* **134**, 5516-5519, doi:10.1021/ja300897h (2012).

34 Müller, J. & Niemeyer, C. M. DNA-directed assembly of artificial multienzyme complexes. *Biochemical and Biophysical Research Communications* **377**, 62-67, doi:https://doi.org/10.1016/j.bbrc.2008.09.078 (2008).

3.8 SUPPLEMANTARY MATERIAL

3.8.1 Preparation of dimeric single-chain Lac headpiece with N-terminal cysteine (cys-dHP)

3.8.1.1 Cloning

The monomeric DNA binding domain of the *Escherichia coli* Lac repressor protein headpiece (HP) gene with a V52C mutation was obtained from the HP62-V52C construct [15] kindly provided by Dr. Gert Folkers (Utrecht University, Netherlands). In order to engineer a single chain homodimeric HP with an N-terminal cysteine residue (cys-dHP), the monomeric HP gene was initially PCR amplified from the HP92-V52C construct using primers P31 and P26 in order to revert the V52C mutation (C52V) and allow overlap extension PCR to construct the dimeric gene. The product of the first PCR reaction was then used as the template for the second PCR with primers P32 and P28 to generate the second part. The two PCR products (approximately 200 bp each) were then used in overlap extension PCR with external primers P29 and P30 and the resulting product (dHP) of approximately 400 bp was digested with *Nco*I and *Hind*III restriction enzymes and ligated into digested pET22b plasmid. The resulting construct pVS11 was sequenced in order to validate the constructed dimeric gene. For the addition of a cysteine residue at the N-terminal of the dHP protein, the dHP gene was amplified with primers P60/P8 from pVS11 construct, digested with NcoI/HindIII restriction enzymes and ligated in digested pBADmychisA plasmid. The final pVS16 construct was verified by DNA sequencing. The sequences of all the primers used for the construction of pVS16 are listed in Table S-3.1.

Table S-3.1: Primers used for the construction of pVS16.

Primer	**Sequence (5’ to 3’)**
P7	TAATACGACTCACTATAGGG
P8	GCTAGTTATTGCTCAGCGG
P26	AACCGCCTTTGCCCGCCAGTTGTTGTGCCACGCGGTTGGGAATGTAATTC
P28	GCTCGATAGCACAAGCTTTTTGCCCGCCAGTTG
P29	GTGCTATCCCATGGCC
P30	GCTCGATAGCACAAGCTTTTTG
P31	GTGCTATCCCATGGCCAAACCAGTAACGTTATACGATGTCGCAGAG
P32	GGCGGGCAAAGGCGGTTCTGGCGGTTCTATGGCCAAACCAGTAACG
P60	CTCTCCCATGGGCTGTAAACCAGTAACGTTATACGATGTCGC

3.8.1.2 Expression and purification

The pVS16 construct was transformed in BL21(DE3) *Escherichia coli* cells and the culture was grown in terrific broth supplemented with ampicillin at 37°C until OD_{600} reached approximately 1, at which point the expression of the protein was induced with 0.02 % arabinose. The culture was grown for another 3 h at 30°C, the cells were harvested and resuspended at 5 ml/g of wet cell weight with lysis buffer (50 mM Tris-HCl pH 7, 5 mM DTT, 5 % glycerol, 5 µg/ml DNaseI, 0.5 % Triton

X-100) and then lysed by sonication on ice for 10 min. The cell lysate was centrifuged at 14,000 rpm at 4°C, the soluble fraction (supernatant) was filtered (0.45 µm) and then loaded on an immobilized metal ion affinity chromatography (IMAC) gravity column packed with HisPure Ni-NTA-agarose resin pre-equilibrated with equilibration buffer (10 mM phosphate buffer pH 7.4, 300 mM NaCl). The column was washed with equilibration buffer containing 7.5 mM imidazole and the protein was eluted with the same buffer containing 500 mM imidazole. The buffer of the elution fraction was exchanged to 50 mM potassium phosphate pH 7 with 1 mM EDTA and the sample was loaded on a gravity column packed with SP Sepharose FF strong cation exchange resin equilibrated with the same buffer. The column was washed with the same buffer containing 50 mM NaCl and cys-dHP was finally eluted with the same buffer containing 1 M NaCl. The buffer of the elution fraction was exchanged to PBS (pH 7) supplemented with 50 % glycerol before storage at -20°C. The whole process was monitored by SDS-PAGE, as shown in Figure S-3.1.

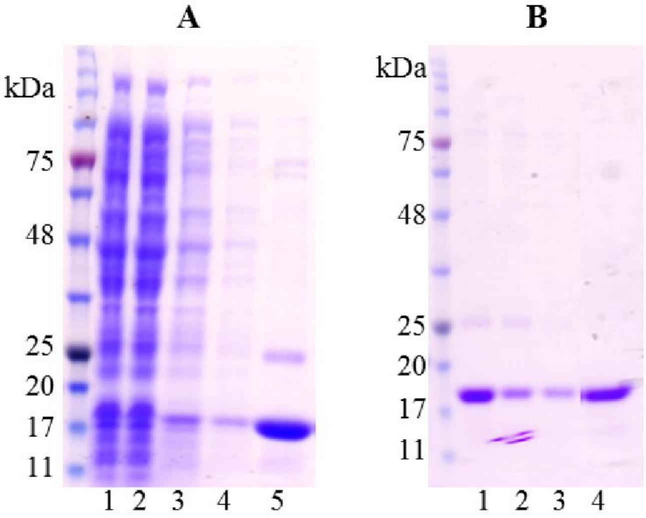

Figure S-3.1: SDS-PAGE analysis for the expression and purification of cys-dHP. (A) IMAC purification. 1: *Escherichia coli* soluble fraction; 2: flowthrough fraction; 3-4: wash fractions; 5: elution fraction. (B) IEC purification. 1: IMAC elution fraction after buffer exchange; 2: flowthrough fraction; 3: wash fraction; 4: elution fraction.

3.8.2 Preparation of the hybrid ssDNA-dsDNA detection probes

Table S-3.2: Oligonucleotides used for the preparation of the HPV16 detection probes. The target complementary part is denoted in bold, the HRP-scCro binding sites are shown in italics and the GOX-dHP binding sites are underlined.

Oligo (length)	scCro/dHP stoichiometry	Sequence (5' to 3')
P88 (69 nt)	1:1	**TTGGAAGACCTGTTAATGGGC**GCAAC*TATCACCGCAAGTGATA*AAAGAATTGTGAGCGGATAACAATTT
P89 (48 nt)		AAATTGTTATCCGCTCACAATTCTTT*TATCACTTGCGGTGATA*GTTGC
P94 (89 nt)	2:1	**TTGGAAGACCTGTTAATGGGC**GCAAC*TATCACCGCAAGTGATA*AAAGAATTGTGAGCGGATAACAATTTAAA*TATCACCGCAAGTGATA*
P95 (68 nt)		*TATCACTTGCGGTGATA*TTTAAATTGTTATCCGCTCACAATTCTTT*TATCACTTGCGGTGATA*GTTGC
P92 (95 nt)	1:2	**TTGGAAGACCTGTTAATGGGC**GCAACGAATTGTGAGCGGATAACAATTTAAA*TATCACCGCAAGTGATA*AAAGAATTGTGAGCGGATAACAATTT
P93 (74 nt)		AAATTGTTATCCGCTCACAATTCTTT*TATCACTTGCGGTGATA*TTTAAATTGTTATCCGCTCACAATTCGTTGC

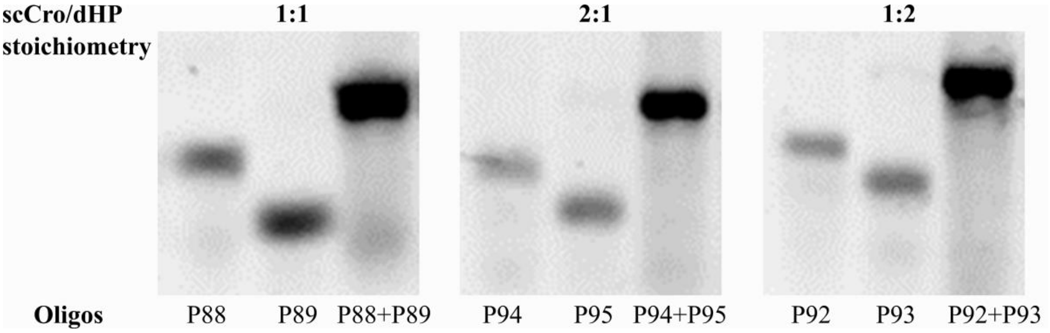
scCro/dHP stoichiometry
1:1
2:1
1:2
Oligos
P88
P89
P88+P89
P94
P95
P94+P95
P92
P93
P92+P93

Figure S-3.2: Agarose gel electrophoresis for the preparation of the HPV16 detection probes with different binding sites stoichiometries.

3.8.3 Characterization of the GOx-dHP conjugate by MALDI-TOF mass spectroscopy

Table S-3.3: Ion species and corresponding mass for GOx and GOx-dHP conjugate. mGOx corresponds to GOx enzyme monomer and dGOx corresponds to the homodimer.

Ion species	GOx (m/z)	GOx-dHP (m/z)
[mGOx+2H]$^{2+}$	37,363.4	38,006.4
[mGOx+H]$^{+}$	74,483.4	75,824.7
3[mGOx+2H]$^{2+}$	113,010.5	
[dGOx+H]$^{+}$	150,056.5	151,251.3
[(mGOx+dHP)+2H]$^{2+}$		46,120.0
[(dGOx+dHP)+3H]$^{3+}$		55,920.4
[(dGOx+dHP)+2H]$^{2+}$		85,129.1
[(mGOx+dHP)+H]$^{+}$		92,909.5
[(dGOx+dHP)+H]$^{+}$		168,158.4

3.8.4 DNA detection with ELONA

Table S-3.4: Sequences of oligonucleotides used for DNA detection with ELONA.

Oligonucleotide (length)	**Sequence (5’ to 3’)**
HPV16 (159 nt)	GCCCATTAACAGGTCTTCCAAAGTACGAATGTCTACGTGTGTGCTTTGTACGCACAACCGAAGCGTAGAGTCACACTTGCAACAAAAGGTTACAATATTGTAATGGGCTCTGTCCGGTTCTGCTTGTCCAGCTGGACCATCTATTTCATCCTCCTCCTC
CDH1 (133 nt)	GGGTTCCCTAAGGGTTGGACCTTGGAGGAATTCTTGCTTTGCTAATTCTGATTCTGCTGCTCTTGCTGTTTCTTCGGAGGAGAGCGATAGGCTGGTTCGTAATCGGTCTAGATTGGATCTTGCTGGCGCGTCC
HUWE1 (137 nt)	GGGTTCCCTAAGGGTTGGACCACCAAGCTGAAGGGCAAAATGCAGAGCAGGTTTGACATGGCTGAGAATGTGGTAATTGTGGCATCTCAGATTACGACGAACTCAATGAATCTAGATTGGATCTTGCTGGCGCGTCC
HLA-DQ1*0201 (97 nt)	GAGAGGAAGGAGACTGCCTGGCGGTGGCCTGAGTTCAGCAAATTTGGAGGTTTTGACCCGCAGGGTGCACTGAGAAACATGGCTGTGGCAAAACACA

Chapter 4

Sandwich-type aptasensor employing modified aptamers and enzyme-DNA binding protein conjugates

Analytical and Bioanalytical Chemistry 2019, 411: 3581–3589.

Chapter 4: Sandwich-type aptasensor employing modified aptamers and enzyme-DNA binding protein conjugates

4.1 ABSTRACT

The use of aptamers in various analytical applications as molecular recognition elements and as an alternative to antibodies, has led to the development of various platforms that facilitate the sensitive and specific detection of targets ranging from small molecules and proteins to whole cells. The goal of this work was to design a universal, target-specific and adaptable sandwich-type aptasensor exploiting the unique properties of DNA binding proteins. Specifically, two different enzyme-DNA binding protein tag conjugates, HRP-scCro and GOx-dHP, which have already been validated for nucleic acid detection in our previous works, were used for the direct detection of protein targets with two aptamers with the function of capture and detection. The specific dsDNA binding sequence for each DNA binding protein tag was incorporated in the form of a hairpin at one end of each aptamer sequence during the synthesis step. Detection was accomplished by an enzymatic cascade (HRP/GOx) reaction after the binding of each enzyme conjugate to its corresponding binding sequence on each aptamer. The proposed sandwich-type aptasensor was validated for the detection of thrombin, which is one of the most commonly used model targets with known dual aptamers and the limit of detection accomplished was 0.92 nM which is comparable with other colorimetric platforms reported in the literature. Moreover, when two LacI binding sites were incorporated in the detection aptamer sequence in an effort to change the enzyme ratio, the limit of detection did not change (0.88 nM) but increased sensitivity was observed. Finally, the compatibility of the two enzyme-DNA binding protein conjugates with paper-based assays was demonstrated by a basic lateral flow assay.

4.2 INTRODUCTION

Over the past decade, researchers have investigated new molecular diagnostics approaches to meet the high demand to detect biomarkers for various diseases [1,2]. Primarily, antibodies have served as biomolecular recognition elements in various systems [3], and they provide highly specific and sensitive detection of their respective targets. They also display some disadvantages such as high cost, long production time, batch to batch variability and instability while in storage. In order to overcome some of these drawbacks, the utilization of aptamers has been explored in different detection platforms as alternative recognition molecules [4-6]. Aptamers are single stranded nucleic acids that fold into specific three-dimensional structures based on their nucleic acid sequence and bind to their target with high affinity and selectivity [7].

Aptamers have been developed to bind a broad range of targets such as proteins [8], peptides [9], amino acids [10], vitamins [11] and whole cells [12]. Due to the ease of chemical modification of oligonucleotides, various reactive groups and labels have been implemented into the sequence of aptamers, such as thiol, amine and biotin among others, to facilitate their oriented immobilization on different sensing platforms [13]. Additionally, pairs of aptamers (dual aptamers) have also been developed for some targets, including proteins and whole cells, that are able to bind to distinct aptatopes on their respective target, thus facilitating the design of sandwich-type biosensors with enhanced sensitivity and specificity [14]. Different platforms employing colorimetric, electrochemical, or SPR-mediated detection have used dual aptamers in sandwich-type aptasensors [15-17]. SPR-based analysis is highly sensitive but the high cost associated with the specific equipment and the requirement for trained personnel limits the use of the technique. On the other hand, colorimetric biosensors in combination with lateral flow assays are favored because of their sensitivity, low cost and straightforward result evaluation by naked eye without the need of a measuring device. However, the labeling of the aptamers (capture and/or detection aptamer) to facilitate immobilization and/or detection in these type of assays results in increased cost.

In our previous work, we developed two DNA binding proteins-enzyme conjugates and demonstrated their use for the sensitive colorimetric detection of ssDNA targets, either alone or in a cascade reaction. Horseradish peroxidase (HRP) was conjugated to a single-chain version of the bacteriophage lambda Cro DNA binding protein (HRP-scCro conjugate) whereas the dimeric form of the headpiece domain of the *Escherichia coli* LacI repressor protein (dHP) was used for conjugation to glucose oxidase (GOX-dHP conjugate) [18]. The reported detection system exploited the high affinity and specificity that the DNA binding proteins display for their specific dsDNA binding sites. Binding of the two enzyme conjugates HRP-scCro and GOx-dHP to the detection probe with incorporated binding sites for the two DNA binding proteins resulted in a cascade reaction and color development after substrate (glucose and AEC) addition.

Herein, we demonstrate the applicability of these two enzyme-DNA binding protein conjugates in sandwich aptasensors for the detection of targets other than DNA. Thrombin, an enzyme involved in blood coagulation and platelet aggregation [19], was used as a model target since dual aptamers for this target are readily available. The two aptamers TBA15 [20] and TBA29 [21] have been widely used for the development of various sandwich-type assays, making thrombin one of the most commonly investigated proteins in aptamer-based sandwich assays [22]. In this work, we present the detection of thrombin in a sandwich system by using modified dual aptamers which include the binding sites for each DNA binding protein and the bi-enzymatic HRP/GOx cascade system. As it can be seen in Fig. 4.1, the two enzyme conjugates were designed to bind individually on each of the modified aptamers and to avoid steric hindrance effects. The system was optimized in terms of choice of capture and detection aptamer in addition to the concentrations of several components (capture aptamer, detection aptamer and enzyme conjugates) to improve the performance and enable the sensitive detection of thrombin. Moreover, the effect of the ratio of the two enzyme conjugates on target detection was also investigated by employing a detection aptamer which incorporated two binding sites for one of the enzyme conjugates. The applicability of the system in paper-based sandwich-type detection of targets was finally evaluated in a lateral flow assay designed as a proof of concept.

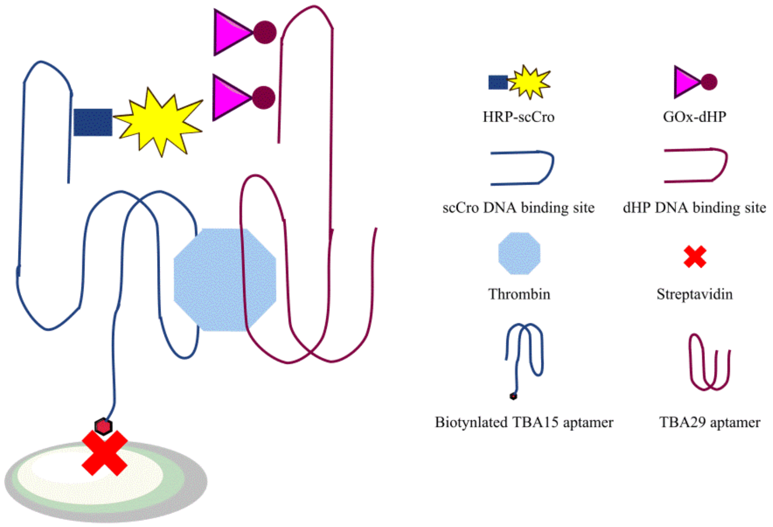
HRP-scCro
GOx-dHP
scCro DNA binding site
dHP DNA binding site
Thrombin
Streptavidin
Biotynlated TBA15 aptamer
TBA29 aptamer

Figure 4.1: The proposed aptamer-based sandwich-type system for target detection via modified dual aptamers and HRP-scCro and GOx-dHP enzyme-DNA binding protein conjugates.

4.3 EXPERIMENTAL

4.3.1 Materials

Thrombin from human plasma, glucose and 3,3',5,5'-tetramethylbenzidine (TMB) were purchased from Sigma Aldrich (Madrid, Spain) and neutravidin-coated microtiter strip plate s from Fisher Scientific (Barcelona, Spain). Thrombin aptamers TBA15 [20] and TBA29 [21] used for detection of thrombin were modified in order to include the specific binding sites for the GOx-dHP and HRP-scCro enzymes conjugates. They were synthesized by Eurofins (Ebersberg, Germany) and their sequences are shown in Table 4.1. All other reagents were purchased from Fisher

Scientific (Barcelona, Spain), Sigma-Aldrich (Madrid, Spain) and Scharlau (Barcelona, Spain).

4.3.2 Preparation and characterization of the modified aptamers

The modified aptamers with one enzyme conjugate binding site were prepared in the form of hairpins whereas in the case of two binding sites, two partially complementary oligonucleotides were hybridized, with one of them part of the aptamer. Twenty microliters of 10 μM modified aptamer with one enzyme conjugate binding site in buffer A (10 mM Tris-HCl pH 8, 1 mM EDTA, 100 mM KCl) were heated up to 95°C for 5 min to dissociate any intermolecular interactions, and then gradually cooled to room temperature to allow the aptamer to fold properly and also to form the hairpin with the DNA binding protein binding site. For the modified aptamer with two GOx-dHP binding sites, the oligonucleotide pair (P109 with P110) were mixed in buffer A at a final concentration of 10 μM each oligo in a total of 20 μl, heated for 5 min at 95°C and then slowly cooled down to room temperature. The hybridization efficiency was evaluated by agarose gel electrophoresis (Fig. S-4.1). Electrophoretic mobility shift assay (EMSA) was used to evaluate the binding of thrombin and the enzyme conjugates GOx-dHP and HRP-scCro to the modified aptamers. The binding mixtures (20 μl total) were prepared in buffer B (20 mM potassium phosphate pH 7.5, 140 mM NaCl, 5 mM KCl, 1 mM $MgCl_2$, 1 mM $CaCl_2$, 0.05 % Tween-20, 5 % glycerol) and they contained 200 nM of modified aptamer and 400 nM of each protein species. The mixtures were incubated for 1 hour at room temperature and then resolved on a 5 % non-denaturing polyacrylamide gel for 60 min at 80V in TAE buffer. The gel was finally stained for 30 min with GelRed before visualization.

Table 4.1: Oligonucleotides used for thrombin detection. The thrombin aptamer sequences are in bold, the binding site for HRP-scCro in italics and for GOX-dHP underlined.

Oligo (length)	Description and sequence (5’ to 3’)
P96 (74 nt)	5'-biotin-TBA29-T7-1xCro-3' **AGTCCGTGGTAGGGCAGGTTGGGGTGACT**TTTTTTT*TATCACCGCAAGTGATA*TTTT*TATCACTTGCGGTGATA*
P97 (68 nt)	5'-TBA15-T4-1xLacI-3' **GGTTGGTGTGGTTGG**TTTTGAATTGTGAGCGGATAACAATTTTTTAATTGTTATCCGCTCACAATTCA
P106 (70 nt)	5'-biotin-T10-TBA15-T7-1xCro-3' TTTTTTTTTT**GGTTGGTGTGGTTGG**TTTTTTT*TATCACCGCAAGTGATA*TTTT*TATCACTTGCGGTGATA*
P107 (87 nt)	5'-1xLacI-T7-TBA29-3' GAATTGTGAGCGGATAACAATTTTTTTTTAATTGTTATCCGCTCACAATTCTTTTTTT**AGTCCGTGGTAGGGCAGGTTGGGGTGACT**
P109 (80 nt)	5'-2xLacI-T7-TBA29-3' GAATTGTGAGCGGATAACAATTTTGAATTGTGAGCGGATAACAATTTTTTT**AGTCCGTGGTAGGGCAGGTTGGGGTGACT**
P110 (44 nt)	5'-2xLacI complementary-3' TTGTTATCCGCTCACAATTCAAAATTGTTATCCGCTCACAATTC
Probe 8 (47 nt)	5'-1x-Cro-N6-1xLacI-3' TAT*TATCACCGCAAGTGATA*CGACATGAATTGTGAGCGCTCACAATT AATTGTGAGCGCTCACAATTCATGTCG*TATCACTTGCGGTGATA*ATA

4.3.3 Thrombin colorimetric detection with enzyme-linked aptamer assay (ELAA)

The biotinylated capture and the detection aptamer with one enzyme conjugate binding site (prepared in buffer A) were heated for 5 min at 95°C and then cooled down to room temperature prior to use. Then, 50 µl of the capture aptamer in buffer C (20 mM potassium phosphate pH 7.5, 140 mM NaCl, 5 mM KCl, 1 mM $MgCl_2$, 1 mM $CaCl_2$, 0.05 % Tween-20, 0.5 % BSA) were added to a neutravidin-coated plate and incubated for 30 min at room temperature. The wells were washed three times with 300 µl of wash buffer (buffer C without BSA) and then 50 µl of thrombin in buffer C were added and incubated for 1h at room temperature. The wells were washed again three times with 300 µl of wash buffer and 50 µl of detection aptamer, with one or two LacI binding sites, were added and binding to thrombin proceeded for 1 h at room temperature. After three washes with 300 µl wash buffer, 50 µl of HRP-scCro enzyme conjugate in buffer C was added and incubated for 30 min at room temperature, the wells were washed three times with 300 µl wash buffer and 50 µl of GOx-dHP enzyme conjugate in buffer D (20 mM potassium phosphate pH 7.5, 100 mM NaCl, 5 mM KCl, 1 mM $MgCl_2$, 1 mM $CaCl_2$, 0.05 % Tween-20, 0.5 % BSA) were added and incubated for 30 min at room temperature. The wells were finally washed three times with 300 µl buffer D without BSA and then 50 µl of freshly prepared mixture of 250 mM glucose and 1 mM TMB were added to the wells. Color development was stopped after 45 min by the addition of 50 µl of 1M H_2SO_4 and the absorbance at 450 nm was measured using a Cary 100 Bio UV visible Spectrophotometer. Optimization of the ELAA was performed for capture aptamer choice, capture and detection aptamer concentration and the enzyme-DNA binding proteins conjugates concentration using the general ELAA setup described above. Optimized conditions were finally used to obtain thrombin calibration curves.

4.3.3.1 Capture aptamer choice

The two thrombin aptamers used in this work that bind to different aptatopes were evaluated for serving as the capture aptamer. For this, 50 µl of 50 nM of each biotinylated modified capture aptamers P106 and P96 (bt-TBA15-1xCro and bt-TBA29-1xCro respectively) with one scCro binding site were individually immobilized on neutravidin-coated wells. Thrombin was used at 10 nM, the detection aptamers, P107 (1xLacI-TBA29) for P106 capture aptamer and P97 (TBA15-1xLacI) for P96 capture aptamer, at 50 nM and the enzyme conjugates HRP-scCro and GOx-dHP) at an equimolar mixture of 25 nM each in buffer E.

4.3.3.2 Optimization of capture aptamer concentration

The capture aptamer P106 concentration was titrated from 10 nM to 150 nM. Thrombin was used at 10 nM, the detection aptamer P107 with one LacI binding site at 50 nM and the enzyme conjugates (HRP-scCro and GOx-dHP) at 25 nM.

4.3.3.3 Optimization of detection aptamer concentration

Using an optimized concentration of the capture aptamer P106 at 75 nM and thrombin at 10 nM, the detection aptamer P107 with one LacI binding site was titrated from 50 nM to 125 nM. The enzyme conjugates (HRP-scCro and GOx-dHP) were used as a mixture with an equimolar concentration of 25 nM each for detection.

4.3.3.4 Optimization of DNA binding protein conjugates concentration

With the capture aptamer P106 at 75 nM, thrombin at 10 nM and the detection aptamer P107 with one LacI binding site at 100 nM, the concentration of both enzyme conjugates GOx-dHP and HRP-scCro were titrated from 5 to 25 nM.

4.3.4 Detection of thrombin using the enzyme conjugates in a lateral flow assay

A lateral flow assay was developed as a proof of concept for the applicability of the enzyme conjugates in a paper-based method for the detection of thrombin. FF170HP nitrocellulose membrane (Whatman, Germany) and glass cellulose absorbent pad (Whatman, UK) were used. The test line comprised of streptavidin (1 mg/ml) with biotinylated capture aptamer P106 (30 uM) and the control line of streptavidin (1 mg/ml) with biotinylated control probe 8 (see Table 4-1) which contains one binding site for each enzyme conjugate. The streptavidin-biotinylated DNA mixtures were incubated in buffer C for 30 min at room temperature before deposition on the nitrocellulose membrane using a pipette tip. Subsequently, the membrane was dried at room temperature for 1 hour and blocked with 1% w/v skimmed milk powder and 0.1% w/v Empigen detergent in PBST for 15 minutes, under shaking conditions at room temperature. The membrane was finally allowed to dry for 1 hour and stored at 4°C until use. For detection, thrombin and the detection aptamer P107 (at 2 µM each in buffer C) were incubated for 30 minutes at room temperature. Then, 20 µl of the mixture were wicked on to the membrane and incubated until dry. Following, 20 µl of 50 nM of HRP-scCro enzyme conjugate in buffer C was flowed along the strip until dry and finally, 20 µl of 50 nM GOx-dHP enzyme conjugate in buffer C supplemented with 100 mM NaCl was added. For naked-eye detection, a freshly prepared substrate solution (1 mM AEC, 250 mM glucose in 100 mM potassium phosphate pH 5) was added to the strip and allowed to develop (red color) for 5 min at room temperature.

4.4 RESULTS AND DISCUSSION

4.4.1 Design of the colorimetric sandwich-type aptasensor

The proposed sandwich-type target detection system relies on the use of dual modified aptamers by incorporating in each of their sequences a different dsDNA binding site specific for a DNA binding protein in the form of a hairpin. The two DNA binding proteins required for this system, which in this case are scCro and dHP, are used as GOx and HRP enzyme conjugates and provide the link between target recognition and signal generation. As it is illustrated in Fig. 4.1, recognition of the model target thrombin by the capture aptamer enables its consequent detection by the detection aptamer. The GOx-dHP and HRP-scCro enzyme conjugates can then bind on the dsDNA part of the modified aptamers and form an enzymatic cascade system that provides a colorimetric signal for the detection of thrombin. In our previous work, we demonstrated the use of these enzyme conjugates and enzymatic cascade for the sensitive detection of target ssDNA [18]. Herein, we provide an example of the application of the enzymes conjugates for the detection of non-nucleic acid targets using aptamers as molecular recognition elements. The dsDNA binding site for each enzyme conjugate was introduced into the sequence of each aptamer during the synthesis step, thus avoiding additional post-synthesis modification steps, with the exception of biotin modification of one of the aptamers that was required to facilitate immobilization through affinity interactions. The enzyme conjugates binding sites on the modified aptamers were formed through hairpin assembly (see Table 4.1 for sequences). When two identical binding sites for dHP were required on the detection aptamer in order to study the effect of enzyme ratio on signal generation, a hybridization step of partially complementary oligos was performed (Fig. S-4.1) to avoid the formation of half-sites because of the palindromic nature of this particular binding sequence. The capture aptamer (with the biotin modification) always contained the binding site for the HRP-scCro enzyme conjugate and the detection aptamer the binding site for the GOx-dHP, in order to minimize any possible background signal in the absence of target.

4.4.2 Preparation and characterization of the modified aptamers

The two aptamers used, TBA15 and TBA29, have been extensively used as dual aptamers models for the development of different types of biosensors. The reported three-dimensional structures of the complexes between thrombin and TBA15 aptamer (PDB code 4DIH) and TBA29 aptamer (PDB code 4I7Y) have shed light on the way these two aptamers bind their target at two parts of the protein that are more than 30 Å apart [23]. To maintain the distance between the two modified aptamers and to avoid any possible steric hindrance effects between HRP-scCro and the bulky GOx-dHP, TBA15 was extended with the DNA binding sequence at the 3' end and TBA29 at the 5' end since, according to the crystal structures, these ends are distanced from the target protein binding sites. This configuration would facilitate the co-binding of the two modified aptamers and the subsequent co-binding of the two enzyme conjugates.

The binding properties of the modified aptamers were evaluated using an electrophoretic mobility shift assay (EMSA). The aptamers were incubated separately with different protein species and the samples were resolved on a non-denaturing polyacrylamide gel. Unbound sequences run faster on the gel compared to their counterparts with a protein species bound on them, resulting in gel retardation due to the increased size. As it can be seen in Fig. 4.2, the modified aptamers are able to bind both their target thrombin and the corresponding DNA binding protein whose specific dsDNA binding site has been incorporated into their sequence. These results confirm the correct folding of each aptamer into their respective G-quadruplex configuration and the simultaneous formation of the hairpin loops containing the DNA binding protein binding sites.

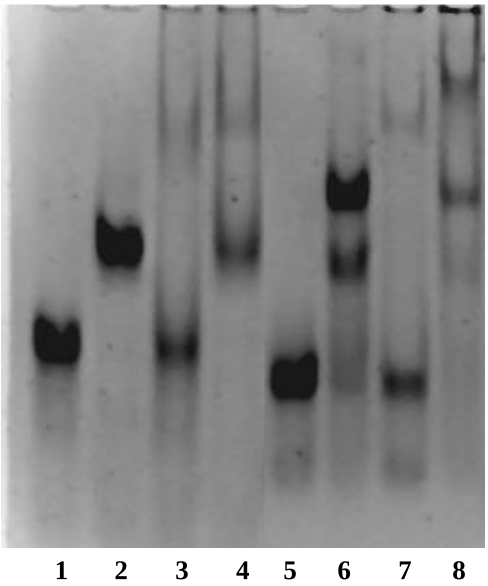

Figure 4.2: Binding of different protein species to the modified thrombin aptamers by EMSA. Lane 1: Capture aptamer P106 (TBA15-1xCro); lane 2: P106 + scCro; lane 3: P106 + thrombin; lane 4: P106 + scCro + thrombin; lane 5: detection aptamer P96 (1xLacI-TBA29); lane 6: P96 + dHP; lane 7: P96 + thrombin; lane 8: P96 + dHP + thrombin.

4.4.3 Colorimetric detection by ELAA

In the aptamer-based target detection, HRP-scCro and GOx-dHP are utilized for simultaneous signal generation after binding to the specific sequence extensions on the aptamers (Fig. 4.1). The Enzyme Linked Aptamer Assay (ELAA) was optimized for each element in the platform: capture aptamer choice (a), capture and detection aptamer concentration (b), DNA binding protein enzymes concentration (c). The signal generated with HRP and GOx enzyme cascade reaction results from the conversion of glucose to gluconic acid and hydrogen peroxide and subsequent electron transfer from hydrogen peroxide to reduced TMB to form the blue colored product.

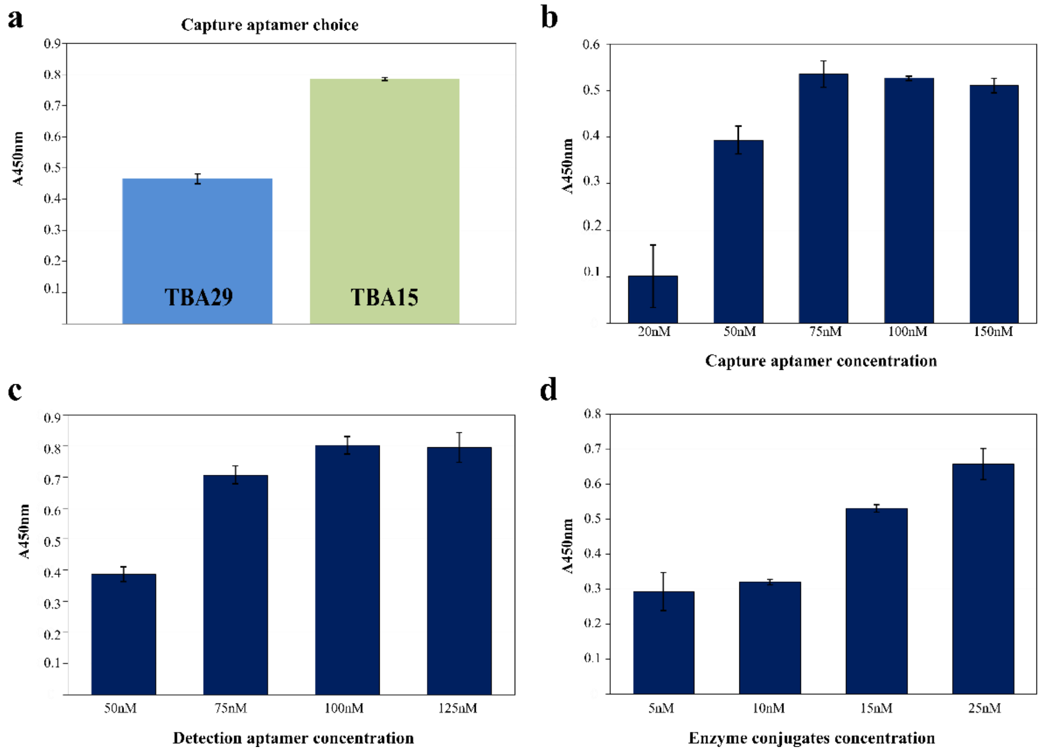

Figure 4.3: Aptamer-based target detection with Enzyme Linked Aptamer Assay. a) Choice of capture aptamer. b) Optimization of capture aptamer concentration. c) Optimization of the detection aptamer concentration. d) Optimization of the enzyme-DNA binding protein conjugates concentration. The error bars show the standard deviation from triplicate samples.

We provide two different capture aptamer strategies to be chosen; TBA15 or TBA29 with scCro DNA binding site. Many studies used TBA15 as capture aptamer since TBA29 can bind stronger to the thrombin and can provide a good signal as the detection aptamer [22]. In this report, we evaluated the optimum capture aptamer choice for our modified aptamers. As the Fig. 4.3 (a) shows the TBA15 aptamer provided a better signal (about 40% more) over TBA29 as capture aptamer, therefore, TBA15 was chosen as capture aptamer. Next, the effect of capture aptamer concentration was assessed by changing its immobilization concentration from 20 to 150 nM while keeping the concentrations of the rest of the components the same. As shown in Fig. 4.3 (b), the optimum signal is achieved with a 75 nM capture aptamer concentration. A possible explanation for the observed trend is an increase in aptamer immobilization until saturation of binding sites is reached. The concentration of detection aptamer was also optimized by changing its immobilization concentration from 50 to 125 nM while keeping the rest of components at the same concentration. As it can be seen in Fig. 4.3 (c), a signal increase occurs with the increase of the detection aptamer concentration up to 100 nM and then it plateaus, therefore 100 nM was chosen for further work. Finally, the effect of the enzyme conjugates concentration was evaluated. The enzyme conjugates were titrated from 5 nM to 25 nM and the highest signal was obtained for the maximum enzyme conjugate concentration (Fig. 4.3 (d)).

Thrombin was titrated to obtain the target calibration curves with one and two LacI DNA binding sites on the detection aptamer using the optimized conditions for the colorimetric assay. The calibration curve of colorimetric signal (absorbance 450 nm) versus thrombin concentration fitted a quadratic model (Fig. 4.4). The limit of detection (LOD) of the assay was also calculated as three times the standard deviation of the blank plus the average of blank measurements. The LOD calculated was 0.92 and 0.88 nM for one and two LacI binding site respectively. These results also show improved sensitivity by the addition of an additional LacI binding site. Most of the thrombin colorimetric assays, based on enzymatic or non-enzymatic detection, have LODs in the low nanomolar range and for some systems based on gold nanoparticles it can go down to the picomolar range (Table S-4.1). The reported LOD of our system in the low nanomolar range is in line with most thrombin colorimetric assays. Detection with gold nanoparticles can result in high sensitivity and very low LODs, but depending on the configuration these nanoparticles need to be modified when changing the target/aptamer base [24,25]. On the other hand, the aptamer-based target detection with two enzyme-DNA binding protein conjugates that we propose, provides a sensitive, simple and a direct universal detection platform.

The enhanced signal with an excess of GOx enzyme over HRP on thrombin detection is in agreement with our previous work for ssDNA target detection and utilizing the same enzymatic cascade [18].

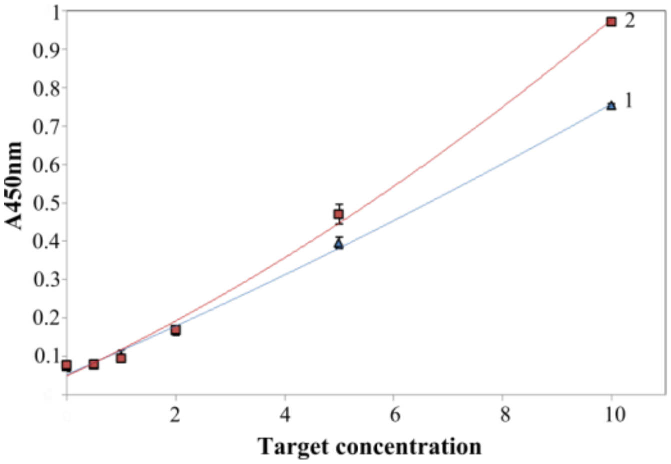

LacI binding sites on detection aptamer	LOD (nM)	Equation	R^2
1	0.92	0.0009x2 + 0.061x + 0.0541	0.99
2	0.88	0.0026x2 + 0.0662x + 0.0501	0.99

Figure 4.4: Target calibration curves using detection aptamers with one or two LacI DNA binding sites. The error bars show the standard deviation from triplicate samples and three independent experiments.

4.4.4 Lateral flow assay

Point-of-care devices using paper-based lateral flow assays have gained a lot of interest in the field of rapid diagnostics due to their low cost and straightforward detection. As a simple proof of concept, we evaluated the ELAA platform in a paper-based lateral flow configuration for the detection of thrombin. Some studies have focused on the aptamer-based lateral flow devices that can be used as simple "dipsticks" or a litmus-test type of assay [26], while others detected thrombin with sandwiched aptamers in lateral flow configuration [25]. In both cases, gold nanoparticles were utilized for the qualitative aptamer-based target detection. Gold nanoparticles are widely used in lateral flow assays and they provide an easily detectable red color signal [27]. On the other hand, many gold nanoparticles detection configurations need the nanoparticles to be modified with aptamers depending on the target. The proposed work eliminates the need of nanoparticle modification and it also eliminates the need to store the unstable hydrogen peroxide. The paper-based thrombin detection via two enzyme-DNA binding protein and dual aptamers is suitable for these type of assays (Fig. 4.5). Due to the non-optimized conditions the background is still quite high, but there is still a significant difference between signal from the negative and positive controls. This high background may be a consequence of the fact that HRP is always bound to the capture aptamer at the test line as well as from some non-specific interaction of the GOx-dHP enzyme conjugate in the absence of the target with the test line. Future work will focus on the optimization of the system in order to reduce this background.

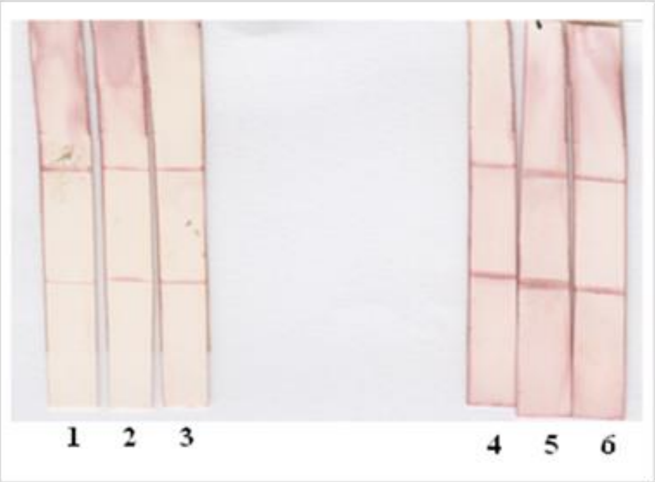

Figure 4.5: Lateral flow assay for thrombin detection with enzyme-DNA binding protein conjugates. Lane 1-2-3: Negative control (triplicate); lane 4-5-6: Positive control (triplicate).

4.5 CONCLUSIONS

We have developed a universal aptamer-based target detection system using HRP-scCro and GOx-dHP conjugates. Two distinct thrombin-binding aptamers were modified to include specific DNA binding sites of the enzyme conjugates to enable recognition and detection of the target. The optimized thrombin detection system provided a direct, universal and sensitive method. In addition, the suitability of the method for lateral flow assays was shown. Overall, the performance of the proposed assay was comparable to other colorimetric thrombin detection systems with a limit of detection achieved in the subnanomolar range. One of the main advantages of the proposed system is the simplicity and low cost of the aptamer modification.

4.6 ACKNOWLEDGEMENTS

This work was supported financially by the FP7-PEOPLE-2011-CIG DeCoDeB project grant awarded to LM. GBA acknowledges the Universitat Rovira i Virgili for the doctoral fellowship. The authors thank Dr. Gert Folkers (Utrecht University, Netherlands) for the generous gift of the construct containing the LacI headpiece domain gene.

4.7 REFERENCES

1 Jain, K. K. Nanodiagnostics: application of nanotechnology in molecular diagnostics. *Expert review of molecular diagnostics* **3**, 153-161, doi:10.1586/14737159.3.2.153 (2003).

2 Tang, Y. W., Procop, G. W. & Persing, D. H. Molecular diagnostics of infectious diseases. *Clinical chemistry* **43**, 2021-2038 (1997).

3 Jayasena, S. D. Aptamers: an emerging class of molecules that rival antibodies in diagnostics. *Clinical chemistry* **45**, 1628-1650 (1999).

4 Song, S., Wang, L., Li, J., Fan, C. & Zhao, J. Aptamer-based biosensors. *TrAC Trends in Analytical Chemistry* **27**, 108-117, doi:10.1016/j.trac.2007.12.004 (2008).

5 Tuerk, C. & Gold, L. Systematic evolution of ligands by exponential enrichment: RNA ligands to bacteriophage T4 DNA polymerase. *Science* **249**, 505-510 (1990).

6 Ellington, A. D. & Szostak, J. W. In vitro selection of RNA molecules that bind specific ligands. *Nature* **346**, 818-822, doi:10.1038/346818a0 (1990).

7 Nimjee, S. M., Rusconi, C. P. & Sullenger, B. A. Aptamers: an emerging class of therapeutics. *Annual review of medicine* **56**, 555-583, doi:10.1146/annurev.med.56.062904.144915 (2005).

8 Klug, S. J., Huttenhofer, A. & Famulok, M. In vitro selection of RNA aptamers that bind special elongation factor SelB, a protein with multiple RNA-binding sites, reveals one major interaction domain at the carboxyl terminus. *Rna* **5**, 1180-1190 (1999).

9 Baskerville, S., Zapp, M. & Ellington, A. D. Anti-Rex aptamers as mimics of the Rex-binding element. *Journal of virology* **73**, 4962-4971 (1999).

10 Geiger, A., Burgstaller, P., von der Eltz, H., Roeder, A. & Famulok, M. RNA aptamers that bind L-arginine with sub-micromolar dissociation constants and high enantioselectivity. *Nucleic acids research* **24**, 1029-1036 (1996).

11 Wilson, C., Nix, J. & Szostak, J. Functional requirements for specific ligand recognition by a biotin-binding RNA pseudoknot. *Biochemistry* **37**, 14410-14419, doi:10.1021/bi981371j (1998).

12 Herr, J. K., Smith, J. E., Medley, C. D., Shangguan, D. & Tan, W. Aptamer-conjugated nanoparticles for selective collection and detection of cancer cells. *Analytical chemistry* **78**, 2918-2924, doi:10.1021/ac052015r (2006).

13 Chen, A. & Yang, S. Replacing antibodies with aptamers in lateral flow immunoassay. *Biosensors & bioelectronics* **71**, 230-242, doi:10.1016/j.bios.2015.04.041 (2015).

14 Seo, H. B. & Gu, M. B. Aptamer-based sandwich-type biosensors. *Journal of biological engineering* **11**, 11, doi:10.1186/s13036-017-0054-7 (2017).

15 Higuchi, A. *et al.* Preparation of a DNA aptamer-Pt complex and its use in the colorimetric sensing of thrombin and anti-thrombin antibodies. *Analytical chemistry* **80**, 6580-6586, doi:10.1021/ac8006957 (2008).

16 Schlecht, U., Malave, A., Gronewold, T., Tewes, M. & Lohndorf, M. Comparison of antibody and aptamer receptors for the specific detection of thrombin with a nanometer gap-sized impedance biosensor. *Analytica chimica acta* **573-574**, 65-68, doi:10.1016/j.aca.2006.01.016 (2006).

17 Nguyen, V. T. *et al.* Highly sensitive sandwich-type SPR based detection of whole H5Nx viruses using a pair of aptamers. *Biosensors & bioelectronics* **86**, 293-300, doi:10.1016/j.bios.2016.06.064 (2016).

18 Aktas, G. B., Skouridou, V. & Masip, L. Nucleic acid sensing with enzyme-DNA binding protein conjugates cascade and simple DNA nanostructures. *Analytical and bioanalytical chemistry*, doi:10.1007/s00216-017-0304-z (2017).

19 Davie, E. W. & Kulman, J. D. An overview of the structure and function of thrombin. *Seminars in thrombosis and hemostasis* **32 Suppl 1**, 3-15, doi:10.1055/s-2006-939550 (2006).

20 Bock, L. C., Griffin, L. C., Latham, J. A., Vermaas, E. H. & Toole, J. J. Selection of single-stranded DNA molecules that bind and inhibit human thrombin. *Nature* **355**, 564-566, doi:10.1038/355564a0 (1992).

21 Tasset, D. M., Kubik, M. F. & Steiner, W. Oligonucleotide inhibitors of human thrombin that bind distinct epitopes. *Journal of molecular biology* **272**, 688-698, doi:10.1006/jmbi.1997.1275 (1997).

22 Park, J. H. *et al.* A colorimetric sandwich-type assay for sensitive thrombin detection based on enzyme-linked aptamer assay. *Analytical biochemistry* **462**, 10-12, doi:10.1016/j.ab.2014.05.015 (2014).

23 Pica, A. *et al.* Through-bond effects in the ternary complexes of thrombin sandwiched by two DNA aptamers. *Nucleic acids research* **45**, 461-469, doi:10.1093/nar/gkw1113 (2017).

24 Li, J. *et al.* General colorimetric detection of proteins and small molecules based on cyclic enzymatic signal amplification and hairpin aptamer probe. *Analytical chemistry* **84**, 5309-5315, doi:10.1021/ac3006186 (2012).

25 Xu, H. *et al.* Aptamer-functionalized gold nanoparticles as probes in a dry-reagent strip biosensor for protein analysis. *Analytical chemistry* **81**, 669-675, doi:10.1021/ac8020592 (2009).

26 Liu, J., Mazumdar, D. & Lu, Y. A simple and sensitive "dipstick" test in serum based on lateral flow separation of aptamer-linked nanostructures. *Angewandte Chemie* **45**, 7955-7959, doi:10.1002/anie.200603106 (2006).

27 Famulok, M. & Mayer, G. Chemical biology: aptamers in nanoland. *Nature* **439**, 666-669, doi:10.1038/439666a (2006).

28 Zheng, C. *et al.* One-pot synthesized DNA-templated Ag/Pt bimetallic nanoclusters as peroxidase mimics for colorimetric detection of thrombin. *Chemical communications* **50**, 13103-13106, doi:10.1039/c4cc05339g (2014).

29 Nie, J. *et al.* A self-assemble aptamer fragment/target complex based high-throughput colorimetric aptasensor using enzyme linked aptamer assay. *Talanta* **106**, 309-314, doi:10.1016/j.talanta.2012.11.018 (2013).

30 Li, T., Wang, E. & Dong, S. G-quadruplex-based DNAzyme for facile colorimetric detection of thrombin. *Chemical communications*, 3654-3656, doi:10.1039/b805565c (2008).

31 Zhang, L., Zhu, J., Li, T. & Wang, E. Bifunctional colorimetric oligonucleotide probe based on a G-quadruplex DNAzyme molecular beacon. *Analytical chemistry* **83**, 8871-8876, doi:10.1021/ac2006763 (2011).

32 Li, W., Li, J., Qiang, W., Xu, J. & Xu, D. Enzyme-free colorimetric bioassay based on gold nanoparticle-catalyzed dye decolorization. *The Analyst* **138**, 760-766, doi:10.1039/c2an36374g (2013).

4.8 SUPPLEMANTARY MATERIAL

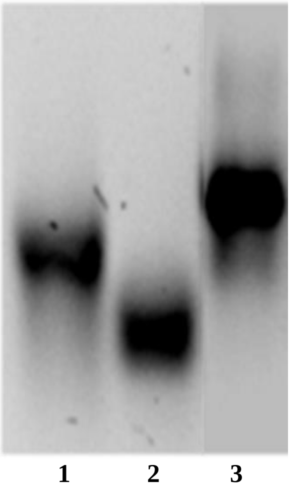

Figure S-4.1: Agarose gel electrophoresis for the preparation of the detection aptamer with 2xLacI binding sites. Lane 1: Detection aptamer with two LacI DNA binding sites (P109); lane 2: Complementary to P109 (P110); lane 3: Hybridization reaction of P109 + P110.

Table S-4.1: Comparison of various colorimetric detection approaches employed for thrombin detection.

Description	**LOD**	**Reference**
Ag/Pt Nanoclusturs for peroxidase-like detection	2.6 nM	[28]
Single aptamer sequence based enzyme-linked assay	10 nM	[29]
DNAzyme mimics peroxidase for a colorimetric detection assay	20 nM	[30]
Label-free molecular beacon based detection	20.5 nM	[31]
AuNPs-based sensing technique with a hairpin aptamer probe	50 pM	[24]
Enzyme-free colorimetric bioassay based on gold nanoparticles	30-320 pM	[32]
Aptamer-based strip biosensor detection with gold nanoparticles	2.5 nM	[25]
Universal enzyme-DNA binding protein conjugates for aptamer based target detection	0.88-0.92 nM	This work

Chapter 5

Paper-based detection of Shiga toxin-producing *Escherichia coli* using carbon nanoparticles-DNA binding protein conjugates

Microchimica Acta 2019, 2019, 186: 426.

Chapter 5: Paper-based detection of Shiga toxin-producing *Escherichia coli* using carbon nanoparticles-DNA binding protein conjugates

5.1 ABSTRACT

Nucleic acid lateral flow assays (NALFA) are widely used to detect specific DNA sequences due to their simplicity, speed and low cost. These assays are very suitable for point-of-care applications. Detection on NALFA strips is usually accomplished by means of DNA hybridization using gold nanoparticles conjugated to specific detection ssDNA sequences or through affinity interactions of labeled PCR amplicons with protein conjugates specific to the labels. The ssDNA form of the target is required for hybridization-based detection and it is usually generated after the PCR amplification step. On the other hand, for the detection methods based on affinity interactions, the target DNA is amplified by PCR using labeled primers and the incorporated labels are detected through protein-label interactions. To avoid the need to generate ssDNA and to reduce the cost associated with primer labeling and usage of specific antibodies, we have developed a NALFA assay that allows the direct detection of PCR amplicons using DNA binding proteins and carbon nanoparticles (CNPs). The target gene was amplified by PCR using a single fluorophore-labeled forward primer and a reverse primer whose sequence was extended with the binding sequence of bacteriophage lambda Cro repressor protein. As a result, the dsDNA amplicons could be detected directly with NALFA using Cro-carbon nanoparticles conjugates. Specifically, the carbon nanoparticles were separately conjugated to the monomeric single-chain format of the Cro DNA binding protein (scCro) and its HRP conjugate (HRP-scCro). Three different detection approaches were evaluated: scCro/CNPs conjugate for carbon black color, HRP-scCro enzyme conjugate for enzymatically generated red color and HRP-scCro/CNPs conjugate for dual color development combining the carbon black color and the enzymatically generated red color. The proposed system was validated for the detection of Shiga

toxin-producing *Escherichia coli* through the amplification and detection of the specific gene target 16S ribosomal RNA from the O157:H7 serotype pathogenic strain. The scCro/CNP detection approach proved to be the fastest one to perform while the HRP-scCro/CNP the most sensitive one. Nevertheless, comparable visual limits of detection were accomplished with all three detection approaches, with 3.75 ng of PCR product (corresponding to 6.5 x 10^3 cfu/ml) being the lowest visual LOD obtained.

5.2 INTRODUCTION

The interest for point-of-care (POC) diagnostics is rapidly increasing due to the need for fast and accurate detection in low resource settings. Therefore, different types of biosensors suitable for this purpose have been developed. Lateral flow assays (LFAs) are one example and they have been widely adopted for POC analysis because of their simplicity, low-cost, user friendly nature and their ability to successfully deliver qualitative and in certain cases quantitative results [1-3]. LFA assays for DNA targets (Nucleic Acid Lateral Flow, NALFA) have gained a lot of interest because of their usefulness for the detection of pathogens [4] and biological warfare agents, DNA diagnostics, gene analysis and forensic applications [5-7]. For increased sensitivity and specificity, the target is amplified by PCR prior to use in NALFA and then visualized through a reporter molecule. Different strategies have been developed and the most commonly used reporters are gold nanoparticles [8], carbon nanoparticles [9], enzymes [10], colored latex beads [11], magnetic particles [12,13], selenium nanoparticles [14], silver nanoparticles [15], quantum dots [16], organic fluorophores [17] and others [1]. Detection of the target is accomplished through complementary base pairing [18-19] or through affinity interactions. In the case of complementary base pairing, the dsDNA target after amplification is used for the preparation of the ssDNA form and used for hybridization with the target-specific complementary probe conjugated with a reporter. This approach is complex and requires many steps whereas discrepancies might arise during the ssDNA preparation step. Also, it requires the preparation of target-specific reporters for each target. On the other hand, for detection through affinity interactions, labeled primers are used during PCR amplification and the labeled amplicon can then be detected through a reporter conjugated to a specific protein that recognizes this label. Typically, a biotinylated primer is used along with streptavidin/neutravidin-conjugated reporter [20-21]. Other examples are small fluorophores incorporated in the primer sequence after oligonucleotide synthesis and specific antibodies conjugated to the reporters are used for target detection. The use of labeled primers circumvents the need for ssDNA preparation and allows the direct detection of the PCR product through universal reporters. This approach is associated with increased primer costs of more than 40% deriving from oligonucleotide post-synthesis modifications. Moreover, the biotinylated PCR product can only bind one reporter-streptavidin conjugate per molecule, suggesting that the signal obtained can be limited.

In this work, an alternative direct detection of the PCR product on NALFA tests is proposed based on DNA binding protein-carbon nanoparticles conjugates. The forward primer used for amplification is labeled with a fluorophore whereas the reverse primer is modified during oligonucleotide synthesis with a DNA extension corresponding to the specific binding sequence of the bacteriophage lambda Cro DNA binding protein. The resulting PCR amplicon contains a fluorophore at one end and the Cro dsDNA binding site at the other and it is captured on the NALFA test line by fluorophore-specific antibody. It should be pointed out that the fluorophore label is just present as an antigen to be recognized by the antibody, there is no utilization of its fluorescent properties. Detection is accomplished through carbon nanoparticles (CNPs) conjugated to the single-chain format of Cro (scCro) or to its HPR conjugate (HRP-scCro), as shown in Fig. 5.1. scCro is a small (17 kDa) single-chain monomeric variant of the Cro protein and it has been shown to retain the high affinity of the wild-type homodimeric protein for its binding sequence [22]. The CNPs were chosen for visualization on NALFA tests because of their good sensitivity and signal-to-noise ratio owing to the high contrast between the dark black color of carbon on the white nitrocellulose membrane background. Also, they are easy to prepare and stable in their conjugated form. They do not require chemical crosslinking but rather direct adsorption of the desired protein and they have a low cost compared to other labels [23,1,24,9,25].

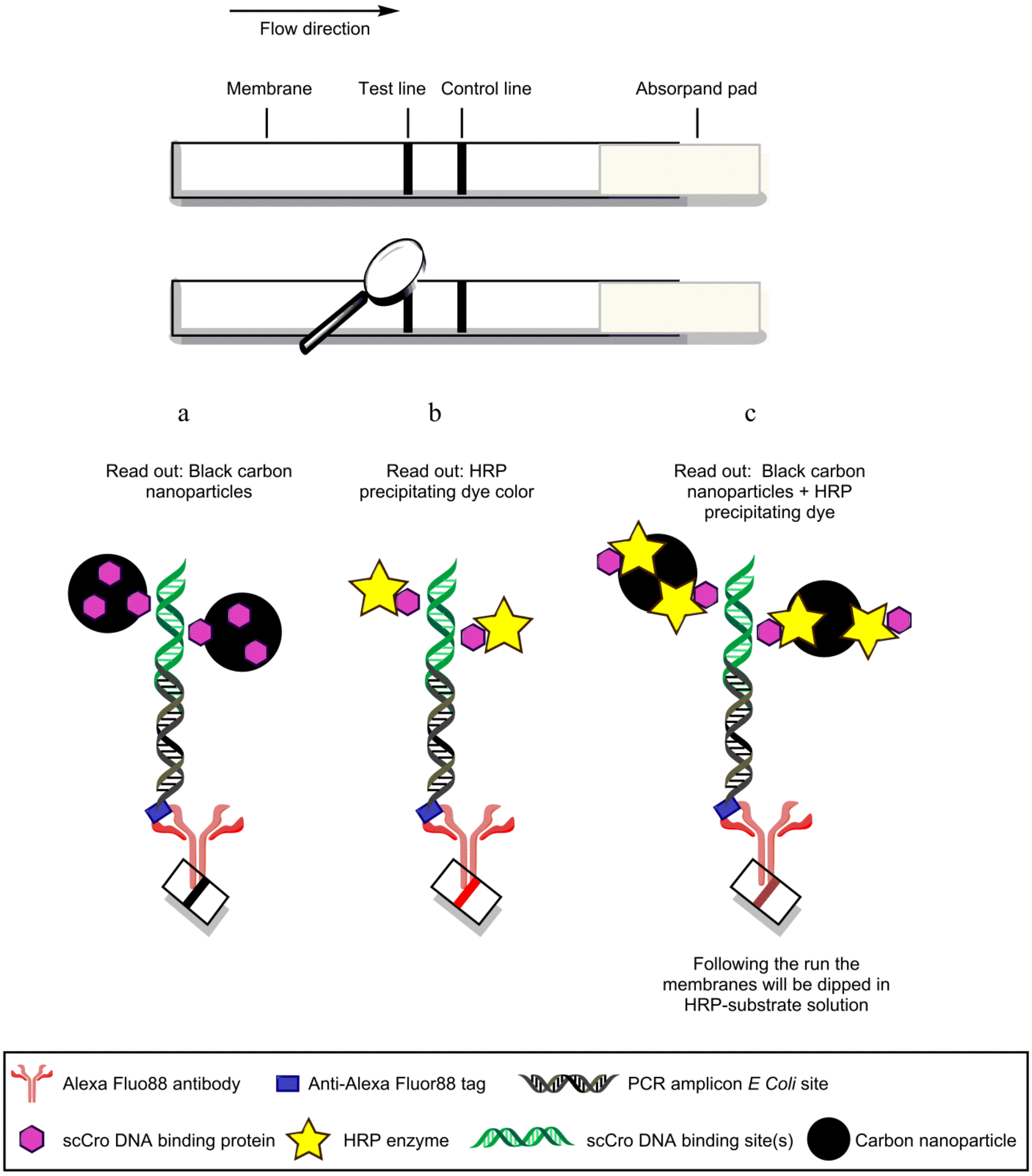
Flow direction
Membrane
Test line
Control line
Absorpand pad
a
b
c
Read out: Black carbon nanoparticles
Read out: HRP precipitating dye color
Read out: Black carbon nanoparticles + HRP precipitating dye
Following the run the membranes will be dipped in HRP-substrate solution
Alexa Fluo88 antibody
Anti-Alexa Fluor88 tag
PCR amplicon *E Coli* site
scCro DNA binding protein
HRP enzyme
scCro DNA binding site(s)
Carbon nanoparticle

Figure 5.1: Scheme of different approaches on the control line NALFA test for the Shiga toxin-producing *E. coli* detection: a) scCro/carbon nanoparticles; b) HRP-scCro enzyme conjugate; and c) HRP-scCro/carbon nanoparticles conjugate.

Three different approaches were evaluated as summarized in Fig. 5.1: (a) scCro immobilized on carbon nanoparticles (scCro/CNP) for CNP-mediated visualization (carbon black color); (b) HRP-scCro conjugate for enzymatically generated red color; and (c) HRP-scCro immobilized on carbon nanoparticles (HRP-scCro/CNP) for dual color development (black + red color). The dual color development was performed in an effort to increase the sensitivity of the assay, since enzyme-based dual-labeled nanoparticles have been demonstrated before and their use in NALFA was successful in enhancing the signal obtained [26,27]. In our previous works we have shown the use of the HRP-scCo enzyme conjugate for signal amplification in the detection of ssDNA targets in ELONA assays, alone or in a cascade reaction with GOx-dHP enzyme conjugate [22,30]. We have also developed paper-based assays for the detection of DNA targets using biotinylated PCR amplicons and neutravidin-carbon nanoparticles conjugates, in dipstick and in microarray formats [20]. Herein, we demonstrate the compatibility of the DNA binding protein scCro and its HRP-scCro enzyme conjugate as carbon nanoparticle conjugates with POC applications such as the NALFA dipsticks. We provide an example of the use of these alternative detection methods that minimize the amount of antibodies required, avoids the use of the (neutr)avidin-biotin system and reduces the need of additional post-synthesis chemical labeling of primers, ultimately leading to lower costs. The assay was validated for the detection of Shiga toxin-producing *Escherichia coli*. Even though many *E. coli* strains are harmless, some of them produce Shiga toxin and are thus pathogenic, causing diarrhea, hemorrhagic colitis or hemolytic uremic syndrome. The O157:H7 serotype, frequently associated with illness outbreaks [28] was chosen as the target strain and specifically the gene encoding for 16S ribosomal RNA (hui) was amplified from genomic DNA purified from this strain using the modified primers described above and detected through the developed method.

5.3 EXPERIMENTAL

5.3.1 Materials

The DNA oligonucleotides were purchased from Biomers.net (Ulm, Germany) and Eurofins Genomics (Netherlands) and their sequences are shown in Table 5.1. High binding Nunc microplates were provided from Grenier Bio-One (Netherlands). Polyclonal antibody against Alexa Fluor 488 was obtained from ThermoFisher and monoclonal anti-His-tag antibody from GE HeathCare (Finland). The Shiga toxin-producing *Escherichia coli* strain EDL 933 (O157:H7 serotype) was used for the isolation of genomic DNA as described before [1], with 5 x 10^8 cfu/mL corresponding to a DNA concentration of 831 ng/µL. All other reagents were purchased from Fisher Scientific (Barcelona, Spain) and Sigma-Aldrich (Madrid, Spain).

5.3.2 Polymerase Chain Reaction

The *hui* gene encoding for the *E. coli* 16S ribosomal RNA was used as the target for the specific detection of *E. coli*. The primers used for the amplification of the gene from genomic DNA were designed according to the literature.[1] The forward primer was labeled with Alexa Fluor 488 while the sequence of the reverse primer was modified in order to include one or two copies of the specific binding sequence of scCro DNA binding protein. A PIKO Thermal cycler and Phire Hot Start DNA Polymerase (Finnzymes, Espoo, Finland) were used for fast PCR amplification within 30 min. Each PCR reaction (total volume 20 µl) included 2 µl of template (diluted *E. coli* genomic DNA), 0.4 µL Phire Hot Start DNA polymerase (Finnzymes), 1.5 mM $MgCl_2$, 0.25 µM dNTPs and 0.9 µM of each primer (forward primer labeled with AlexaFluor 488 and reverse primer with one or two copies of scCro binding sites). Amplification was performed with an initial denaturation of 30 sec at 98°C, followed by 30 cycles with a denaturation step of 5 sec at 98°C, annealing step of 5 sec at 61°C and an extension step of 5 sec at 72°C, followed by a final extension step of 1 min at 72°C. Negative controls of PCR mix in the absence of the template were included in all runs. The PCR reactions were quantified and stored at -20°C until the use on NALFA strip tests.

Table 5.1: Primer sequences used in this work. The scCro DNA binding site(s) are underlined.

Primers	**Primer sequences (5’ - 3’)**	**Amplicon size (bp)**	**Label or Extension**
hui-FW	CATGCCGCGTGTATGAAGAA	96	Alexa Fluor 488
hui-Rv	CGGGTAACGTCAATGAGCAAA		-
hui-Rv-1xCro	TATCACCGCAAGTGATACGGGTAACGTCAATGAGCAAA	113	1x Cro binding site
hui-Rv-2xCro	TATCACCGCAAGTGATATTTTATCACCGCAAGTGATACGGGTAACGTCAATGAGCAAA	133 bp	2x Cro binding sites

5.3.3 Enzyme-Linked Immunosorbent Assay (ELISA)

The PCR products were tested with ELISA to ensure correct incorporation of the labels. Specifically, the plate was coated with 100 µl of 5 mg/ml anti-Alexa Fluor 488 antibody in 50 mM carbonate buffer pH 9.6 overnight at 4°C. The plate was washed three times with 300 µl PBS-T and then the PCR product (100 µl of up to 475 ng diluted in PBS) was added and incubated for 1 h at 37°C. The wells were then washed with PBS-T and 100 µl of 5 nM HRP-scCro conjugate (in PBS) was added and incubated for 30 min at room temperature. After a final washing step, 100 µl of TMB substrate was added and color development was allowed to proceed for 10 min before the addition of 100 µl of 1M H_2SO_4 and absorbance was recorded at 450 nm. Triplicate sample measurements were performed with three independent experiments whereas the blank measurements were conducted in sextuplets. Data was fitted with a sigmoidal curve and the limit of detection (LOD) for each detection approach was calculated as the calculated bottom of the fitted curve plus three times the standard deviation (SD) of the bottom.

5.3.4 Preparation of the carbon nanoparticles-protein conjugates

Carbon nanoparticles were labeled with scCro DNA binding protein or its HRP conjugate (HRP-scCro) by physical adsorption according to the reported method [20] with minor modifications. In brief, 1 % (w/v) carbon (Spezial Schwartz 4, Degussa AG, Frankfurt, Germany) was prepared in MilliQ water and sonicated for 5 min (Branson model 250 Sonifier, Danbury, CT, USA). The carbon suspension was diluted five times in binding buffer (5 mM carbonate-bicarbonate buffer pH 10.6) and sonicated for another 5 min. Next, 70 µg of either scCro protein or 35 µg of HRP-scCro conjugate (prepared as detailed before [2]) were added to 200 µl or 100 µl of 0.2 % (w/v) carbon suspension respectively and both individual suspensions were stirred overnight at 4°C. Then, the suspensions were centrifuged at 13,636 xg for 15 min, the supernatants were removed and the pellets were washed with wash buffer (5 mM borate pH 8.8, 1 % w/v BSA) to remove unbound protein. The washing process was repeated two more times. After the last washing step, each pellet was resuspended in 200 µl or 100 µl of storage buffer (100 mM borate pH 8.8, 1% w/v BSA) for Cro/CNPs or HRP-scCro/CNPs, respectively. The two conjugate suspensions, which contained 0.2% (w/v) carbon nanoparticles, were stored at 4°C until use.

5.3.5 Preparation of the nucleic acid lateral flow assay (NALFA) strips

Hi-Flow Plus HFB13502 nitrocellulose membrane (Millipore) was cut to 2.5 cm height. The antibody solutions, 200 ng/µl for the anti-Alexa Fluor 488 and 250 ng/µl for the anti-His tag, were prepared in 5 mM borate buffer pH 8.8 and dispensed on the nitrocellulose membrane using a Linomat IV TLC dispenser (Camag, Berlin, Germany) for the test and control line, respectively. The membranes were dried and then fixed on a plastic backing along with a 3 cm high cellulose absorbent pad (Schleicher and Schuell's-Hertogenbosch, Netherlands). Finally, the strips were cut at a width of 5 mm using a Bio-Dot Cutter CM4000 (Irvine, CA, USA), packaged in aluminum pouches (Nefab, Barneveld, The Netherlands) along with a silica desiccation pad (Multisorb Technologies, Inc., NY, USA) and the ready-to-use strips were stored at room temperature until use.

5.3.6 Detection of PCR amplicon by NALFA

The PCR amplicon was detected with NALFA strips using three different approaches: (i) scCro/CNPs conjugate for carbon black signal, (ii) HRP-scCro enzyme conjugate for precipitating dye (red color) signal and (iii) HRP-scCro/CNPs conjugate for carbon black plus precipitating dye (red color) mixed signal. The amplicons with one (1x) or two (2x) Cro specific binding sequences at the 3' were captured on the test line by the anti-Alexa Fluor 488 antibody and detected with the three different approaches to compare their performances. Strips were dipped vertically in a low-binding 96-well microplate wells containing 100 µl of running buffer (1% dry milk and 0.1 % Tween-20 in PBS) including the desired amount of the PCR amplicon. After the strips adsorbed completely the introduced solution, the three detection methods were applied to the strips separately. In the case of the CNPs conjugates, the strips were dipped in 100 µl of running buffer mixed with 1 µl of scCro/CNPs or HRP-scCro/CNPs conjugate suspensions. For detection with the HRP-scCro enzyme conjugate, 135 ng of the conjugate was added to 100 µl of running buffer. Black color signals from the carbon nanoparticles were observed after 10 min in the case of the CNPs conjugates. In the case of detection with the HRP-scCro conjugate or the HRP-scCro/CNPs conjugate suspension, an additional development step was required using an HRP substrate. The chromogenic dye solution (1 mM 3-amino-9-ethylcarbazole (AEC) and 1 mM hydrogen peroxide in 100 mM potassium phosphate pH 5) was freshly prepared and incubated on the strips for 5 min. The strips were dried and the visual limit of detection was determined by naked-eye detection. Additionally, the pixel grey intensities of the test lines were evaluated using the ImageJ program and the signal intensities were plotted against the amount of PCR amplicon using the GraphPad Prism program. The limits of detection (LOD) were then calculated quantitatively as the bottom value from the fitted curve plus three times the standard deviation (SD) of the bottom.

5.4 RESULTS AND DISCUSSION

5.4.1 Target gene PCR amplification and ELISA validation

A fragment of the target gene was amplified from genomic DNA isolated from the Shiga toxin-producing *E. coli* strain EDL 933 using the primers shown in Table 5-1. After a fast 30 min PCR amplification protocol, the reactions were resolved by agarose gel electrophoresis and the size of the amplicons ranged from 96-133 bp depending on the primer pair used (Supplemantary Material, Fig. S-5.1). When both forward and reverse primers were labeled, the resulting amplicons contained a 5'-Alexa Fluor 488 label at one end and one or two dsDNA binding sites for Cro on the other end, depending on the reverse primer used. Correct incorporation of the fluorophore label and the dsDNA sequence extension in the PCR amplicon was verified with an ELISA assay. The PCR products were captured on the plate by the immobilized anti-Alexa Fluor 488 antibody whereas detection was achieved using the HRP-scCro enzyme conjugate. The two amplicons containing one or two binding sites for the Cro DNA binding protein, 1xCro and 2xCro respectively, were tested (with three independent experiments) and the results are shown in Fig. 5.2. Both amplicons were successfully detected and the limits of detection (LOD) achieved were 5.3 ng and 2.4 ng of PCR product with 1x and 2xCro binding sites, respectively. The results show that the incorporation of two binding sites for Cro in the PCR amplicon resulted in more than two times improved LOD, suggesting that two HRP-scCro enzyme conjugate molecules could bind on each amplicon and provide signal enhancement with higher sensitivity when more than 2 ng of PCR product was used.

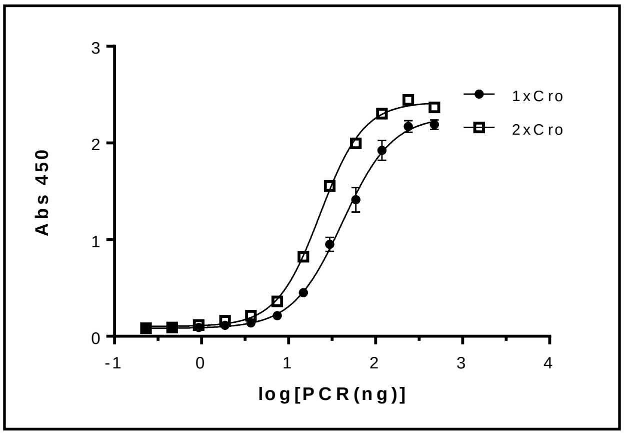

Figure 5.2: PCR amplified *E. coli* 16S rRNA gene detection by ELISA for one or two scCro DNA binding site.

5.4.2 NALFA

After verification of the correct incorporation of the label and sequence extensions in the PCR amplicons, the target amplicons were detected on NALFA strips. Three different detection approaches were performed as shown in Fig. 5.1 with the objective to evaluate the performance of each one on the test strips. The PCR amplicon was captured on the test line by the anti-Alexa Fluor 488 antibody, whereas excess reporter conjugate was captured by the anti-His tag antibody on the control line recognizing the 6xHis tag on the C-terminal of the scCro and HRP-scCro proteins.

5.4.2.1 Detection with scCro/CNP conjugate

When the scCro/CNPs conjugate was used for the detection of the PCR amplicon, black color was visualized on the test lines after the specific interaction of the conjugate with the dsDNA sequence extension incorporated in the target sequence after PCR amplification. As it can be seen in Fig. 5.3, the intensity of the test line increased with increasing amounts of PCR product until a maximum plateau was reached when more than 500 ng were used. To verify that the NALFA test works properly and no false positive result is obtained, a negative control PCR reaction (absence of target in the reaction mix) was also applied on the strip and only the control line gave signal as expected. The evaluation of the line intensities calculated with the ImageJ program clearly show a signal enhancement when the PCR product contained 2xCro binding sites compared to 1xCro. As one of the NALFA tests drawbacks is the lack of sensitivity, this approach shows that the detection signal can be improved just by incorporating more Cro binding sites in the PCR amplicon. This could result in the association of more than one carbon nanoparticle conjugates per target molecule, as opposed to other detection methods which are limited to one carbon nanoparticle conjugates per target molecule [1,3]. The visual limit of detection when scCro/CNPs were used was estimated as 15 ng and 7.5 ng PCR product with 1xCro and 2xCro binding sites respectively. These LODs were calculated at 13.8 and 20.8 ng respectively when a sigmoidal model was used to fit the data in the graph of Fig. 5.3 (see Table S-5.2).

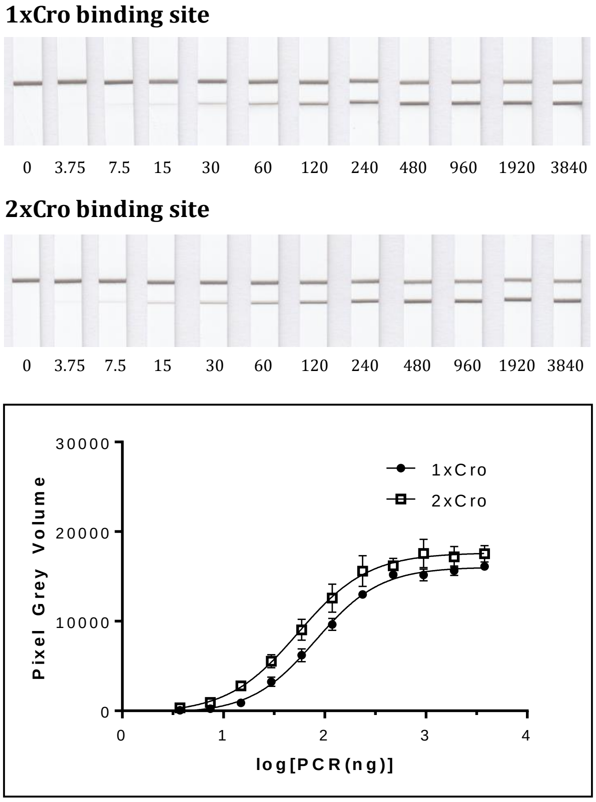

Figure 5.3: Detection of the PCR amplicon with 1x and 2xCro binding sites on NALFA strips using the scCro/CNPs conjugate.

5.4.2.2 Detection with HRP-scCro enzyme conjugate

The HRP enzyme has been widely used in lateral flow assays as a detection tool because of the sensitivity it provides as a consequence of the rapid conversion of chromogenic substrates to precipitating colored products that can be easily visualized on the test strips [4,5]. High sensitivity is crucial for the detection of low concentrations of targets and HRP can enhance the sensitivity of the biosensor. We hypothesized that the HRP-scCro detection approach could provide a higher signal in the NALFA test compared to CNPs detection due to the enzymatic signal amplification. For this reason, we also evaluated the performance of the HRP-scCro enzyme conjugate on NALFA tests and compared the obtained sensitivity to the scCro/CNPs detection strategy described above. After PCR amplicon capture on the test line, the HRP-scCro conjugate was flowed over the strips and the corresponding signals were obtained after incubation with the HRP chromogenic substrate. As it is shown in Fig. 5.4, the signals obtained from the enzymatic development of the strips were higher compared to the signal from the scCro/CNPs shown in Fig. 5.3, confirming the initial hypothesis. It can also be observed that the background color of the strips is not as white as in the case of scCro/CNPs detection due to residual color from the enzyme-generated precipitating colored product. At low target amounts, the signal obtained was not affected by the number of Cro binding sites on the PCR amplicon but when more than 100 ng were used, a signal increase of up to 25 % was observed. The visual limit of detection was estimated as 3.75 ng regardless of the number of Cro binding sites on the PCR amplicon. The LODs calculated after curve fitting were 21 and 45 ng for PCR amplicon with 1x and 2xCro binding sites, respectively (Table S-5.3).

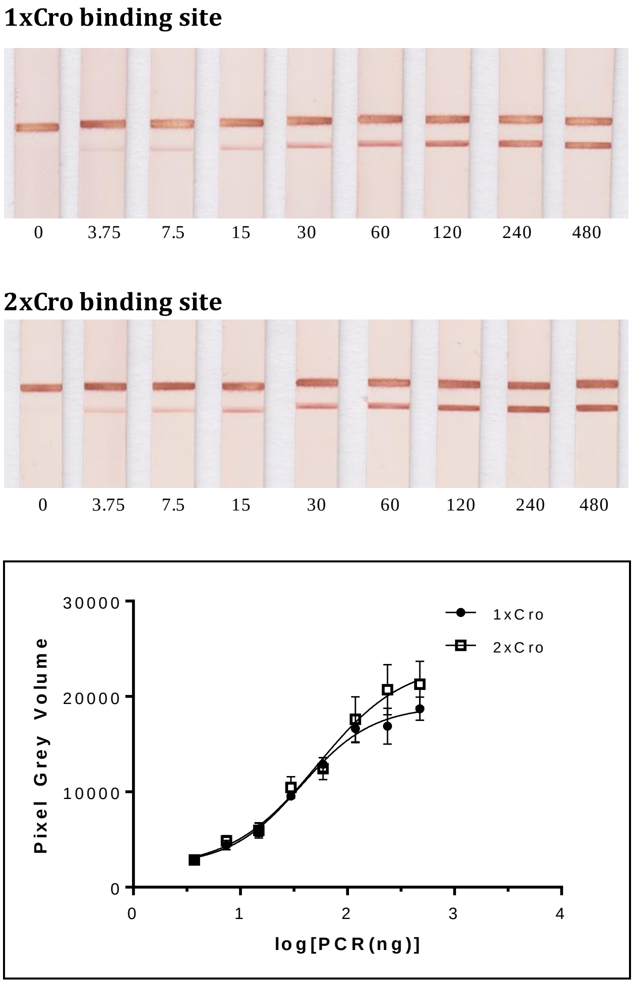

Figure 5.4: Detection of the PCR amplicon with 1x and 2xCro binding sites on NALFA strips using the HRP-scCro enzyme conjugate.

5.4.2.3 Detection with HRP-scCro/CNP conjugate

The third approach for PCR amplicon on NALFA involved the dual color development using the HRP-scCro/CNPs conjugate. Dual signals in lateral flow assays have been reported before by using a dual labeled reporter. Typically, gold nanoparticles are combined with HRP and ultrasensitive detection signals can be achieved [6] [27]. In this work, by using the HRP-scCro/CNPs reporter, the black color from the CNPs is combined with the red color produced from the HRP chromogenic substrate 3-amino-9-ethylcarbazole. After applying the substrate solution (AEC +

H_2O_2) on the strips, a reddish black band was developed on the NALFA strips (Fig. 5.5). The visual effect was enhanced significantly due to dual color development with an approximate signal enhancement of 30 % compared to scCro/CNPs and HRP-scCro detection strategies. Even though the visual limit of detection, as evaluated from the strips shown in Fig. 5.5 is 3.75 ng regardless of the number of Cro binding sites on the PCR amplicon, increased sensitivity is obtained at both low and high target concentrations. The LODs calculated after curve fitting were 25 and 35 ng for PCR amplicon with 1x and 2xCro binding sites, respectively (Table S-5.5).

We also have evaluated the performance of the HRP-sCro/CNPs detection strategy without substrate addition and dual color development. Fig. S-5.2 clearly shows that the signal obtained is lower than the signal observed in the strips visualized with the scCro/CNPs (Fig. 5.3). This could be explained by steric hindrance effects and lower accessibility of scCro to the binding site on the PCR amplicon when the bulkier HRP-scCro is used as a CNPs conjugate. Nonetheless, when the HRP-scCro/CNPs conjugate is used for detection, improved signals were obtained after the dual color development compared to using scCro/CNPs or HRP-scCro alone.

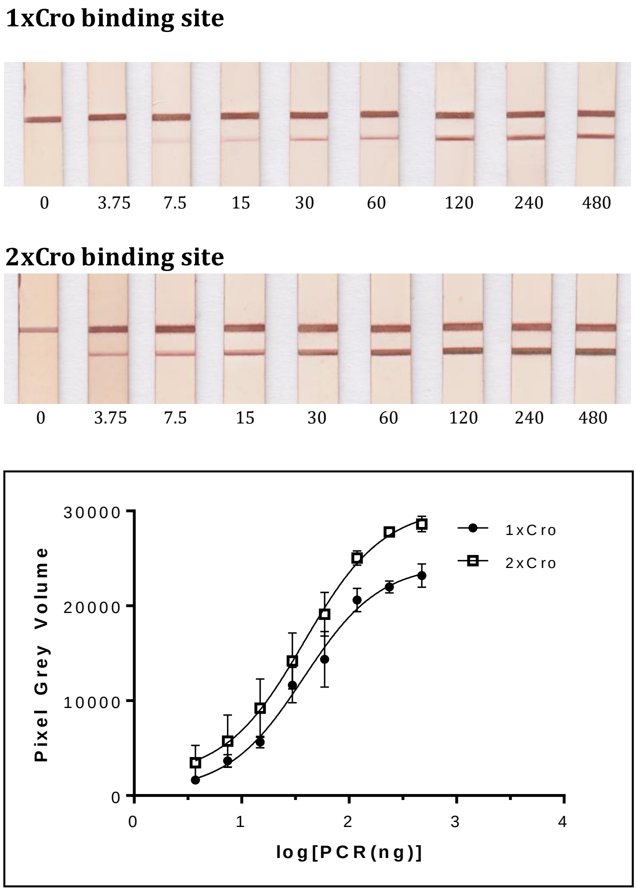

Figure 5.5: Detection of the PCR amplicon with 1x and 2xCro binding sites on NALFA strips using the HRP-scCro/CNPs enzyme conjugate

Table 5.2: Detection limits achieved by ELISA and NALFA.

Limits of detection (ng of PCR product)				
	ELISA	**Visual limit of detection in NALFA**		
Cro binding sites on the PCR product	**HRP-scCro**	**scCro/CNPs**	**HRP-scCro**	**HRP-scCro/CNPs**
1x	5.27	15.00	3.75	3.75
2x	2.40	7.50	3.75	3.75

5.5 CONCLUSION

We have successfully developed three different strategies for the detection of DNA targets after PCR amplification on NALFA strips based on a DNA binding protein and carbon nanoparticles. By using a fluorophore-labeled primer and a sequence-extended primer with the specific binding site of Cro DNA binding protein, the PCR amplicon was successfully detected by the reporter conjugates scCro/CNPs, HRP-scCro and HRP-scCro/CNPs. By increasing the number of Cro binding sites on the PCR amplicon, we were able to increase the obtained signal in a controlled manner. Also, when the HRP-scCro/CNPs detection strategy was utilized, dual color development was accomplished by the combination of the black color read out properties of the carbon nanoparticles and the enzymatically-generated red color from the HRP precipitating chromogenic substrate, leading to signal enhancement. A summary of the visual limits of detection achieved are shown in Table 5.2. We have also demonstrated that a different detection strategy can be chosen depending on the specific requirements of the assay; scCro/CNPs can be used for fast detection within less than 20 min whereas when higher sensitivity is required, the dual color development through the HRP-scCro/CNPs conjugate is more appropriate. Overall, these alternative detection strategies minimize the amount of antibodies required, avoid the use of the (neutr)avidin-biotin system and the preparation of ssDNA target and lower the assay costs associated with the additional post-synthesis chemical labeling of both primers. To further optimize the NALFA tests using DNA binding protein/carbon nanoparticles conjugates, additional work will be performed by replacing the fluorophore label of the forward primer with a sequence extension of the binding site of a DNA binding protein with different sequence specificity, allowing the detection of the PCR amplicon without the use of antibodies or chemically-modified primers.

5.6 ACKNOWLEDGEMENTS

This work was supported financially by the FP7-PEOPLE-2011-CIG DeCoDeB project grant awarded to LM. GBA acknowledges the Universitat Rovira i Virgili for the doctoral fellowship and EMBO for the short term fellowship. The authors thank Prof. M. C. Mossing (University of Mississippi, USA) for the gift of the pscCro16 construct.

5.7 REFERENCES

1 Sajid, M., Kawde, A.-N. & Daud, M. Designs, formats and applications of lateral flow assay: A literature review. *Journal of Saudi Chemical Society* **19**, 689-705, doi:10.1016/j.jscs.2014.09.001 (2015).

2 Sher, M., Zhuang, R., Demirci, U. & Asghar, W. Paper-based analytical devices for clinical diagnosis: recent advances in the fabrication techniques and sensing mechanisms. *Expert Review of Molecular Diagnostics*, null-null, doi:10.1080/14737159.2017.1285228 (2017).

3 Posthuma-Trumpie, G. A., Korf, J. & van Amerongen, A. Lateral flow (immuno)assay: its strengths, weaknesses, opportunities and threats. A literature survey. *Analytical and Bioanalytical Chemistry* **393**, 569-582, doi:10.1007/s00216-008-2287-2 (2009).

4 Lazcka, O., Del Campo, F. J. & Munoz, F. X. Pathogen detection: a perspective of traditional methods and biosensors. *Biosensors & bioelectronics* **22**, 1205-1217, doi:10.1016/j.bios.2006.06.036 (2007).

5 Sassolas, A., Leca-Bouvier, B. D. & Blum, L. J. DNA Biosensors and Microarrays. *Chemical Reviews* **108**, 109-139, doi:10.1021/cr0684467 (2008).

6 Cordray, M. S. & Richards-Kortum, R. R. Emerging nucleic acid-based tests for point-of-care detection of malaria. *The American journal of tropical medicine and hygiene* **87**, 223-230, doi:10.4269/ajtmh.2012.11-0685 (2012).

7 Carter, D. J. & Cary, R. B. Lateral flow microarrays: a novel platform for rapid nucleic acid detection based on miniaturized lateral flow chromatography. *Nucleic acids research* **35**, e74, doi:10.1093/nar/gkm269 (2007).

8 Aveyard, J., Mehrabi, M., Cossins, A., Braven, H. & Wilson, R. One step visual detection of PCR products with gold nanoparticles and a nucleic acid lateral flow (NALF) device. *Chemical communications*, 4251-4253 (2007).

9 Posthuma-Trumpie, G. A., Wichers, J. H., Koets, M., Berendsen, L. B. J. M. & van Amerongen, A. Amorphous carbon nanoparticles: a versatile label for rapid diagnostic (immuno)assays. *Analytical and Bioanalytical Chemistry* **402**, 593-600, doi:10.1007/s00216-011-5340-5 (2012).

10 Kawde, A.-N. *et al.* Moving Enzyme-Linked ImmunoSorbent Assay to the Point-of-Care Dry-Reagent Strip Biosensors. *American Journal of Biomedical Sciences*, 23-32, doi:10.5099/aj100100023 (2010).

11 Mao, X., Wang, W. & Du, T. E. Dry-reagent nucleic acid biosensor based on blue dye doped latex beads and lateral flow strip. *Talanta* **114**, 248-253, doi:10.1016/j.talanta.2013.04.044 (2013).

12 Zheng, C., Wang, X., Lu, Y. & Liu, Y. Rapid detection of fish major allergen parvalbumin using superparamagnetic nanoparticle-based lateral flow immunoassay. *Food Control* **26**, 446-452, doi:10.1016/j.foodcont.2012.01.040 (2012).

13 Taton, K., Johnson, D., Guire, P., Lange, E. & Tondra, M. Lateral flow immunoassay using magnetoresistive sensors. *Journal of Magnetism and Magnetic Materials* **321**, 1679-1682, doi:10.1016/j.jmmm.2009.02.113 (2009).

14 Wang, Z. *et al.* Lateral flow test strip based on colloidal selenium immunoassay for rapid detection of melamine in milk, milk powder, and animal feed. *International journal of nanomedicine* **9**, 1699-1707, doi:10.2147/IJN.S58942 (2014).

15 Jiang, H. *et al.* Silver Nanoparticle-Based Fluorescence-Quenching Lateral Flow Immunoassay for Sensitive Detection of Ochratoxin A in Grape Juice and Wine. *Toxins* **9**, doi:10.3390/toxins9030083 (2017).

16 Taranova, N. A., Berlina, A. N., Zherdev, A. V. & Dzantiev, B. B. 'Traffic light' immunochromatographic test based on multicolor quantum dots for the

simultaneous detection of several antibiotics in milk. *Biosensors & bioelectronics* **63**, 255-261, doi:10.1016/j.bios.2014.07.049 (2015).

17 Khreich, N. *et al.* Detection of Staphylococcus enterotoxin B using fluorescent immunoliposomes as label for immunochromatographic testing. *Analytical biochemistry* **377**, 182-188, doi:10.1016/j.ab.2008.02.032 (2008).

18 Xu, Y. *et al.* Fluorescent probe-based lateral flow assay for multiplex nucleic acid detection. *Analytical chemistry* **86**, 5611-5614, doi:10.1021/ac5010458 (2014).

19 Mao, X. *et al.* Disposable nucleic acid biosensors based on gold nanoparticle probes and lateral flow strip. *Analytical chemistry* **81**, 1660-1668, doi:10.1021/ac8024653 (2009).

20 Noguera, P. *et al.* Carbon nanoparticles in lateral flow methods to detect genes encoding virulence factors of Shiga toxin-producing Escherichia coli. *Anal Bioanal Chem* **399**, 831-838, doi:10.1007/s00216-010-4334-z (2011).

21 Moers, A. P. *et al.* Detection of single-nucleotide polymorphisms in Plasmodium falciparum by PCR primer extension and lateral flow immunoassay. *Antimicrobial agents and chemotherapy* **59**, 365-371, doi:10.1128/AAC.03395-14 (2015).

22 Aktas, G. B., Skouridou, V. & Masip, L. Novel signal amplification approach for HRP-based colorimetric genosensors using DNA binding protein tags. *Biosensors & bioelectronics* **74**, 1005-1010, doi:10.1016/j.bios.2015.07.077 (2015).

23 Linares, E. M., Kubota, L. T., Michaelis, J. & Thalhammer, S. Enhancement of the detection limit for lateral flow immunoassays: evaluation and comparison of bioconjugates. *Journal of immunological methods* **375**, 264-270, doi:10.1016/j.jim.2011.11.003 (2012).

24 Quesada-Gonzalez, D. & Merkoci, A. Nanoparticle-based lateral flow biosensors. *Biosensors & bioelectronics* **73**, 47-63, doi:10.1016/j.bios.2015.05.050 (2015).

25 Oliveira-Rodriguez, M. *et al.* Point-of-care detection of extracellular vesicles: Sensitivity optimization and multiple-target detection. *Biosensors & bioelectronics* **87**, 38-45, doi:10.1016/j.bios.2016.08.001 (2017).

26 He, Y. *et al.* Ultrasensitive nucleic acid biosensor based on enzyme-gold nanoparticle dual label and lateral flow strip biosensor. *Biosensors & bioelectronics* **26**, 2018-2024, doi:10.1016/j.bios.2010.08.079 (2011).

27 Gao, X. *et al.* An enzyme-amplified lateral flow strip biosensor for visual detection of microRNA-224. *Talanta* **146**, 648-654, doi:10.1016/j.talanta.2015.06.060 (2016).

28 Karmali, M. A., Gannon, V. & Sargeant, J. M. Verocytotoxin-producing Escherichia coli (VTEC). *Veterinary microbiology* **140**, 360-370, doi:**HTTP://DX.DOI.ORG/10.1016/J.VETMIC.2009.04.011** (2010).

29 Jana, R., Hazbun, T. R., Fields, J. D. & Mossing, M. C. Single-chain lambda Cro repressors confirm high intrinsic dimer-DNA affinity. *Biochemistry* **37**, 6446-6455, doi:10.1021/bi980152v (1998).

30 Aktas, G. B., Skouridou, V. & Masip, L. Nucleic acid sensing with enzyme-DNA binding protein conjugates cascade and simple DNA nanostructures. *Anal Bioanal Chem* **409**, 3623-3632, doi:10.1007/s00216-017-0304-z (2017).

31 Shan, S., Lai, W., Xiong, Y., Wei, H. & Xu, H. Novel strategies to enhance lateral flow immunoassay sensitivity for detecting foodborne pathogens. *Journal of agricultural and food chemistry* **63**, 745-753, doi:10.1021/jf5046415 (2015).

5.8 SUPPLEMANTARY MATERIAL

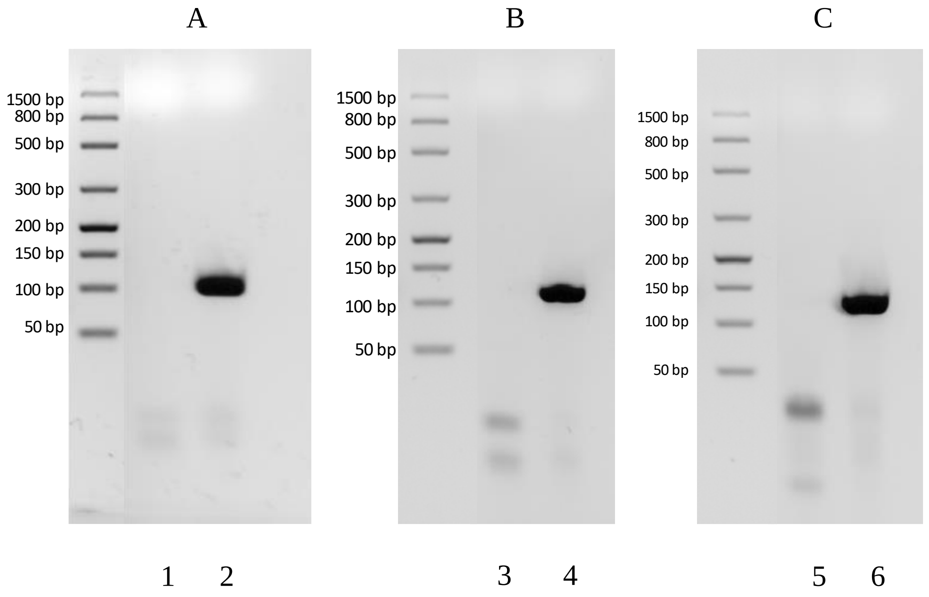
A
1500 bp
800 bp
500 bp
300 bp
200 bp
150 bp
100 bp
50 bp
1
2
B
1500 bp
800 bp
500 bp
300 bp
200 bp
150 bp
100 bp
50 bp
3
4
C
1500 bp
800 bp
500 bp
300 bp
200 bp
150 bp
100 bp
50 bp
5
6

Figure S-5.1: Agarose gel electrophoresis of the PCR reactions for *E. coli* 16S rRNA target gene amplification with Alexa Fluor 488-labeled forward primer and (A) unlabeled reverse primer, (B) reverse primer with 1xCro binding site, and (C) reverse primer with 2xCro binding sites. Lanes 1, 3, 5 represent the PCR controls and lanes 2, 4, 6 the PCR reactions with genomic DNA template.

Table S-5.1: ELISA calibration curve results and statistics for the PCR amplicons with (A) 1xCro and (B) 2xCro DNA binding sites. Each replicate corresponds to the average of triplicate sample from three independent experiments, while the sextuplets were used for the blank sample.

(A) ELISA HRP-scCro detection – PCR amplicon with 1x Cro binding site

PCR (ng)	Replicate 1	Replicate 2	Replicate 3	Model: Sigmoidal 4PL $R^2 = 0.985$ Top: 2.277 ± 0.07 Bottom: 0.083 ± 0.03 IC50: 41.7 ng LOD: 5.27 ng
0.000	0.075	0.085	0.077	
0.230	0.075	0.089	0.085	
0.460	0.076	0.084	0.089	
0.930	0.083	0.097	0.097	
1.860	0.103	0.115	0.122	
3.710	0.132	0.126	0.159	
7.420	0.193	0.188	0.257	
14.840	0.370	0.462	0.524	
29.690	0.805	0.937	1.110	
59.380	1.374	1.168	1.696	
118.750	1.880	1.730	2.158	
237.500	2.168	2.046	2.298	
475.000	2.207	2.081	2.285	

(B) ELISA HRP-scCro detection – PCR amplicon with 2x Cro binding sites

PCR (ng)	Replicate 1	Replicate 2	Replicate 3	Model: Sigmoidal 4PL $R^2 = 0.998$ Top: 2.424 ± 0.02 Bottom: 0.102 ± 0.015 IC50: 23.06 ng LOD: 2.4 ng
0.000	0.071	0.080	0.080	
0.230	0.081	0.085	0.084	
0.460	0.087	0.095	0.090	
0.930	0.107	0.127	0.115	
1.860	0.148	0.172	0.162	
3.710	0.207	0.207	0.226	
7.420	0.346	0.334	0.407	
14.840	0.734	0.916	0.825	
29.690	1.479	1.632	1.559	
59.380	2.021	1.968	2.002	
118.750	2.306	2.324	2.277	
237.500	2.513	2.450	2.376	
475.000	2.399	2.362	2.345	

Table S-5.2: PCR amplicon detection by NALFA using scCro/CNPs. Calibration curve results and statistics for (A) 1x Cro and (B) 2x Cro DNA binding sites. Data shows three independent replicates.

(A) NALFA scCro/CNPs detection – PCR amplicon with 1x Cro binding site

PCR (ng)	Replicate 1	Replicate 2	Replicate 3	
3.7	35.1	51.6	66.2	Model: Sigmoidal 4PL (Three independent values) $R^2 = 0.999$ Top: 16045 ± 343.9 Bottom: -301.2 ± 442.5 IC50: 81.45 ng LOD: 13.8 ng
7.4	129.7	377.3	198.5	
14.8	435.6	1079.5	1155.6	
29.7	2080.3	4264.8	3393.6	
59.3	4474.8	7098.3	7038.6	
118.7	8028.2	10425.9	10477.7	
237.3	12750.3	12906.7	13314.9	
474.6	14687.3	14776.8	16079.0	
949.2	13684.8	15416.9	16379.1	
1898.4	14651.7	15397.1	16871.5	
3796.8	15846.0	15788.3	16727.6	

(B) NALFA scCro/CNPs detection – PCR amplicon with 2x Cro binding sites

PCR (ng)	Replicate 1	Replicate 2	Replicate 3	
3.7	397.4	409.9	181.3	Model: Sigmoidal 4PL (Three independent values) $R^2 = 0.926$ Top: 17645 ± 781.7 Bottom: -289.5 ± 1382 IC50: 54.34 ng LOD: 20.8 ng
7.4	1373.8	840.7	619.7	
14.8	3710.1	2584.8	2040.7	
29.7	7288.6	4850.1	4450.2	
59.3	11899.5	7775.2	7465.7	
118.7	16379.0	10713.2	10639.1	
237.3	19747.0	13954.9	13081.3	
474.6	18188.8	15444.0	14948.9	
949.2	21430.6	15544.2	15749.5	
1898.4	20036.8	15755.4	15739.1	
3796.8	19747.5	16470.8	16372.6	

Table S-5.3: PCR amplicon detection by NALFA using HRP-scCro. Calibration curve results and statistics for (A) 1x Cro and (B) 2x Cro DNA binding sites. Data shows three independent replicates.

(A) NALFA HRP-scCro detection – PCR amplicon with 1x Cro binding site

PCR (ng)	Replicate 1	Replicate 2	Replicate 3	
3.7	2209.4	2757.9	3863.1	Model: Sigmoidal 4PL (Independent values) $R^2 = 0.906$ Top: 18984 ± 1598 Bottom: 2289 ± 1857 IC50: 36.82 ng LOD: 21 ng
7.4	3881.5	3772.5	5619.7	
14.8	5282.2	5077.1	7727.5	
29.7	9705.4	10237.4	8737.5	
59.3	13600.6	13886.2	11142.2	
118.7	18303.3	18588.5	13024.4	
237.3	20167.5	18012.7	12460.1	
474.6	21703.7	17102.7	17366.8	

(B) NALFA HRP-scCro detection – PCR amplicon with 2x Cro binding sites

PCR (ng)	Replicate 1	Replicate 2	Replicate 3	
3.7	3276.9	2218.8	3096.8	Model: Sigmoidal 4PL (Independent values) $R^2 = 0.8414$ Top: 23571 ± 434 Bottom: 2024 ± 334 IC50: 52.21 ng LOD: 45 ng
7.4	5069.4	3621.0	5899.0	
14.8	7715.5	4328.6	5869.1	
29.7	12563.2	10966.8	7857.5	
59.3	15255.7	11286.1	10771.8	
118.7	21578.9	19251.9	11988.9	
237.3	25043.7	22665.7	14434.1	
474.6	26700.0	20535.3	16653.6	

Table S-5.4: PCR amplicon detection by NALFA using HRP-scCro/CNPs. Calibration curve results and statistics for (A) 1x Cro and (B) 2x Cro DNA binding sites. Data shows two independent replicates.

(A) NALFA HRP-scCro/CNPs detection – PCR amplicon with 1x Cro binding site			
PCR (ng)	**Replicate 1**	**Replicate 2**	
3.7	2222.4	1077.2	Model: Sigmoidal 4PL (Independent values) $R^2 = 0.933$ Top: 24361 ± 266 Bottom: 482.7 ± 3 IC50: 37.79 ng LOD: 25 ng
7.4	4588.9	2714.2	
14.8	6500.5	4789.3	
29.7	14269	9024.0	
59.3	18507.7	10225.5	
118.7	22338.3	18888.5	
237.3	22877.1	21094.6	
474.6	24926.6	21449.7	

(B) NALFA HRP-scCro/CNPs detection – PCR amplicon with 2x Cro binding sites			
PCR (ng)	**Replicate 1**	**Replicate 2**	
3.7	6051.8	884.4	Model: Sigmoidal 4PL (Independent values) $R^2 = 0.906$ Top: 30417 ± 4066 Bottom: 1942 ± 4562 IC50: 38.05 ng LOD: 35 ng
7.4	9615.8	1866.4	
14.8	13556.1	4865.6	
29.7	18358.7	10028.0	
59.3	22369.1	15846.5	
118.7	26100.8	23978.8	
237.3	27288.8	28266.8	
474.6	27464.9	29771.1	

1xCro binding site

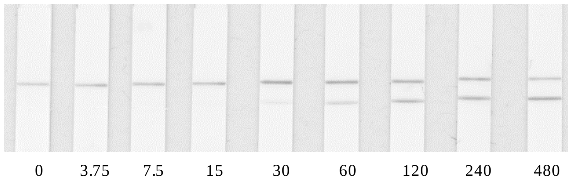
0
3.75
7.5
15
30
60
120
240
480

2xCro binding site

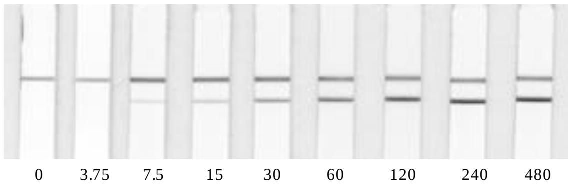
0
3.75
7.5
15
30
60
120
240
480

Figure S-5.2: NALFA strips for PCR amplicon detection using HRP-scCro/CNPs before HRP substrate addition and color development.

Chapter 6

General conclusion

Chapter 6: General conclusion

6.1 GENERAL CONCLUSION

The overall objective of this thesis was to develop a protein fusion tag system that would allow the controlled and orderly precise co-immobilization of proteins and its application to biosensors. To immobilize the target proteins of interest, specific DNA binding proteins were used as tags in combination with a dsDNA tether as the template to direct protein co-immobilization by specific positioning of the target DNA sequences of the DNA binding proteins. Fundamental aspects such as the preparation and characterization of two novel enzyme-DNA binding protein conjugates (HRP-scCro and GOx-dHP) and their use for detection and signal amplification in biosensors have been described. The enzyme-DNA binding protein conjugates were then utilized in several biosensor configurations to provide sensitive, rapid and universal target-independent detection which can be easily adapted in point-of-care tests.

We utilized the enzyme-DNA binding protein conjugate HRP-scCro as a signal generator for the detection of ssDNA targets, and demonstrated that the DNA binding protein tags were able to facilitate the association of more HRP molecules per target molecule. The signal generation was compared with direct conjugation of the ssDNA detection probe with HRP (ssDNA–HRP conjugate) under the same conditions, and a clear enhancement of the signal was achieved when multiple dsDNA binding sequences for the scCro where included.

The sensitive detection signal plays a very important role in biosensors by means of low analyte amount detection and disease detection on early stage. The specific DNA binding proteins as tags provides a direct and controlled protein co-immobilization by specific positioning, increasing the the HRP enzyme ratio per target, thus for amplifying the signal and lowering the limit of detection. HRP-scCro demonstrated that it can be used as a universal signal amplification tool in biosensors with reduced cost due to their target-independent dsDNA binding tags.

A second enzyme-DNA binding protein conjugate, glucose oxidase- dimeric headpiece domain of *Escherichia coli* LacI repressor protein (GOx-dHP) was then prepared and used with the HRP-scCro enzyme conjugate and simple DNA nanostructures in a versatile and universal DNA sensing platform that uses glucose instead of hydrogen peroxide as one of the enzymatic substrates. This avoids the issue of the storage of the unstable hydrogen peroxide which can be important for point-of-care biosensors. A simple DNA nanostructure allows target recognition and signal generation simultaneously. Target recognition takes place through hybridization to its target-complementary single-stranded DNA (ssDNA) part and signal generation happens after conjugate binding on the double-stranded DNA (dsDNA) containing the specific binding sites for the dHP and scCro DNA binding proteins. Due to the co-immobilization of the GOx and HRP, the signal is obtained in the absence of externally added hydrogen peroxide, which can be integrated to the point-of-care assays. As in the first approach, just by changing the ssDNA part of the detection probe, the system can be used for the detection of different ssDNA target sequences which makes the platform universal.

The first two applications of the enzyme-DNA binding protein tag conjugates showcased the utility of the developed protein immobilization system in DNA biosensors for signal amplification. In the next part of the work, a protein target (thrombin) was detected using the two conjugates together with dual modified aptamers that include the DNA binding sites of the DNA binding protein tags in a sandwich configuration. The binding of the conjugates (HRP-scCro and GOx-dHP) to the modified aptamers allows detection through an HRP/GOx enzymatic cascade reaction. The limit of detection obtained was in the low nanomolar range which is comparable with other colorimetric platforms reported in the literature.

The DNA binding protein scCro and its HRP-scCro conjugate were used to directly detect PCR amplicons with a modified primer that includes the corresponding DNA binding sequence of scCro. These proteins were used in conjuction with carbon nanoparticles in a lateral flow assay for the detection of a pathogenic Shiga toxin-producing *Escherichia coli* strain. This work validates the use of the developed immobilization methods in paper-based lateral flow biosensors.

In summary, the main contribution of this thesis to the state-of-the-art is the development of a system that allows controlled protein co-immobilization. The utility of this system was demonstrated in various biosensor platforms, highlighting its great potential in the field as an alternative to existing immobilization approaches. A lot of possibilities and applications still remain to be explored, especially in the context of multiplex biosensors. For this to happen, more DNA binding proteins with different sequence specifities need to be identified and evaluated.